PERFORMANCE IMPROVEMENT OF VAPOUR COMPRESSION REFRIGERANT SYSTEM USING GRAPHENE AND MULTI-WALLED CARBON NANOTUBE NANO-LUBRICANTS

By

VIRA CUT

Thesis Submitted to the School of Graduate Studies, Universiti Putra Malaysia, in Fulfilment of the Requirements for the Degree of Master of Science

July 2024

FK 2024 3

Abstract of thesis presented to the Senate of Universiti Putra Malaysia in fulfilment of the requirement for the degree of Master of Science

PERFORMANCE IMPROVEMENT OF VAPOUR COMPRESSION REFRIGERANT SYSTEM USING GRAPHENE AND MULTI-WALLED CARBON NANOTUBE NANO-LUBRICANTS

By

VIRA CUT

July 2024

Chairman : Assoc. Prof. Abdul Aziz bin Hairuddin, PhD
Faculty : Engineering

The use of Vapour Compression Refrigerant (VCR) systems is very common in households and industries. Owing to the system's widespread utilisation, an analysis of the vapour compression refrigeration system's performance is required. Consequently, it has been discovered that the system's electricity consumption remained extremely high and that the output was incompatible with the input, which reduced its efficiency. To solve this issue, more research is needed to produce higher system performance, such as using nanoparticles as additional ingredients in pure compressor oil to yield higher performance. In the VCR systems, different results can be achieved depending on the type of nanoparticle selected and the concentration of the nano-lubricant. Among the nanoparticles with suitable characteristics are graphene and Multi-Walled Carbon Nanotubes (MWCNT). Therefore, this research aims to determine the optimal concentration of graphene and MWCNT in Polyolester (POE) oil and the impact of using nano-lubricants in the R134a system, such as reducing compressor work and exergy destructions, as well as improving the Coefficient of Performance (COP) system. The initial method was to characterise each graphene sample (0.1-0.3 g/L) and MWCNT (0.5-0.7 g/L) to eliminate the unstable concentrations. The characterization findings revealed that the three most optimal concentrations of each nano-lubricant are 0.1, 0.15, and 0.2 g/L for graphene and 0.5, 0.55, and 0.65 g/L for MWCNT nano-lubricant. The following step was to inject nano-lubricant into the compressor part. Among other graphene nano-lubricant concentrations, working with 0.2 g/L showed the highest reduction of compressor work and total exergy destruction, as well as improvement of $COP_{heating}$. The value of each parameter was 30%, 30%, and 16.94%, respectively. The same thing also happened in the system when using MWCNT nano-lubricant with 0.65 g/L as the most stable concentration compared to other concentrations. The value of each parameter was 39.33%, 40.42%, and 50.26%, respectively. By comparing the result, the best performance of VCR system was achieved by using 0.65 g/L MWCNT nano-lubricant. In conclusion, replacing pure POE oil with nano-lubricants indicated higher system performance by increasing the COP value, saving more energy in the compressor part and minimising energy loss in the system.

Keywords: Graphene, MWCNT, nano-lubricants, performance system, and VCR system.

SDG: GOAL 9: Industry, Innovation and Infrastructure

Abstrak tesis yang dikemukakan kepada Senat Universiti Putra Malaysia
sebagai memenuhi keperluan untuk ijazah Master Sains

PENINGKATAN PRESTASI SISTEM PENYEJUK MAMPATAN WAP MENGGUNAKAN PELINCIR NANO GRAFIN DAN NANOTIUB KARBON BERBILANG DINDING

Oleh

VIRA CUT

Julai 2024

Pengerusi : Prof. Madya. Abdul Aziz bin Hairuddin, PhD
Fakulti : Kejuruteraan

Penggunaan sistem Vapor Compression Refrigerant (VCR) adalah sangat biasa di dalam isi rumah dan industri. Disebabkan penggunaan sistem yang meluas, analisis prestasi sistem penyejuk mampatan wap diperlukan. Akibatnya, didapati bahawa penggunaan elektrik sistem kekal tinggi dan output tidak memadai dengan input, yang mengurangkan kecekapannya. Untuk menyelesaikan isu ini, lebih banyak penyelidikan diperlukan untuk menghasilkan prestasi sistem yang lebih tinggi, seperti menggunakan nanopartikel sebagai bahan tambahan dalam minyak pemampat tulen untuk menghasilkan prestasi yang lebih tinggi. Dalam sistem VCR, keputusan yang berbeza boleh dicapai bergantung pada jenis zarah nano yang dipilih dan kepekatan pelincir nano. Antara nanopartikel yang mempunyai ciri yang sesuai ialah grafin dan Nanotiub Karbon Berbilang Dinding (MWCNT). Oleh itu, penyelidikan ini bertujuan untuk menentukan kepekatan optimum grafin dan MWCNT dalam minyak Polyolester (POE) dan kesan penggunaan pelincir nano dalam sistem R134a, seperti mengurangkan kerja pemampat dan kemusnahan eksergi, serta meningkatkan Pekali Prestasi sistem (COP). Kaedah awal adalah untuk mencirikan setiap sampel grafin (0.1-0.3 g/L) dan MWCNT (0.5-0.7 g/L) untuk menghapuskan kepekatan yang tidak stabil. Penemuan pencirian mendedahkan bahawa tiga kepekatan paling optimum bagi setiap pelincir nano ialah 0.1, 0.15, dan 0.2 g/L untuk grafin dan 0.5, 0.55, dan 0.65 g/L untuk pelincir nano MWCNT. Langkah berikut ialah menyuntik pelincir nano ke dalam bahagian pemampat. Antara kepekatan pelincir nano grafin yang lain, bekerja dengan 0.2 g/L menunjukkan pengurangan tertinggi kerja pemampat dan jumlah pemusnahan eksergi, serta peningkatan COPheating. Nilai setiap parameter ialah 30%, 30%, dan 16.94%, masing-masing. Perkara yang sama juga berlaku dalam sistem apabila menggunakan pelincir nano MWCNT dengan 0.65 g/L sebagai kepekatan paling stabil berbanding kepekatan lain. Nilai setiap parameter ialah 39.33%, 40.42%, dan 50.26%, masing-masing. Dengan membandingkan kedua-dua kepekatan ini, prestasi terbaik sistem VCR dicapai dengan menggunakan pelincir nano 0.65 g/L MWCNT. Kesimpulannya, menggantikan minyak POE tulen dengan pelincir nano menunjukkan prestasi sistem yang lebih tinggi dengan meningkatkan nilai COP, menjimatkan lebih banyak tenaga dalam bahagian pemampat dan meminimumkan kehilangan tenaga dalam system.

Kata Kunci: Graphene, MWCNT, pelincir nano, sistem prestasi, dan sistem VCR.

SDG: MATLAMAT 9: Industri, Inovasi dan Infrastruktur

ACKNOWLEDGEMENTS

This endeavor would not have been possible without my family and my supervisors, Assoc. Prof. Dr. Abdul Aziz Hairuddin and Assoc. Prof. Ts. Dr. Norkhairunnisa Mazlan. Thank you for all forms of assistance that have been provided during this study. There are many things to learn while studying at Putra Malaysia University.

Additionally, I would like to extend my sincere thanks to Nuralyia Atieka Binti Noor Mahadi who has helped me a lot in this research. The success of this final project is due to the cooperation of both of us. I am very grateful that you have been my research partner during the last year I studied at University Putra Malaysia. Hopefully, we can continue to be friends even though this project is finished.

I would remiss in not mentioning all of my Indonesian friends who struggled together in Malaysia to complete this lecture. You all succeeded in convincing me to be able to finish this lecture on time. Hopefully, we can all meet again on another occasion with the highest achievements we have in the future.

This thesis was submitted to the Senate of Universiti Putra Malaysia and has been accepted as fulfilment of the requirement for the degree of Master of Science. The members of the Supervisory Committee were as follows:

Dr. Abdul Aziz bin Hairuddin
Associate Professor
Faculty of Engineering
Universiti Putra Malaysia
(Chairman)

Dr. Norkhairunnisa binti Mazlan
Associate Professor.Ts
Faculty of Engineering
Universiti Putra Malaysia
(Member)

____
ZALILAH MOHD SHARIFF, PhD
Professor and Dean
School of Graduate Studies
Universiti Putra Malaysia

Date: 7 November 2024

TABLE OF CONTENTS

LIST OF TABLES

LIST OF FIGURES

LIST OF ABBREVIATIONS

AKB	Alkyl Benzene
Al_2O_3	Aluminium oxide
CNT	Carbon Nanotubes
COF	Coefficient of Friction
COP	Coefficient of Performance
COP_{HP}	Coefficient of Performance Heat-Pump/ Heating
COP_{RE}	Coefficient of Performance Refrigerant-Effect/ Cooling
CTAB	Cetrimonium Bromide
DI	Deionized
rGO	Reduced Graphene Oxide
GWP	Global Warming Potential
HP	Heat Pump
HVAC-R	Heating, Ventilation, Air Conditioning and Refrigeration
LPG	Liquefied Petroleum Gas
MO	Mineral Oil
MWCNT	Multi-Walled Carbon Nanotubes
ODEA	Oleic acid Diethanolamide
ODP	Ozone layer Depletion
PAG	Polyalkylene Glycol
POE	Polyolester
PVE	Polyvinyl Ether
RE	Refrigerant Effect

SDBS	Sodium Dodecyl Benzene Sulfonate
SiO_2	Silicon dioxide
SP	Sepiolite
SWCNT	Single-Walled Carbon Nanotubes
TiO_2	Titanium dioxide
UV–vis	Ultraviolet-visible
VCR	Vapour Compression Refrigeration
ZnO	Zinc oxide
ZP	Zeta Potential

LIST OF SYMBOLS

c_w	Specific heat capacity of water (4.2 kJ/kg°C)	kJ/kg°C
COP	Coefficient of Performance	-
COP_{HP}	Coefficient of Performance heat-pump/ heating	-
COP_{RE}	Coefficient of Performance refrigerant-effect/ cooling	-
$\dot{E}x$	The flow rate of exergy	kJ/s
$\dot{E}x_{dest}$	Flow rate of exergy destructions	kJ/s
$\dot{E}x_{dest.comp}$	Flow rate of exergy destruction in compresor part	kJ/s
$\dot{E}x_{dest.condenser}$	Flow rate of exergy destruction in condenser part	kJ/s
$\dot{E}x_{dest.evap}$	Flow rate of exergy destruction in evaporator part	kJ/s
$\dot{E}x_{dest.exp.val}$	Flow rate of exergy destruction in expansion valve part	kJ/s
$\dot{E}x_1$	Flow rate of exergy destruction inlet compressor	kJ/s
$\dot{E}x_2$	Flow rate of exergy destruction outlet compressor	kJ/s
$\dot{E}x_3$	Flow rate of exergy destruction outlet condenser	kJ/s
$\dot{E}x_4$	Flow rate of exergy destruction outlet expansion valve	kJ/s
$\dot{E}x_5$	Flow rate of exergy destruction inlet water	kJ/s
$\dot{E}x_6$	Flow rate of exergy destruction outlet water	kJ/s
h_1	Specific enthalpy point 1	kJ/kg
h_2	Specific enthalpy point 2	kJ/kg
h_3	Specific enthalpy point 3	kJ/kg
h_4	Specific enthalpy point 4	kJ/kg
$\dot{m}_{ref}$	Mass flow rate refrigerant	kg/s

m_w	Mass of water	kg
$\dot{m}_w$	Mass flow rate of water	kg/s
P_{cond_inlet}	High pressure of the system at point 2	kPa
P_{cond_outlet}	High pressure of the system at point 3	kPa
P_0	The pressure in the dead state (101.325 kPa)	kJ/s
P_1	Compressor suction pressure	kPa
P_2	Compressor delivery pressure	kPa
P_3	Condenser outlet pressure	kPa
P_4	Evaporator inlet pressure	kPa
Q	The supplied or discharged heat by the system	kJ
Q_{cond}	The heat transferred from condenser	kJ
Q_{evap}	The heat absorbed by evaporator	kJ
$\dot{Q}_{cond}$	The rate of heat transferred from condenser	kJ/s
$\dot{Q}_{evap}$	The rate of heat absorbed by evaporator	kJ/s
Q_w	The heat energy of water	kJ
$\dot{Q}_w$	The rate of heat energy of water	kJ/s
s_1	Entropy point 1	kJ/kg.K
s_2	Entropy point 2	kJ/kg.K
s_3	Entropy point 3	kJ/kg.K
s_4	Entropy point 4	kJ/kg.K
T_{wi}	Water inlet temperature	°C
T_{wo}	Water outlet temperature	°C
T_0	The temperature in the dead state (25°C)	kPa

T_1	Compressor suction temperature	°C
T_2	Compressor delivery temperature	°C
T_3	Condenser outlet temperature	°C
T_4	Evaporator inlet temperature	°C
T_5	Water inlet temperature	°C
T_6	Water outlet temperature	°C
W	The required power by the system	kJ
W_{comp}	Compressor work	kJ
$\dot{W}_{comp}$	The rate of compressor work	kJ/s
$\dot{W}_{comp.EL}$	The flow rate of compressor input	kJ/s

CHAPTER 1

INTRODUCTION

1.1 Research Background

It has been years since researchers have paid more attention to environmental obstacles: energy insecurity, global warming and air pollution (Jacobson et al., 2022). Nowadays, the global temperature is getting higher, with readings that have broken the record rate every year (Bian, 2020). Based on data in the year 2021, the temperature of the global surface drastically increased to 1.12 °C, relative to the temperature in 1880, which was around 0.2 °C; this temperature has been predicted to set a new record in the future (Hansen et al., 2022). Hansen et al. (2023) mentioned that before 2030, global warming will reach a new peak at 1.5 °C and will continue to increase by 0.5 °C in 2050. According to Yıldırım et al. (2023), the Heating, Ventilation, Air Conditioning and Refrigeration (HVAC-R) system significantly contributes to greenhouse gas emissions. There are two types of emissions based on how they influence the environment: direct and indirect emissions. The Vapour Compression Refrigeration (VCR) system contributes as much as 80% of indirect emissions obtained from electricity used, equipment production, and materials and 20% of total greenhouse gases caused by refrigerant leaks (direct emissions) (Yıldırım et al., 2023). In addition, air conditioning units in domestic regions only consume around 15% of global electricity (She et al., 2018).

Kulkarni et al. (2023) reported that people worldwide have been using the VCR system as it serves residential areas and large industrial facilities. The four most important components of the system are the compressor, condenser, evaporator and expansion valve. The system can be employed in various applications such as refrigeration, freezer storage, air conditioning, cooling systems, as well as heating rooms and buildings, among others. Most of these applications only utilise an evaporator as a cold producer or a condenser as a heat producer. Besides the components, the refrigerant in the system has an essential role of helping to absorb the heat from the environment, then transfer it to other components and remove the heat from the components. Additionally, the compressor lubricant oil can contribute to the system's energy efficiency by decreasing its electricity usage. Therefore, a strategy for optimal performance from the VCR system relies on the selected refrigerant and compressor oil.

A vapour compression refrigeration system requires a working fluid (refrigerant) to produce cold or heat. Manoj Kumar et al. (2021) stated that working fluid can significantly affect the efficiency of a given system. However, it may be detrimental to the environment due to the potential for Ozone layer Depletion (ODP) and Global Warming Potential (GWP) (Husainy et al., 2018). In Canada (Montreal) and Japan (Kyoto), R12 and R123 have been stopped from being utilised in the HVAC-R system as they have a high value of GWP and ODP (Nair et al., 2020). Utilising eco-friendly materials, using less electricity and improving system efficiency, besides other measures, are necessary to immediately resolve this issue due to the detrimental environmental effects. Carefully considering and choosing environmentally friendly refrigerants (low GWP and ODP) can effectively reduce harmful emissions. For instance, R134a is a refrigerant used in industrial and residential areas. Many instruments today still use R134a owing to its zero potential for global warming, lower ODP and a class of non-flammable gases (Vaghela, 2017). Other than that, changing the energy sources from conventional to renewable and improving the performance system (efficiency) can help reduce emissions produced by VCR systems (Shakya et al., 2019; Yıldırım et al., 2023).

While greenhouse gases contribute to global warming, residual heat becomes the primary driver of this issue (Bian, 2020). Occasionally, the energy loss from waste heat has never been considered a significant issue, which partly happened because certain technologies, such as air conditioning for cooler production and water heaters for heater production, are only effective for one outcome. The combination of these two outcomes has been observed by researchers (Nikhil Babu et al., 2021). Furthermore, simultaneously employing heating and cooling enhances the value of this operation, optimises system performance and reduces gas emissions (Xu et al., 2021; Yaakop et al., 2023). Several studies have demonstrated a great potential to reduce electricity consumption and increase the efficiency of the system (Srithar et al., 2018; Vashisht & Rakshit, 2021; Nikhil Babu et al., 2021; Saxena & Tangellapalli, 2022).

Compared to other sectors, higher electricity usage is demanded in buildings, about 40% of the total energy consumption (Deymi-Dashtebayaz et al., 2022; Pinamonti & Baggio, 2020). Furthermore, from the percentage mentioned above, air conditioning consumes the largest proportion, representing 50% of the overall energy consumption (D. Liu et al., 2023). The reduction of energy electricity has a positive-remarkable impact on the high efficiency of the VCR system (Liu et al., 2023; Otsuka, 2023; Xia et al., 2023). Hence, keeping these aspects in the long-term relationship would make it possible to reduce greenhouse and the effects of global warming, thereby contributing to the improvement of environmental sustainability (D. Liu et al., 2023).

1.2 Problem Statement

Regarding the Vapour Compression Refrigeration (VCR) system, many experiments have been conducted by researchers over the years to improve its performance (Nandanwar et al., 2023; Patel et al., 2024; Senthilkumar et al., 2023). The high energy required for work input, the small amount of heat absorbed by the evaporator, and heat rejection by the condenser are the main problems by using the vapor compression refrigeration system. These will affect the coefficient of performance (COP), which generally assesses whether the system is more working efficiently or not. Many aspects can influence, such as refrigerant and compressor oil. Choosing an appropriate refrigerant for the compressor's working design is necessary, especially for long-term use. The value of GWP and ODP are the important parameter before selecting the refrigerant. Some studies also showed the alternative of environmentally unfriendly refrigerant or HVAC system (Kasi & Cheralathan, 2023; Kulkarni et al., 2023; Sarsam, 2024).

In addition to refrigerant selection, lubricant compressor oil is one part of the VCR system that can be modified namely by mixing it with nanoparticles and research has increased from year to year. The results obtained were also very amazing, such as the large reduction in work input on the compressor, increasing the energy absorbed by the evaporator and the energy released by the condenser (Bahman & Saleh, 2024; Ogbonnaya et al., 2023; Sakhir & Qaid, 2023). However, researchers are still looking for the most optimal type of nanoparticles to replace pure compressor oil because the types vary greatly, plus determining the right concentration and preparation method is also needed to achieve the most efficient VCR performance.

Most current experiments were conducted with metal oxide and metal hybrid nanoparticles (Chavhan et al., 2023; Dağıdır & Bilen, 2023; Sharif et al., 2022). While the outcomes of the previous experiment were noteworthy, carbon-based materials (graphene and carbon nanotubes) exhibited greater promise compared to metal, metal oxide and metal hybrid nanoparticles (Akhtar & Rajput, 2024; Hiralal & Ali, 2024; Madyira & Babarinde, 2024). The production process of nano-lubricants is also crucial since it determines the degree of nanoparticle separation within the lubricant and the period that the nanoparticles remain stable or well dispersed. Madyira et al. (2022) investigated the effects of three different concentrations of graphene/ Mineral Oil in R600a and discovered that the Coefficient of Performance Refrigerant-Effect (COP_{RE}) experienced more than 25% improvement and an approximate 18% reduction in pure lubricant oil energy consumption at a concentration of 0.2 g/L. With the same lubricant oil and mass of R600a refrigerant, Babarinde et al. (2020) conducted a study with multi-walled carbon-nanotube (MWCNT), showing that the highest concentration, 0.6 g/L, had improved COP_{RE} to around 23.8% and the minimum required energy consumption of around 12.42% reduction compressor work. From both studies above, using the right concentrations can have a great impact on the performance system, with lower concentrations of graphene lubricant and higher concentrations of MWCNT lubricant.

Therefore, in this study, the selection of refrigerants with low Global Warming Potential (GWP) and Ozone layer Depletion (ODP) value categories, carbon-based nanoparticles were chosen as materials dissolved in pure compressor oil with various value ranges. This is done so that this study provides different results than past studies that can be applied in the long term because it is more environmentally friendly and produces an enhanced level of performance.

1.3 Objectives

The general objective of this study is to improve the Vapour Compression Refrigeration (VCR) system through graphene and Multi-walled Carbon Nanotube (MWCNT) nano-lubricants. The specific objectives to achieve the main aim are:

i. To investigate the stability of graphene and MWCNT in Polyolester oil (POE) lubricant oil.
ii. To determine the power consumption, coefficient of performance (COP), and exergy analysis for graphene and MWCNT nano-lubricants.

1.4 Hyphothesis

The hypothesis is raised in this experiment and investigated using graphene and Multi-walled Carbon Nanotube (MWCNT) nano-lubricant.

Ho: Both nano-lubricants Graphene/ Cetrimonium Bromide (CTAB) and MWCNT have higher system efficiency than pure lubricant oil. Having more concentrations of graphene and MWCNT nano-lubricant would reduce the required work input, thus optimising the performance of the system.

1.5 Scope of Study

i. Experimenting with a mechanical heat pump (VCR system), a multi-functional air conditioner integrated with water heaters.

ii. Using carbon-based nanoparticles (Graphene and Multi-walled Carbon Nanotube) and POE oil as lubricant in the R134a system. Cetrimonium Bromide (CTAB), as a surfactant, has a contribution to graphene nano-lubricant.

iii. The concentrations of graphene nano-lubricants are 0.1-0.3 g/L and Multi-walled Carbon Nanotube (MWCNT) nano-lubricants are 0.5-0.7 g/L. These numbers were chosen because of the performance of previous experimental results where for graphene it was 0.2 g/L and for MWCNT it was 0.6 g/L.

iv. Testing on room temperature at T = 25 ^oC (298.15 K) and pressure at P= 101.325 kPa (1 atm) in the laboratory for avoiding external factor such as change of temperature and pressure.

v. The water flow rate integrated with the condenser remained at 4 g/s to obtain the maximum difference between temperature water input and output.

1.6 Thesis Outline

The thesis research proposal consists of five main chapters supported by sub chapters for further explanation.

1. Chapter 1 explains the research background, problem statement, objectives, and scope of the research.

2. Chapter 2 reviews the previous related research and compares them to show the results of experiments. The main theory is supported by other theories from the experimental results of other studies. This chapter aids in obtaining a more in-depth explanation, theoretically and practically, for the following process: experimental work.

3. Chapter 3 is concerned with experimental work design. Research materials and procedures are listed in this chapter. The process of selecting nanoparticles and the preparation process into nano-lubricant oil is clearly explained. Before using it in the system, monitoring the quality of each material used will help produce the expected experimental results.

4. Chapter 4 discusses and evaluates all collected experimental data. All the data obtained are used in the appropriate formulas so that the value of Coefficient of Performance (COP), compressor work, and refrigerant effect can be obtained from each experiment for a particular time.

5. Chapter 5 is the last chapter of the research proposal, containing the conclusion of the evaluation work and the recommendations for further research.

CHAPTER 2

LITERATURE REVIEW

2.1 Overview

Vapour compression refrigeration systems are the most prevalent methods embraced around the world. Nevertheless, the development of this system continues to attract researchers' attention. Various innovations have been made to improve this system's performance, including the replacement of pure lubricant oil in the refrigerant system with nano-lubricant oil. Among the many nanoparticles, carbon-based (graphene and multi-walled carbon nanotubes) are among the most promising in overcoming researchers' concerns about the long-term use of refrigeration systems, such as the high energy required and deficient system performance. This chapter presents previous related studies revealing the extent of nanoparticles mixed with compressor oil in refrigerant systems, primarily using graphene and Multi-Walled Carbon Nanotubes (MWCNT). Previous research tended to use other nanoparticles with various types of lubricant oil available and according to the compressor used (Sakhir & Qaid, 2023; Senthilkumar et al., 2021; Senthilkumar et al., 2023; Senthilkumar et al., 2021; Subhedar et al., 2022). As this chapter explains the factors influencing the performance of the refrigerant system, such as the type of nanoparticles, concentrations and nano-lubricant preparation techniques, theoretical and research bases are discussed before being considered for further research so that the results are expected to be much better than the previous.

2.2 Vapour Compression Refrigeration System

The Vapour Compression Refrigeration system (VCR) is the most widely used refrigerant cycle in commercial and industrial sectors (Alrwashdeh & Ammari, 2019) for electronics cooling, cold storage and heat storage (Kutlu et al., 2019; Liang et al., 2019; Yan et al., 2019). Due to its high usage in various places, such as office buildings, homes and factories, the VCR system consumes at least 15% of electricity globally and 10% of greenhouse gas emissions (She et al., 2018). In this experiment, the VCR system would be assumed as the Ideal Vapour Compression Refrigeration system

2.2.1 Component and Ideal Vapour Compression Refrigeration System

The single-stage VCR system's four main components are the compressor, condenser, expansion valve and evaporator (Poachaiyapoom et al., 2019). Each component has the important role of making the refrigerant in the system flow evenly, starting from the compressor to evaporator and back to the compressor.

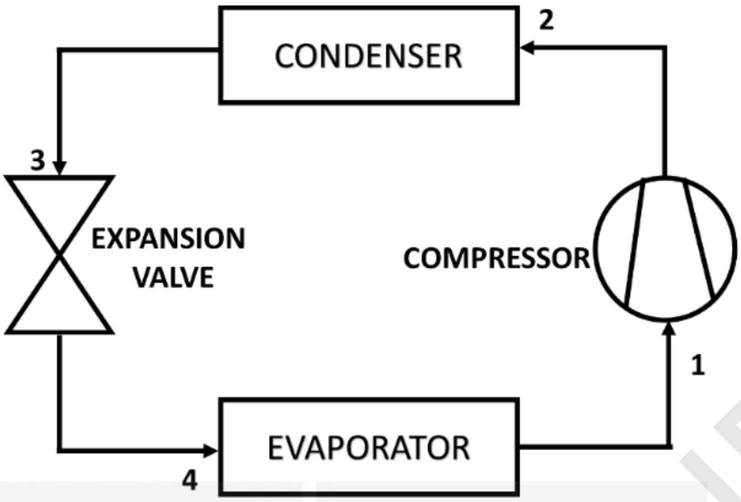

Figure 2.1 : Schematic of Single-stage Vapor Compression Refrigeration System (Source : V. Kumar et al., 2020)

Generally, the ideal VCR system utilises the work of a compressor as a tool for compressing refrigerants to allow refrigerant cycles. When the refrigerant is under pressure, it enters the suction side of the compressor and is discharged under high pressure at the exhaust side of the compressor. This pressure difference allows the refrigerant to flow from one component to another, eventually forming a refrigerant cycle. In the refrigerant cycle, four basic processes or changes are involved in the state of the refrigerant (Duarte et al., 2017), which are illustrated in detail in Figure 2.2, with all the following equations (Malwe et al., 2022):

(a)

(b)

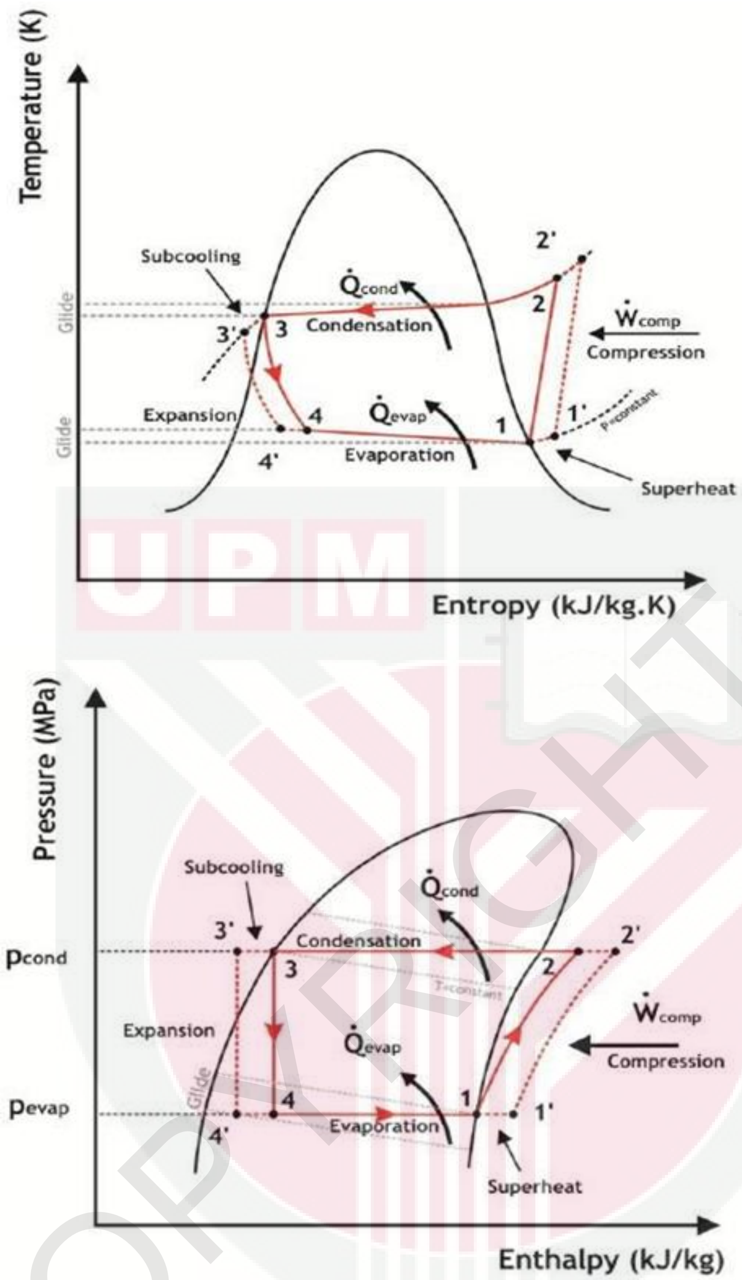

Figure 2.2 : Vapour Compression Refrigeration cycle (a) T-s diagram (b) P-h diagram

The four stages of processes are explained below**:**

1. Compression Process (Point 1-2)

Point 1: Low pressure and low temperature.

Point 2: High pressure and high temperature.

This process is known as compression, where energy is used to compress the saturated gas into high-pressure steam for increasing the temperature and enthalpy (Wu et al., 2021). The results of the compression process are superheated refrigerant. The amount of energy required ($\dot{W}_{comp}$) to perform the compression process is:

$$\dot{W}_{comp} = \dot{m_{ref}}(h_2 - h_1) \quad (2.1)$$

where:

$\dot{W}_{comp}$ = Compressor work (kJ/s)

$\dot{m_{ref}}$ = Mass flow rate refrigerant (kg/s)

h_1, h_2 = Specific enthalpy (kJ/kg)

2. Condensation Process (Point 2-3)

Point 2: High pressure and high temperature.

Point 3: High pressure and sub-cooled temperature.

This process is known as condensation, whereby heat must be discharged into the environment to change the refrigerant phase from superheated vapour to saturated liquid. An electrical fan is required to facilitate this cooling performance process (Fukuchi, Yoshitake, & Yokota, 2019). The amount of heat discharged is:

$$\dot{Q}_{cond} = \dot{m_{ref}}(h_3 - h_2) \quad (2.2)$$

where:

$\dot{Q}_{cond}$ = The heat transferred from condenser (kJ/s)

h_2, h_3 = Specific enthalpy (kJ/kg)

In this process, water is used as a medium for dissipating heat from the condenser. The presence of additional media, like water, can aid the heat-releasing process more efficiently. One of the benefits that can be obtained is water heating by integrating the water pipe into the condenser pipe. When the flowing water optimally absorbs the heat produced by the condenser, it is necessary to isolate the pipe. Apart from water, fans are also among the tools used to help release heat into the environment. However, the perceived benefit only increases environmental temperature and does not provide other benefits (Sonawan et al., 2018).

As mentioned above, water is a heat absorption medium that has many applications. Several studies have been carried out, including that by Yıldız et al. (2022), which used continuous flowing water. Other researchers have also opted to incorporate a condenser within a water tank. For instance, Dai and Li (2018) conducted their experiment by placing the condenser coil in an 80-litre-sized water tank without insulation. Their experiment showed the relation between dissipation energy (Equation 2.2) and heat-absorbed water, as shown in Equation 2.3.

$$Q_w = m_w c_w \left(T_{wo} - T_{wi}\right) \quad (2.3)$$

where:

Q_w = The heat energy of water (kJ)

m_w = Mass of water (kg)

c_w = Specific heat capacity of water (kJ/kg°C) (4.2 kJ/kg°C)

T_{wo} = Water outlet temperature (°C)

T_{wi} = Water inlet temperature (°C)

To determine the amount of energy absorbed by water, Equation 2.3 was applied. However, should the water flow continuously, the formula changes, as shown in Equation 2.4.

$$\dot{Q}_w = \dot{m}_w c_w (T_{wo} - T_{wi}) \quad (2.4)$$

where:

$\dot{Q}_w$ = The heat energy of water (kJ/s)

$\dot{m}_w$= Mass flow rate of water (kg/s)

$$\dot{Q}_{condenser} = \dot{Q}_{water} \quad (2.5)$$

$$\dot{m_{ref}} (h_3 - h_2) = \dot{m}_w c_w (T_{wo} - T_{wi}) \quad (2.6)$$

The heat transfer rate of water is equal to the condenser if there is no heat loss to the environment. Therefore, it is essential to isolate the condenser coil to avoid it. The magnitude of heat loss can be calculated as in Equation. 2.7.

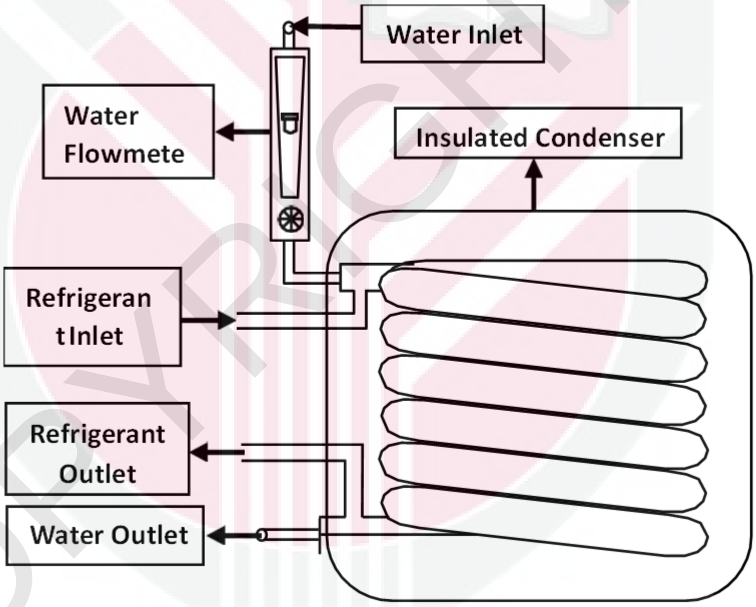

Figure 2.3 : Schematic of the used flowing water in the condenser

3. Expansion Process (Point 3-4)

Point 3: High pressure and sub-cooled temperature.

Point 4: Low pressure and low temperature.

This process is known as the irreversible limiting process. Expansion is a process of decreasing temperature and pressure, ideally assumed not to involve heat transfer. The decrease in temperature is expected to make the final temperature of this process below ambient temperature. If that is not the case, then heat absorption cannot occur in the evaporator. Apart from that, a phase change process also occurs, from saturated liquid to saturated mixture, with no absorption or release of heat. Thus, the enthalpy is assumed to be constant (Megdouli et al., 2017).

$$h_4 = h_3 \tag{2.8}$$

4. Vapourising Process (Point 4-1)

Point 4: Low pressure and low temperature.

Point 1: Low pressure and low temperature.

This process absorbs heat and changes the mixture's phase into a saturated vapour. The absorption of environmental heat by the system can produce a cooling process. Under ideal cycle conditions, this process is isothermal and isobaric. The amount of heat absorbed is:

$$\dot{Q}_{evap} = \dot{m_{ref}}(h_4 - h_1) \tag{2.9}$$

where:

$\dot{Q}_{evap}$ = The heat absorbed by evaporator (kJ/s)

h_4 = Specific enthalpy (mixture) (kJ/kg)

2.2.2 Parameters Performance of VCR system

The coefficient of performance (COP) shows the efficiency of heating and cooling machines. The ratio of heat dissipation and electrical power intake defines the value of COP. In general, the formula for COP is as in Equation. 2.10.

$$COP = \frac{Q}{W} \tag{2.10}$$

where:

COP = Coefficient of Performance

Q = The supplied or discharged heat by the system

W = The required power by the system

Generally, the COP is divided into two formulas, namely the cooling coefficient of performance (COP_{RE}) (Ozsipahi et al., 2022; Senthilkumar et al., 2023) and the heating coefficient of performance (COP_{HP}) (Jing et al., 2023; Sánta, 2022). It depends on the component to be investigated, as in Equation 2.11 and 2.12. In addition, there is the relation between the COP_{RE} and COP_{HP} (Kaygusuz, 2017) as in Equation 2.13.

$$COP_{HP} = \frac{Q_{cond}}{W_{comp}} = \frac{Heating\ Effect}{Work\ Input} \tag{2.11}$$

$$COP_{RE} = \frac{Q_{evap}}{W_{comp}} = \frac{Cooling\ Effect}{Work\ Input} \tag{2.12}$$

$$COP_{HP} = 1 + COP_{RE} \tag{2.13}$$

2.2.3 Working Fluids in the VCR system

Known as a refrigerant, working fluid is a substance used in the heat cycle to transfer heat from one component to another. R134a, chemically known as 1,1,1,2- Tetrafluoroethane (CF3CH2F), is the most common and widely used refrigerant in the sector, such as commercial refrigeration, industrial refrigeration, air-conditioning chillers and mobile air-conditioning (Kasaeian et al., 2018). One of the advantages is that R134a is a non-flammable gas (Vaghela, 2017). Other characteristics of R134a are shown in Table 2.1.

Table 2.1 : Characteristics of R134a refrigerant

Normal boiling point	-26
Critical temperature [°C]	101
Critical pressure [kPa]	4059
Liquid density at 25 °C [kg/m^3]	1207
Vapor density at 25 °C [kg/m^3]	32.37
ODP (Ozon Depleting Potential)	0
GWP (Global Warming Potential)	1370
Atmospheric lifetime [years]	13.4
ASHRAE 34-Safety code	A1

(Source : de Paula, Duarte, Rocha, de Oliveira, & Maia, 2020; Li, Jiang, Chen, & Liang, 2019; Ohunakin et al., 2018)

Table 2.1 presents various characteristics of R134a, a widely used refrigerant in various applications. However, it has a Global Warming Potential (GWP) value of 1370, leading researchers to explore and analyse its alternatives. For example, Sánchez et al. (2017) studied alternatives to R134a, such as R290 and R600a. In another study, Kandhaswamy et al. (2017) concluded that the mixture of R290/R600a could be a feasible alternative to R134a in the VCR system. Moreover, Devecioğlu and Oruç (2018) tested R1234ze(E) and found a lower GWP value and a comparable COP value.

The GWP value of refrigerant should be considered; however, other values or characteristics should also be reviewed, such as Ozone layer Depletion (ODP) and level of flammability refrigerant. Most of these working fluids belong to category A2L or A3, the ASHRAE 34-Safety code that can potentially create an ozone layer. A2L is a milder flammability refrigerant, while A3 is a higher flammability refrigerant (Colbourne et al., 2020; Kim & Sunderland, 2021).

Ozair Arshad et al. (2021) investigated the effect of a performance vapour compression refrigeration system using three different refrigerants, namely R12, R22 and R134a. The result revealed that the COP was higher while working with R12 and R22. However, the characteristics of both refrigerants were high regarding global warming and ozone depletion potential, as mentioned in Table 2.2.

Table 2.2 : Comparison of GWP and ODP among refrigerants

Type of Refrigerant	GWP	ODP
R12	8500	1
R22	1700	0.055
R134a	1300	0

(Source: Kulkarni et al., 2023)

Another result obtained by Raviram et al. (2020) indicated that compared to R22 and R410a, the system with R134a and R290 could reduce the compressor energy consumption by around 24%, although the COP improved by almost 40%. Hence, employing eco-friendly refrigerants can be safer in the long term, and the system's performance can be enhanced by other methods, such as replacing the pure compressor oil or installing new equipment (integrated water pipeline in the condenser).

2.3 Impact nano-lubricants in VCR system

Most of the research on vapour compression refrigeration systems aims to enhance the refrigeration effect and reduce the compressor work. Improving the absorbed heat in the evaporator and minimising work in the compressor automatically has been seen to increase the heat dissipated to other mediums, including air and water. Meanwhile, replacing the pure lubricant oil compressor with the nano-lubricant oil effectively was observed to improve the system without changes to the main components. However, the result of each experiment revealed different improvements in Coefficient of Performance refrigerant-effect (COP_{RE}), Coefficient of Performance heat-pump (COP_{HP}), compressor work, heat-absorbed evaporator (RE) and heat-dissipated condenser (HP). Refrigerant, type of lubricant oil and nanoparticles (size, shape, concentrations, and more) are the factors for determining the experiment results.

- **R134A / POE**

In the R134a system, many lubricant oils can be used as compressor oil, such as Polyolester (POE), Polyalkylene Glycol (PAG) and Mineral Oil (MO). Each lubricant oil has its special characterisations, with values that need to be considered before mixing with the selected nanoparticles and substituting the conventional one in the VCR system. The recent experiment nanoparticle was conducted by Zawawi et al. (2024) with different concentrations of TiO2-SiO2/POE nano-lubricants. Among 0.01, 0.03, 0.05, 0.07 and 0.1 vol%, the most optimal concentration was 0.03 vol% in terms of enhancement of Qcond (42.46%), Qevap (50%) and COP_{HP} (23.39%), while in work input, the compressor worked more than pure one and still showing a minimum increment compared to other concentrations. The researchers assumed that internal factors such as pumping force, heat production, and energy loss can influence the compressor work.

Another experiment by Akhtar and Rajput (2023) investigated the MWCNT/POE with different concentrations (0- 1 g/L, with interval 0.2). The most significant improvement in the performance of R134a was while working with 0.8 g/L concentration, caused by the decreasing compressor work by around 21.46% and the increase of $COP_{cooling}$ and cooling capacity of 40.09% and 11.40%, respectively. Meanwhile, Zawawi et al. (2023) tested the SiO_2/POE lubricant on hybrid electric vehicle air-conditioning. Their findings revealed a $COP_{cooling}$ value of 3.36 with 0.01 vol%, which improved by 53.8% from pure POE oil. These significant results marked the potential of mixing nanoparticles in lubricating oil for optimal system performance.

Previous research has shown that mixing nanoparticles in POE oil has good results applied in R134a. However, researchers continue to vary various types of additional materials to give the VCR system the best performance. For instance, Akkaya et al. (2023) mixed two lubricant oil ingredients as the basis for the nano-lubricant solution with rod-shaped sepiolite in POE oil. The nanoparticles chosen were carbon-based, namely Carbon Black, reduced Graphene Oxide (rGO) and MWCNT. The $COP_{cooling}$ of the R134a-test rig has even increased by 10.7% after adding Sepiolite (SP) to pure POE oil. The addition of nanoparticles made the system performance much more efficient. When compared with pure POE oil, the increase in COP was 16.7%, 23.6% and

18.73%. So, it can be concluded that POE/SP-rGO lubricant is the most optimal type of lubricant oil over other types of carbon lubricant and pure POE/SP.

- **R134A/ PAG**

Apart from POE oil, Polyalkylene Glycol (PAG) oil is a type of lubricant oil that can be used in compressors on the R134a system. Anwar and Randa (2020) observed Al2O3 nano-lubricant in the vapour compression refrigeration test rig with various concentrations. Compared to others, 0.3 wt% was the excellent concentration due to the highest coefficient of the performance system. However, the required work of the compressor also increased by nearly 50% at the same time. Even so, the outcome (refrigerant effect) of the system still resulted in more than twice that of pure MO and other samples, which was about 910.4 kJ/s.

- **R600A/MO**

The high GWP value of R134a encouraged researchers to look for alternative refrigerants. In VCR systems, r600a is an option frequently used to replace R134a. This is supported by the low GWP value of the refrigerant, namely zero potential. However, in terms of level of flammability, R600a is classified as a flammable refrigerant. Babarinde and Madyira (2023) observed the effect of vapour compression system performance after using pure R134a, pure R600a and adding nanoparticles in R600a. After substituting R134a/POE, the enhancement of the performance system was 10.53% higher using R600a/MO. In detail, adding TiO_2, Al_2O_3, and SiO_2 in R600a/MO caused the COP value to get higher, which were around 2.8, 2.4 and 2.7, subsequently.

Another investigation on the metal oxide group was conducted by Chavhan et al. (2023). In their study, three different concentrations of CuO/MO were employed: namely 0.02, 0.04 and 0.06 wt%. The presence of CuO in this nano-lubricant caused heat transfer to increase due to its high thermal conductivity and surface area. More specifically, the value increased with the presence of more nanoparticles in the base oil. From the supporting nanoparticles properties, the maximum enhancement of COP became 0.06 wt%, which was approximately 30.32% higher than that obtained by pure MO. The following other predominant parameters obviously were presented, such as the effortless compressor working and the pull-down time, which was 12.53% and 20.2%.

Different from previous research, Madyira et al. (2022) studied the impact of using 0.2, 0.4 and 0.6 g/L graphene lubricant. The most significant effect of the performance system in terms of reducing the work input, increasing the $COP_{cooling}$ and cooling capacity, and the lowest evaporation temperature occurred at 0.2 g/L, which was the lowest concentration. The values were 19.36%, 38%, 8.5% and -10 °C, respectively. The researcher also explained that the decrease in work on the compressor was caused by the presence of graphene in the compressor oil, which reduced friction and resulted in low temperatures in the evaporation process.

Utilising hybrid nanoparticles also yielded the greatest potential to enhance the VCR system. Senthilkumar et al., (2023) combined MWCNT and TiO_2 in mineral oil to prepare the 0.2 and 0.4 g/L solution. The lowest COP was 2.5 by pure mineral oil result, whereas adding 0.4 g/L improved the COP by 40%. However, the lack of this research was that there was no experiment and data for the COP value for each of the MWCNT and TiO2 lubricants separately to be compared with the hybrid lubricant.

Babarinde et al. (2021), in their research, tested the effect of replacing mineral oil in 60g-R600a performance with MWCNT as an addictive nanoparticle with different concentrations. The COP value increased to 2.9 while working with the most optimal and highest concentration, which was 0.6 g/L. This value was also compared with the pure MO lubricant result, showing a lower value of 38%.

- **LPG/MO**

In a comparison study with graphene/MO in R600a, the same concentrations of graphene/MO were tested in 50g-Liquefied Petroleum Gas (LPG) as a refrigerant in the system (Babarinde et al., 2021). Working with different types of refrigerants, the most reliable concentrations remained 0.2 g/L graphene/MO. In 60g-R600a, most of the performance parameters displayed remarkable improvement. Nonetheless, changing the refrigerant increased the efficiency of the system, which was roughly -20% in compressor work, 47.8% in $COP_{cooling}$, 19.75% in cooling capacity and -55% in low evaporator temperature (from -9 °C to -14 °C).

- **R32/ PVE**

R32 is an environmentally friendly refrigerant owing to its lower GWP compared to R134a. However, this refrigerant is mildly flammable. Azmi et al. (2024) worked with Polyvinyl Ether (PVE) as a suitable lubricant oil for R32-system and SiO_2-TiO_2 as hybrid nanoparticles. Even though research using PVE as base oil is still very rare compared to POE and MO lubricant, the value of system performance was able to increase by 39.3% using 0.005 vol% compared to results without spreading nanoparticles in lubricant oil. The increase in system performance was apparently supported by tribological nano-lubricants, like the friction effect. The low value of the coefficient of friction (COF) indicates a smaller friction loss in the compressor, which can make the work required by the system become lower.

2.4 Nanoparticles

Nanoparticles are one of the materials that are gaining popularity among researchers owing to the impact of their use in increasing higher outcome values. One example is as an addictive ingredient in base lubricant oil for refrigerant systems. To produce optimal and efficient performance in the system, nanoparticles with high thermal conductivity values are needed. Most nanoparticles that fall into the carbon category have high conductivity values.
Based on the explanation in the previous subsection, graphene and MWCNT are promising nanoparticles as they belong to the carbon group and have higher thermal conductivity compared to other nanoparticles.

2.4.1 Graphene

Graphene is a form of carbon comprising a single layer of sp2-bonded carbon atoms densely arranged in a honeycomb lattice (Le Ba et al., 2020). Many researchers are attracted to graphene by its unique characteristics, such as higher thermal conductivity (up to 5300 W/mK), small size of particle, easy synthesis, more extended suspension stability, larger surface area, high surface energy, high surface activity, lower erosion, and lower demand for pumping power (Le Ba et al., 2020; Yang et al., 2020). Therefore, graphene and its derivatives or composites have great potential for developing innovative high-performance materials (Yu et al., 2017). Besides, graphene is one of the most robust materials owing to its electrical conductivity, tensile strength, relative transparency, impermeability to some gases and liquids, as well as superior thermal and optical properties (Phiri etal., 2017; Silva et al. 2020). Some applications of graphene include electronics, energy storage, water purification, biomedical applications, biosensors, elemental storage, plasmonic, lubricant, radio wave absorption, nanoantenna and sound transducers (Obodo et al., 2019; Rudrapati, 2020).

2.4.2 Multi-walled Carbon Nanotube (MWCNT)

Several advantages of using carbon nanotubes (CNT) are high surface area, high thermal and electrical conductivity, large aspect ratios, as well as high mechanical strength (Venkataraman et al., 2019). There are two types of CNTs: Single-walled carbon nanotubes (SWCNT) and multi-walled carbon nanotubes (MWCNT) (Kinloch et al., 2018). The difference between the two members of the CNT group is the number of layer carbons. SWCNT has one carbon atom layer, while MWCNT consists of several layers of graphene sheets (Che Abdullah & Albert, 2019). Since CNT has a cylindrically shaped material, it comes in various lengths and diameters, which adjust according to the application. This material also plays a role in transistors, electronic devices, sensors, and biomedical applications (Jagadeesan et al., 2020).

2.4.3 Thermal Conductivity

The value of thermal conductivity depicts the ability of a material to transfer heat. Thermal conductivity is the most considered parameter in heat transfer applications, among several other thermophysical properties (Ahmadi et al., 2018). In general, thermal conductivity is related to the concentration of fluids and the temperature. However, the values are sometimes linear as they depend on the nature of nanoparticles and the employed base fluid (Yarmand et al., 2016). In a review by Pavía et al. (2021), relative to some nanoparticles such as copper, carbon monoxide, copper(II) oxide, titanium oxide, aluminium oxide, iron(III) oxide, CNT, graphene, graphene oxide, reduced graphene oxide (rGO), and some base fluids (water and ethylene glycol), Graphene and CNT, which is part of carbon-based nanoparticles, has the highest value of thermal conductivity of around 5000 and 3000 W/m.K, respectively.

Sanukrishna et al. (2019) analysed the result of the minimum concentration of graphene/PAG oil for about 0.05 vol%, which had the highest thermal conductivity of 0.167 W/m-K at 15 °K. Employing different base fluids (POE and mineral oil), Joshi et al. (2022) introduced the reduced-graphene nanoparticles in their experiments. By using all different concentrations of samples (pure, 0.02, 0.05 and 0.1 wt%), the value of thermal conductivity significantly increased from 1 W/m-K (pure) to 2.45 W/m-K (0.1 wt%) in mineral oil based. In addition, for POE nano-lubricants, the thermal conductivity value increased from the pure-oil result of approximately 0.8 W/m-K to around 2 W/m-K. Following an experiment with the same lubricant oil, Joshi et al. (2023) reported that embedding the highest concentration in their work, which is 0.09 wt% of graphene-nanoplatelets nano-lubricant, showed an improvement in thermal conductivity of around 51.8% (POE oil) and 40.7% (mineral oil). The addition of MWCNT in POE showed an increment in thermal conductivity value of about 29.75% from 0.121 to 0.157 W/m-K while working with 1 g/L.

Increasing the concentration of Al_2O_3, SiO_2, and ZrO_2 causes the thermal conductivity and Coefficient of Performance(COP) values in the VCR system to become higher (Santhana Krishnan et al., 2018) as the evenly distributed nanoparticles in the lubricating oil cause a large amount of heat transfer in the surface area. As the heat transfer increases, the process of absorption and discharge of heat becomes more optimal, which is the reason why the thermal conductivity of nano-lubricants must be of high value.

2.5 Preparation of nano-lubricant

Preparing nanofluids is the first stage before injecting them into the compressor. Generally, there are two methods to produce nanofluid: the one-step method and the two-step method (Yang et al., 2020). The one-step method is a procedure that mixes the production of nanoparticles and synthesises the nanofluids simultaneously (Kong, Sun, & Bao, 2017). The advantages of this step are that no drying process is required, and agglomeration can be minimised (Kaggwa & Carson, 2019; Sezer, Atieh, & Koç, 2019). However, the drawbacks of the single-step technique are that it is infeasible on an industrial scale, has a high production cost, and limits the control of used particle size. The two-step method initially begins with producing nano-powder by chemical or physical methods, followed by mixing the nano-powder with base fluids to form mixed solutions (Sanjeevi & Loganathan, 2020). This method is beneficial as it is feasible on the industrial scale, has low-cost production, and is mainly used for non-metallic (Kaggwa & Carson, 2019; Sezer et al., 2019).

Ismail et al. (2023) prepared three different types of nano-lubricants, namely TiO_2, SiO_2 and mixed TiO_2-SiO_2, with various times of ultrasonication. TiO2/PVE sonicated for 7 hours possessed the most outstanding stability of all monitored-30-day samples in their work, while other samples showed thick sedimentation. Senthilkumar et al. (2021) tested 0.4 g/L and 0.6 g/L ZnO-SiO_2/POE nano-lubricant in different masses of the R600a-VCR system. Their experimental results showed that using higher concentrations helped the system performance significantly. However, the details of preparation were not mentioned by the researchers. Meanwhile, Ekundayo and Babarinde (2019) employed the same method for preparing TiO_2 nano-lubricant, with 5 hours of sonification and magnetic stirring process to produce 0.2, 0.4 and 0.6 g/L samples. Sharif et al. (2022) prepared Al_2O_3/PAG and SiO_2/PAG nano-lubricants using an ultrasonication bath for two hours. This sonication time was chosen to prevent the sample from overheating in the bath, which would cause the temperature to rise and the volume of water in the bath to decrease from the initial sonication process. All the details of each experiment mentioned above are summarised in Table 2.3.

Table 2.3 : Summary of the previous experiment of preparation of nano-lubricant

No.	Nano-lubricants	Preparations	Details of Preparations	Researchers
1.	TiO_2/PVE/0.01 vol%, SiO_2/PVE/1 vol%, and TiO_2-SiO_2/PVE/0.01 vol%	Two-step method	Magnetic stirrer 60mins + Ultrasonic vibrator 7h	Ismail et al. (2023)
2.	ZnO- SiO_2/ POE/0.6 g/L	Two-step method	Magnetic stirrer + Ultrasonic bath	Senthilkumar et al. (2021)
3.	TiO_2/MO/0.4 g/L	Two-step method	Ultrasonic 5h + magnetic stirrer	Ekundayo and Babarinde (2019)
4.	SiO_2/ POE/0.6 g/L	Two-step method	Mixing	Senthilkumar and Anderson (2021)
5.	Al_2O_3/PAG and SiO_2/PAG	Two-step method	Ultrasonic bath for 2h	Sharif et al. (2022)

2.5.1 Preparation of Graphene nano-lubricant

Babarinde et al. (2020) prepared the graphene nano-lubricant with three different concentrations using a magnetic stirrer for 45 minutes, followed by homogenising for 3 hours. Their result showed that adding 0.2 g/L gave the most optimal concentration compared to unfilled mineral oil. The improvement of Coefficient of Performance (COP) also exhibited variation due to testing with different quantities of R600a, with the highest recorded outcome being 52% at a mass of 60 grams. Babarinde et al. (2021) conducted an experiment involving Liquefied Petroleum Gas (LPG) with varying masses but similar concentrations. Upon observation, it was discovered that the system performance was most impressive while utilising a concentration of 0.2 g/L despite being created using an ultrasonicator for only 2 hours. The graphene in mineral oil was dispersed ultrasonically at 25 °C in the water bath to avoid the excessive overheating of the samples (Yang et al., 2020). However, before mixing all materials, this solution was separately added with nine surfactants (Tween20, Tween60, Tween85, Span20, Span40, Span80, Span85, Oleic acid Diethanolamide (ODEA) and KH570) to obtain excellent stability of nano-lubricant. After 20 days, it was revealed that graphene nano-lubricant with Span-85 was the only solution with good dispersion and minimum sedimentation.

Based on the experiments mentioned earlier, most graphenes have been mixed with mineral oil as a solvent. However, other experiments also used Polyolester (POE) oil as a lubricant oil. The reduced-graphene/POE nano lubricants were synthesised by probe-sonication for 70 minutes without any surfactants, and the samples remained stable after two days (Joshi et al., 2022). Their experiment highlighted that higher concentrations will gradually increase thermal conductivity and viscosity value. Among other less-concentrated samples, the 0.1 wt% sample had the highest thermal conductivity value, which was 2 W/mK. In Joshi et al. (2023) research, the highest thermal conductivity value was obtained using 0.09 wt%, which was the highest concentration, with a value of only 1.5625 W/mK.

The surfactant significantly affects the graphene/POE oil nano-lubricant in the same way as in mineral oil. Other types of surfactants mixed with the graphene/POE nano-lubricant can decrease the potential of possessing sedimentation (Al-Janabi, Hussin, & Abdullah, 2021). In Al-Janabi et al. (2021) experiment, Sodium Dodecyl Benzene Sulfonate (SDBS), Cetrimonium

Bromide (CTAB) and Span-80 were selected as surfactants (ratio 1:1) in 0.1 vol% of nano-lubricant. The result indicated that mixing graphene with CTAB made the solution highly concentrated, followed by no surfactant, while using the other SDBS and Span-80 speeded up the deposition process as theirs are anionic and non-ionic surfactants, respectively. Saufi and Mamat (2022) observed the same surfactants (SDBS, CTAB and Span-80) with two different machines in sample preparation, which were magnetic and overhead stirrer. Based on the visual observation, the result confirmed that CTAB mixed well with both stirrer types, and the SDBS can also be an alternative surfactant only if using the overhead stirrer.

In the investigation carried out by Al-Janabi et al. (2022), more trials were conducted using different ratios, specifically 1:1, 1:2, 1:4 and 1:8, of nanoparticles to CTAB surfactant in mineral oil. Their research study observed that an excessive amount of CTAB led to the formation of micelles (lipid bilayers) on the surface of graphene. This layer hindered the dissolution of the nanoparticles, as depicted in Figure 2.4. After preparation, the samples were tested for zeta potential analysis. The result demonstrated that all samples were between -46.3 and -50.3 mV, representing good stability. However, after monitoring for 14 days, samples with 1:4 and 1:8 ratios had thick sedimentation at the bottom of the layer surface. Another stability test was conducted to determine the best-suited ratio for graphene nano-lubricant, namely Ultraviolet-visible (UV–vis) spectrum. The graphene with CTAB 1:1 had the highest absorbance value even after 14 days of preparation. This result is essential for further experimentation with graphene nano lubricant. All details of each experiment mentioned above are summarised in Table 2.4.

Table 2.4 : Summary of the previous experiment for preparing graphene nano-lubricant.

No.	Lubricant Oil	Concentrations	Preparations	Researchers
1.	Mineral Oil	0.2, 0.4, and 0.6 g/L	Magnetic stirring 45mins + Ultrasonic homogeniser 3h	(T. Babarinde et al., 2020)
2.	Mineral Oil	0.2, 0.4, and 0.6 g/L	Magnetic stirring + Ultrasonic homogeniser	Babarinde et al. (2021)
3.	Mineral Oil/ Span-85	10, 20, and 30 mg/L	Ultrasonic bath 2h	Yang et al. (2020)
4.	POE Oil	0.02, 0.05, 0.1 wt%	Ultrasonic probe homogeniser 70mins	Joshi et al. (2022)
5.	POE Oil	0.03, 0.06, and 0.09 wt%	Ultrasonic probe homogeniser 65mins	Joshi et al. (2023)
6.	SUNISO SL68 (POE)/ CTAB	0.1 vol%	Magnetic stirring 20mins /1250 rpm + Ultrasonic probe homogeniser 30mins	(Al-Janabi et al., 2021)
7.	SUNISO SL68 (POE)/ CTAB	0.1 vol%	Magnetic stirring 20mins/ 1250 rpm + Ultrasonic probe homogeniser 30mins	Al-Janabi et al. (2022)
8.	POE Oil/ CTAB	0.05 vol%	M1 (Magnetic Stirrer 10mins/1000rpm + Sonication 30mins) and Method 2(Overhead Stirrer 10mins/1000rpm + Sonication 30mins)	Saufi and Mamat (2022)

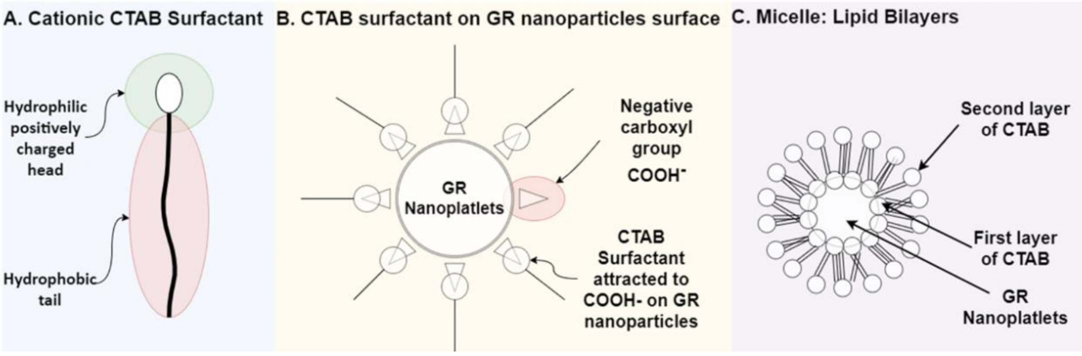

Figure 2.4 : The attachment CTAB and graphene nanoparticle procedure (Source: Al-Janabi et al., 2022).

2.5.2 Preparation of MWCNT nano-lubricant

In recent years, researchers have focused more on carbon-based nanoparticles, graphene and carbon nanotubes (CNTs). Mineral oil (MO) is one of the most common lubricants mixed with nanoparticles. Babarinde et al. (2021) used a magnetic stirrer, followed by a sonicator for 3 hours in total duration at temperatures around 15-20 °C to produce 0.2, 0.4, 0.6 g/L of MWCNT/MO nano-lubricant. Before this experiment, Babarinde et al. (2020) utilised the same nano lubricant and concentrations with the aid of a magnetic stirrer for 45 minutes and a sonicator for 3 hours. Even though it was carried out using different methods, 0.6 g/L nano-lubricant was still the most optimal concentration in the VCR system.

Choi et al. (2021) reported that mixing MWCNT and POE oil in a sonication bath for 5 hours obtained a stable nano lubricant for about 72 hours. With a similar unit of concentration (wt%), Salem (2020) performed the preparation of 0.1, 0.2, 0.3, 0.4 and 0.5 wt% using an agitator bath for 36 hours for four consecutive days, followed by an ultrasonic vibrator for the next 6 hours at room temperature and finally vibrator again for 3 hours at different temperature with SDBS as surfactant. Akhtar and Rajput (2023) conducted a preparation procedure using several concentrations, including 0.2, 0.4, 0.6, 0.8 and 1 g/L. Even after 72 hours, the two highest concentrations remained uniformly dispersed. Nevertheless, the system worked most efficiently with 0.8 g/L in terms of COP, energy consumption and cooling capacity.

The role of surfactant for some nano lubricants is important to create a homogenous solution. Al-Janabi et al. (2021) proved that in MWCNT nano lubricant, the optimal result of stabilisation testing is with CTAB in visual inspection. However, the solution without surfactants showed better results in zeta potential value results. To validate the result, Al-Janabi et al. (2022) confirmed that after 60 days, the higher ratio of CTAB in MWCNT nano lubricant visually indicated its concentrated solution. However, after testing with a zeta analyser, the highest zeta potential value was without CTAB as a surfactant.

Table 2.5 : Summary of the previous experiment for preparing MWCNT nano-lubricant.

No.	Lubricant Oil	Concentrations	Preparations	Researchers
1.	Mineral Oil (MO)	0.2, 0.4, and 0.6 g/L	Magnetic stirring and Ultrasonicator (total process = 3 h)	Babarinde et al. (2021)
2.	Mineral Oil (MO)	0.4 and 0.6 g/L	Magnetic stirring 45 mins and Ultrasonicator 3 h	Babarinde et al. (2020)
3.	POE Oil	0.1 wt%	Ultrasonic bath 5 h	Choi et al. (2021)
4.	POE Oil/ SDBS	0.1-0.5 wt% (with interval 0.1 wt%)	Agitator bath 36 h/ 3450 rpm + Ultrasonic vibrator 6 h (room temp.) + Ultrasonic vibrator 3 h (at 85 °C)	Salem (2020b)
5.	POE Oil	0.2 - 1 g/L (with interval 0.2 g/L)	Magnetic stirring 2 h/ 1500 rpm + Ultrasonic bath 60 mins	Akhtar & Rajput (2023)
6.	SUNISO SL68 (POE Oil) / CTAB	0.1 vol%	Magnetic stirring 20 mins/ 1250 rpm + Ultrasonic probe homogeniser 30 mins	Al-Janabi et al. (2021)
7.	SUNISO SL68 (POE Oil) / CTAB	0.1 vol%	Magnetic stirring 20 mins/ 1250 rpm + Ultrasonic probe homogeniser 30 mins	Al-Janabi et al. (2022)

2.6 Stability test of Nano-lubricant Methods

The most challenging part of having a homogeneous solution is using nano lubricants in the refrigerant system. One of the nanoparticles' characteristics is that they tend to form agglomeration and affect the quality of the nano lubricant (Said, Rahman, Sohail, & B s, 2023). The role of nanoparticles' type, lubricant oil, surfactants, concentrations and preparation methods significantly influence nano-lubricant stability. As a result, stability testing is required to demonstrate the quality of the dispersed nanoparticles in the solution to avoid pipeline blockages and inefficient use of nanoparticles in the compressor part. There are three standard stability tests: visual inspection, zeta potential analyser and Ultraviolet-visible (UV-vis) Spectrophotometry.

2.6.1 Visual Inspection

The visual observation test is the simplest and most cost-effective way to identify whether deposits are in a solution for a particular time. However, this method is also time-consuming (Azman & Samion, 2019). Most investigations of graphene samples were carried out briefly due to their high tendency to form agglomeration. This can be seen in the research of Al-Janabi and Hussin (2020), where it was proved that even after 24 hours of preparation, sediment was present in the bottom layer of the sample bottles, and the investigation was carried out over the next 13 days. Al-Janabi et al. (2021) observed all graphene nano-lubricants with different surfactants in 10 days. While with all MWCNT nano-lubricant samples, there was no significant difference observed after being monitored for 60 days, and the sedimentation slowly appeared in specific samples alone. Al-Janabi et al. (2022) then conducted an experiment where graphene samples were examined using a specific ratio of CTAB over 14 days. They observed substantial sediment formation at the bottom of the surface samples. However, all MWCNT samples were relatively stable in 60 days. A noteworthy discovery was made by Choi et al. (2021) in their research of a brief analysis of MWCNT that only lasted 72 hours using samples of high concentrations.

Sharif et al. (2022) found that for up to 6 months, SiO_2/PAG samples were stable in all concentrations (0.01, 0.03 and 0.05 vol%). However, Al_2O_3/PAG was the only sample consisting of 0.05 vol% with a better dispersion solution. Ismail et al. (2023) effectively identified notable distinctions in various time-sonifications of TiO_2/PVE, SiO_2/PVE and TiO_2-SiO_2/PVE by collecting data for 30 days. Each sample exhibited substantial sedimentation and the presence of white spots, indicating agglomeration. The biggest size was observed in the sample that was not sonicated, whereas the smallest size was observed after 7 hours of sonication. In the same vein, Jatinder et al. (2019) also monitored the white spots in TiO_2/MO samples for 30 days. Even though no clear appearance of white spots was noted, the colour of each solution became less concentrated. The final result of their experiment showed that the most concentrated solution was 0.6 g/L sample, while other concentrations, 0.2 and 0.4 g/L sample, started to create sedimentation.

2.6.2 Zeta Potential Analysis

Zeta potential (ZP) is a parameter employed to determine the nanoparticle's surface charge in a colloidal solution. The higher the value of zeta potential magnitude (positive or negative), the more stable the nano-lubricant (Al-Janabi & Hussin, 2020; Thachnatharen, Khalid, Arulraj, & Sridewi, 2021), as shown in Table 2.6.

Table 2.6 : Zeta Potential Characteristics

Stability Characteristics	Range value of Zeta Potential (mV)
Fast coagulation or flocculation	0 to ±5
Incipient instability	±5 to ±30
Moderate Stability	±30 to ±40
Good Stability	±40 to ±60
Excellent Stability	More than ±60

Many nanoparticles were investigated in the form of nano lubricants. One of the common lubricants is POE oil, which acts as a solvent. Zawawi et al. (2023) obtained excellent stability of SiO_2 nano-lubricant, which was 102.5 mV. Before being tested, the samples were prepared by magnetic stirring for 30 minutes and continued by the sonication process for 3 hours. According to Al-Janabi et al. (2021), the use of various types of surfactants has a significant impact on the appearance of a sample condition, and the results of the experimental investigation were demonstrated by conducting zeta potential testing to ensure the quality of each sample.

The use of CTAB in graphene/POE nano-lubricant (0.1 vol%) caused the solution to become more stable (-49.4 mV), followed by no surfactant at -47.3 mV. In contrast, the zeta potential value for the mixture of MWCNT and POE oil was -45.5 mV, while adding surfactants of CTAB, SDBS or Span-80 decreased the quality of the nano-lubricant. Besides the types of surfactant, its quantity also brings about the quality of nano-lubricants; thus, determining the ratio between surfactant and nanoparticles becomes fundamental. Al-Janabi et al. (2022) proved that the result of zeta potential was it their study was slightly different but still in the good stability category (> 40mV) after testing different ratios of CTAB in graphene/POE. In MWCNT/POE nano lubricant, having no surfactant was the best option (ZP value = 45.5 mV) to replace the pure POE oil in the refrigerant system.

2.6.3 Ultraviolet-Visible Spectrophotometry Analysis

Ultraviolet-visible (UV-vis) spectrometry is an effective method to evaluate the stability of nanofluid by emitting light of varying wavelengths through a solution and measuring the absorbance at each wavelength (Mohd Zaki et al., 2017). Aljuwayhel et al. (2023) promptly analysed the stability of nanodiamond/POE samples after preparation with the range of 200-800 nm wavelength. In the process of UV-vis measurement, not all the light can be absorbed (passed through) by nano lubricant, which is the definition of transmittance. In contrast, the amount of light that can be absorbed is considered absorbance (Nugroho et al., 2021a). Therefore, there are two primary factors influencing the UV-vis result: preferring the highest absorbance at its range of wavelength or choosing the absorbance peak at the shortest wavelength (Ahmad et al., 2020). This is because a higher absorbance level (axis-y) with the peak of wavelength can show excellent dispersion of nanoparticles in the base oil (Awang et al., 2019).

Nugroho et al. (2021) selected 278 nm as the reference wavelength to represent the UV-vis result for Al_2O_3 nano lubricant samples, as the highest absorbance value for each sample was 278 nm. The researchers also showed that the different methods of preparation samples have a significant impact on UV-vis results. After 13 hours of preparing SiO2/POE nano lubricant with magnetic stirring for an hour and sonification for 12 hours, it was displayed that the most stable concentration was 0.2 wt%. It is because the result of UV tended to remain consistent for six days, even when there was a slight decline, which was from 0.893 a.u. day-1 to 0.768 a.u. day-6 at 216.99 nm (Narayanasarma & Kuzhiveli, 2019). Al-Janabi et al. (2022) revealed that the result of UV-vis using a 1:1 ratio for CTAB and graphene has the highest absorbance in three different periods (after preparation, after 7-day preparation and after 14-day preparation). At the same time, the authors also observed that UV-vis data for MWCNT nano-lubricant showed that all the peak absorptions were at 350 nm wavelength and continued to decrease as time went by with higher wavelengths.

2.7 Summary

According to the findings of past research, several parts still need to be developed. In general, when conducting research on Vapour Compressor Refrigerant (VCR) systems, the researchers seek to optimize the system's performance using various methods. Based on prior study, many of them only concentrate on one aspect that they aim to improve, such as condenser performance, evaporator performance, or compressor work reduction only. The approaches used to improve the VCR system differ widely. In general, this involves changing the materials or modifying the system, each of which brings particular challenges in improving the performance of this VCR system.

More details, replacing pure compressor oil is an innovation that is currently being developed. One way is to add nanoparticles to the pure oil. This research is very limited because most researchers employ selected nanoparticles, such as metal and metal oxide nanoparticles in their studies, therefore knowledge on the utilization of carbon-based nanoparticles is currently restricted. However, carbon-based research is now becoming more widely available. Aside from the type of nanoparticle, one of the project's challenges is determining the appropriate concentration. Because past studies have shown that having a high concentration level in a solution is not a stable result, it can cause sediments to form in the solution. Adding surfactant is one approach to address this issue. The amount of surfactant that wishes to dissolve with the nano-lubricants should also be considered. As previously stated, the presence of surfactant actually has the possibility of reducing the action of the nanoparticles themselves in the solution.

Aside from the components, establishing the preparation methods for this nano-lubricant is critical. This is due to the lack of a consistent mechanism for dissolving nanoparticles in liquid. Examples include the tools utilized and the duration of each process. Thus, in this study, graphene and MWCNT will be combined in Polyolester (POE) oil using the method specified to produce various concentration samples before being tested on the VCR system.

CHAPTER 3

RESEARCH METHODOLOGY

3.1 Overview

Chapter 3 will explain in detail the performance carried out to obtain the material being tested, the implementation process on the test rig system, and the processing of the data obtained to determine the resulting changes, starting with a flowchart that briefly describes the work system of the process of carrying out this study. In this experiment, the mechanical heat pump was chosen as the medium for applying nano-lubricant. The location of each main component is explained through pictures taken from several sides. Not only that, the location of each sensor at the data collection point (temperature and pressure) and the refrigerant's flow are also clearly displayed on the schematic test rig system. Moreover, each specification for the materials and tools used in this research is attached. The process of taking and researching samples to experiment with nano-lubricant in actual amounts is explained to facilitate understanding in working with nano-lubricant. The processing of data obtained from each sensor is carried out by calculating the related formula so that the parameters of the system performance can be displayed in the next chapter for more details.

3.2 Flowchart of Experiment

This project started with determining the right materials and concentration to use. This was the first step because of the many types of nanoparticles and concentrations available and makes it possible to replace pure compressor oil in Vapour Compression Refrigeration (VCR) systems. After selecting the type of nanoparticle and the desired concentration range, the nano-lubricants is prepared in sample form first. This was conducted to avoid redundant nano-lubricants in full size form. The next step was stability testing, which starts with a visual inspection first. If at least three of the five available samples were concentrated or had some sedimentation, additional stability tests, such as zeta potential and Ultraviolet-visible (UV-visible) spectrometry, should be performed to corroborate the visual inspection's stability results. If not, it was important to identify new nanoparticles, surfactants, compressor oil, and/or concentrations. If already selecting the three optimal samples, the replacement on pure compressor oil at three different concentrations of the two types of nano-lubricants accessible in the VCR system. Any data collected from temperature, pressure, and compressor meters would be utilised to assess the system's performance, including energy consumption, coefficient of performance, and exergy analysis. All of the experiment's findings were examined and analysed in order to determine the appropriate concentration of each nano-lubricant in the system.

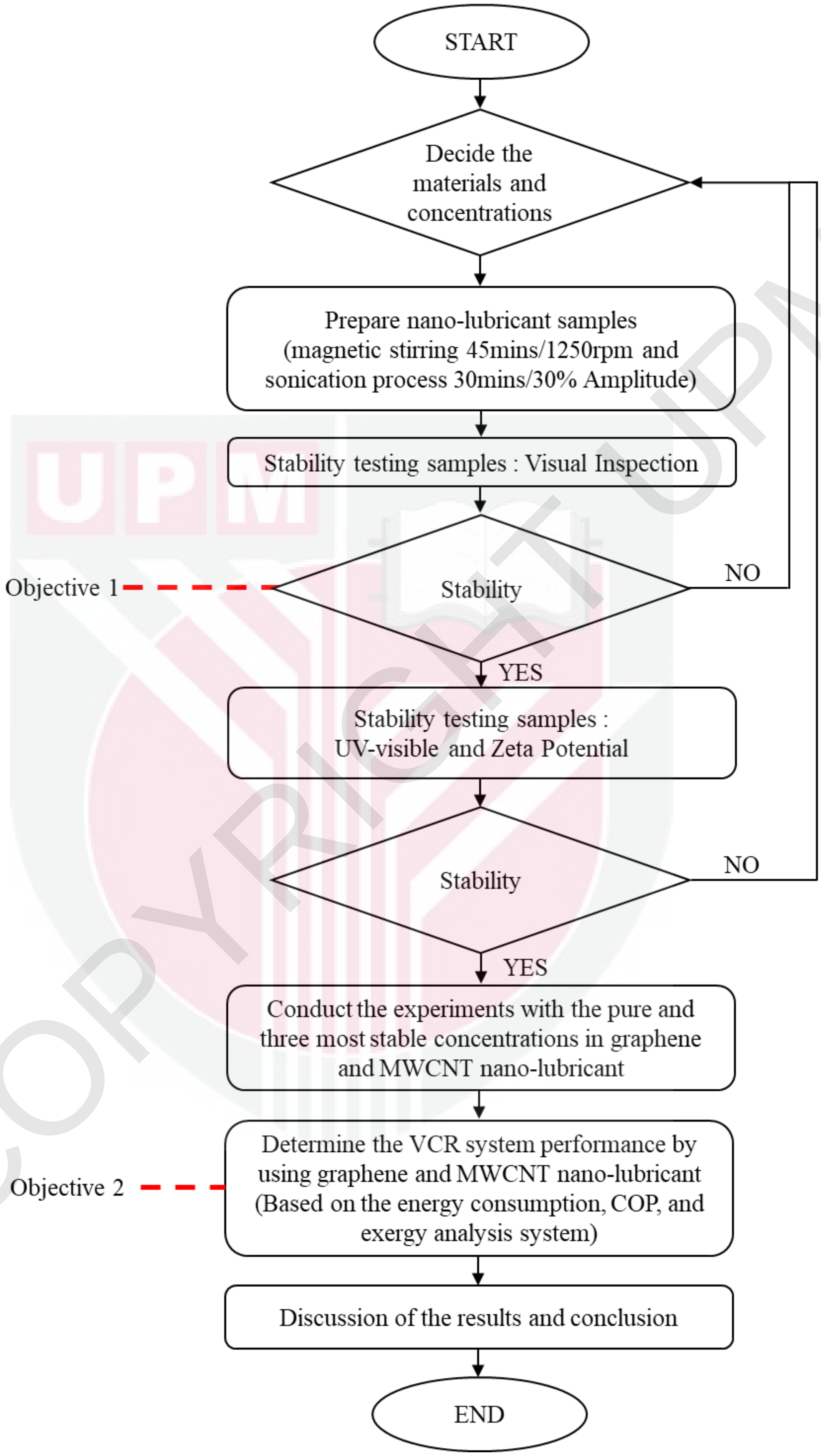

Figure 3.1 : Flowchart of project experiments pure oil, graphene and MWCNT nano-lubricant

3.3 Selection materials of nano-lubricants

There are several types of nanoparticles that already replaced the pure compressor oil in VCR system. However, based on the previous experiment by other researchers and the promising characteristics, the carbon-based nanoparticles, such as graphene and Multi-Walled Carbon Nanotubes (MWCNT) nano-lubricants helped the system worked efficiently (Akhtar & Rajput, 2024; Bibi Cassim, Aziz Hairuddin, & Vira, 2024; Senthilkumar et al., 2023).

Al-Janabi et al., (2021) showed that the mixing of graphene in Polyolester (POE) oil was better by adding the surfactant, namely CTAB with the ration 1:1. However, MWCNT nano-lubricants was possible to mixed without any surfactants. The selecting of type compressor oil also based on the characteristic of compressor itself to avoid the performance of compressor.

Based on the previous experiments of T. O. Babarinde et al., (2020), the reliable concentration to having the best Coefficient of Performance (COP) was using 0.6g/L instead of 0.4 g/L. From this previous result, in this experiment, the concentrations of MWCNT were 0.5, 0.55, 0.6, 0.65, 0.7 g/L. T. Babarinde et al., 2020) presented that compare to 0.4, and 0.6 g/L, by having lower concentration of graphene, namely 0.2 g/L had the better performance in VCR system. Therefore, in this experiment, the variety of graphene concentrations were 0.1, 0.15, 0.2, 0.25, and 0.3 g/L. The different of concentrations nano-lubricants from the previous experiment should be selected to have the chance of better result performance of the system itself.

3.3.1 Nanoparticles

Graphene and carbon nanotubes were two types of carbon nanoparticles in this experimental work. The colour of the resulting nano-lubricant was dark grey, which was similar to the colour of the raw material seen in Figure 3.2. The initial masses provided for graphene and MWCNT were 1.5 and 3 grams, respectively. To prevent sample failure, including the solution containing sediment quickly, this weight was greater than that utilised in the subsequent preparation step. Therefore, this amount was divided according to the previously determined concentration.

Figure 3.2 : The powder of graphene and carbon nanotubes

In addition, the information for each product is attached in Table 3.2 for graphene and Table 3.3 for carbon nanotubes. A high purity value is significant as it can lessen the potential that the nanoparticles include impurities, imperfections, or unwanted byproducts. Aside from that, carbon is the primary component of this substance since these two nanoparticles are members of the carbon group. Not less significant are the raw material's size and form, as these will influence the chosen method of processing. Furthermore, the dispersion process in the solution is significantly influenced by the layer on the nanoparticles. Table 3.3 illustrates that graphene is a multilayered substance, which contributes to its strength and difficulty in separating its layers.

Table 3.1 : The graphene product information

Form	Pure powder
Size	< 10 µm
Purity	> 98%
Graphite carbon	100%
Consist of	20-40 layered
Colour	Dark Grey
Manufactured by	Btcorp Generique Nano Private Ltd

Table 3.2 : The carbon nanotubes product information

Type	MWCNT
Form	Pure powder
Size	20 nm/ 10 µm
Purity	> 99%
Carbon	100%
Colour	Dark Grey
Manufactured by	Btcorp Generique Nano Private Ltd

3.3.2 Base Lubricant Oil

Based on the specifications of the compressor used, the lubricant oil selected was POE oil, with its specification shown in Table 3.4. Apart from using lubricant oil that was suitable for the type of compressor, POE oil brand EMKARATE 32H had many advantages in accordance with the temperature range required in the research (Dağıdır & Bilen, 2023). The value of the viscosity index is 121, which means that the lubricant can reliably carry out its lubricating function over an extensive temperature range. Another important parameter is the pour point temperature level, which is -46 ^{o}C. This value is related to lubricant fluidity; by having a lower temperature, the capability of lubricant to flow smoothly becomes unstable. However, in this test rig, the lower temperature (inlet evaporator) is around -5 ^{o}C, which is higher than the pour point temperature. Moreover, there is a flash point as an indication of the highest tolerated temperature in lubricant oil. In the used VCR system, the highest temperature will be reached in the condenser (inlet and outlet point), and the estimated value is below 100 ^{o}C. It means that overall, the lubricant is operating under standard conditions, and this type of POE oil is the ideal lubricant for the R134a system.

Table 3.3 : The lubricant oil product information

Type Oil	POE oil
Product	Emkarate RL 32H
Viscosity (at 40 ^{o}C) (cSt)	32.5
Viscosity (at 100 ^{o}C) (cSt)	5.8
Viscosity Index	121
Pour point (Celcius)	-46
Density (at 20 ^{o}C) (g/ml)	0.977
Flash Point (Celsius)	258
Water Content (ppm)	< 40
Acid value (mg KOH/g)	0.02
Hydroxyl Value (mg KOH/g)	< 4.5
Colour (Hazen)	60
Miscibility 10% lube in R134a (Celsius)	-42

Figure 3.3 : Used Synthetic Polyol-Ester (POE) as lubricant oil and Base oil in Nano-lubricant.

3.4 Preparation of nano-lubricants

Two steps were involved in obtaining the optimal concentration of nano-lubricant. The first step was the preparation to produce samples nano-lubricants for all concentrations. The next method was to test the stability of each concentration. In this step, three tests were–carried out to obtain the most optimal concentration before replacing the pure oil in the VCR system.

All the samples and full-size form of each nano-lubricant were prepared with 45 minutes of magnetic stirring with 1250 rpm and 30 minutes of sonication process. This method was chosen based on the previous method preparations, such as magnetic stirring for 45 minutes from (T. Babarinde et al., 2020) experiment, 1250 rpm and sonication duration time from (Al-Janabi et al., 2021, 2022) experiments.

3.4.1 Step One (Preparation of samples nano-lubricants)

a. Material Lists:

- 5 different masses of graphene (10,15, 20, 25 and 30 mg)
- 5 different masses of graphene (50, 55, 60, 65 and 70 mg)
- One litre of POE oil
- 30 thirty-millilitre clear glass vials
  - Plastic spoon
  - 150 ml of the sized beakers
  - Magnetic Stirring machine
  - Ultrasonic Probe machine

b. Procedure:

1. Poured 100 ml of POE oil into the beaker.
2. Took 10 mg of graphene with a dry plastic spoon (for example, 0.1 g/L concentration).
3. Placed the measured graphene in the same beaker.
4. Put the stirrer bar in the beaker of oil and nanoparticles.
5. Placed the beaker on top and centre of the stir plate machine.
6. Turned it on for 45 minutes.
7. After the stirring process, placed the beaker in the ultrasonic probe machine.
8. Turned it on for 30 minutes.
9. Split into three vials, 30 ml nano-lubricant to each labelled vial.
10. Repeated steps 1-10 four more times for the same nanoparticles with other concentrations.

11. Repeated steps 1-11 one more time for carbon nanotube (CNT) withthe respective concentrations.

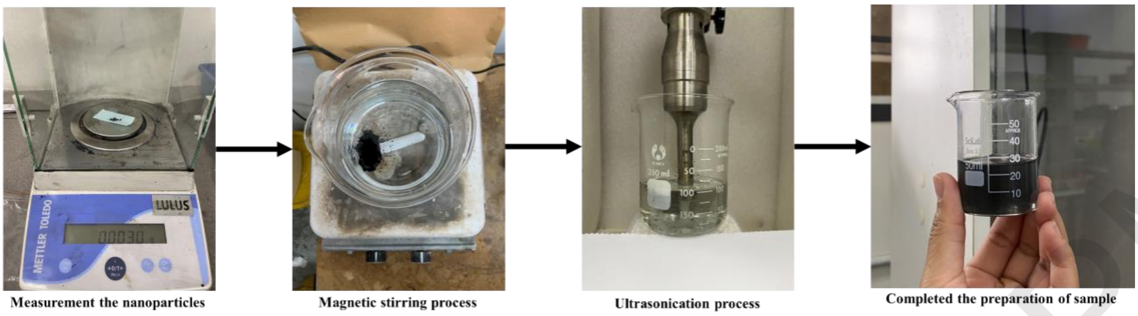

Figure 3.4 : The process of sample preparation

3.4.2 Step Two (Stability test of nano-lubricant samples)

Each type of nanoparticle had five different concentrations. For graphene, the concentrations were 0.1, 0.15, 0.2, 0.25 and 0.3 g/L. Meanwhile, for another nanoparticle, MWCNT, the concentrations were 0.5, 0.55, 0.6, 0.65 and 0.7 g/L. All samples were around 30 ml and were tested to obtain the most optimal concentration based on their stability. The first test was visual observation. The minimum day of monitoring the sample was seven days. After that, the three most stable samples were selected for the next stability testing. However, if the appearance of the sample is similar to the initial condition, the inspection can be extended to a maximum 6-month period. If more than that, the Ultraviolet-visible (UV-vis) testing needs to be done to select the three optimal samples.

The following stability tests were zeta potential and UV-vis spectrophotometry, which were carried out to ensure that the samples to replace the conventional lubricant oil have good stability and can reduce the possibility of blocking the system. After accomplishing all stability tests, the full size of each concentration of graphene and MWCNT can be produced to test in the VCR system.

3.4.2.1 Visual Inspection test

This test is conducted for at least seven days by regularly monitoring all samples of nano-lubricant. If there is no sedimentation, the visual testing is extended until the sedimentation is found.

a. Material Lists:

- Differently labelled sample vials of graphene nano-lubricant
- Differently labelled sample vials of carbon nanotubes nano-lubricant

b. Procedure :

First, placed all vials on the flat table in static conditions and ensure that no significant ambient temperature changes were observed. All the samples should be placed and captured in the first condition after preparation. If there was no sediment, monitor the ten vials for the next 24 hours. Next, capture the condition of all samples to identify the condition of each sample. If there was no sediment, monitor the vials for the next two days. Similarly, captured the conditions for all samples. If there was no significant sedimentation, monitored for the next few days to see the different conditions of each sample.

3.4.2.2 Zeta Potential Testing

a. Material Lists:

- 5 differently labelled sample vials of graphene nano-lubricant
- 5 differently labelled sample vials of carbon nanotubes nano-lubricant
  - The pipette dropper
  - 100 ml of deionised water

- 150 ml of the sized beaker
- Folded capillary zeta cell
- Zeta analyser machine

Figure 3.5 : Malvern Zeta Analyser Machine

b. Procedure :

First, cleaned the folded capillary zeta tube and the pipette dropper with Deionized (DI) water. Next, poured the DI water from the zeta tube into the beaker. Then, repeated steps 1-2 two more times to clean from any residue. After that, took a certain millilitre of the nano-lubricant sample with apipette dropper. Inserted the pipette tip into one of two open ports of the zeta tube. Dropped the sample until the zeta tube was full and ensure no bubbles. Then, plugged two ports with the plastic plugs and insert the zeta tube into the machine. Opened and read the desired information on the appropriate software. Finally, repeated steps 1-8 nine more times for each different concentration sample of nano-lubricant.

3.4.2.3 Ultraviolet-visible spectrophotometry

a. Material Lists:

- 5 differently labelled sample vials of graphene nano-lubricant
- 5 differently labelled sample vials of carbon nanotubes nano-lubricant
   - 5 cuvettes (two opposite transparent and two opposite opaque sides)
   - 5 pipette droppers
   - 100 ml of deionised water
   - 150 ml of the sized beaker
   - Sheets of tissue
   - UV-vis spectrophotometer machine

Figure 3.6 : Biomate 3s UV-vis testing machine

c. Procedure :

First, cleaned the cuvettes and the pipette droppers with DI water. Then, poured the DI water from the cuvettes into the beaker. Repeated steps 1-2 two more times to clean from any residue. After that, uptook a certain millilitre for each concentration of nano-lubricant with a different pipette dropper. Dropped the sample into the cuvettes until complete enough and wipe the cuvette sides with tissue (no fingerprint on sides). The next step was to properly insert the cuvettes into the machine. Opened and read the desired information on the appropriate software. Finally, repeated steps 1-8 one more time for each different concentration of carbon nanotube nano-lubricant.

3.5 Components specifications of the system

The mechanical heat pump is one of the vapour compression refrigeration cycle's applications. In this study, all experiments were carried out on a mechanical heat pump, and the data were read manually. It can be seen in Fig 3.2, there are four main components on the test rig, namely compressor, insulated condenser, expansion valve and evaporator. All connecting pipes between components are isolated to reduce the energy wasted while the engine is running. In the condenser part, the water pipe is integrated into the condenser pipe and insulated so that all heat transfer from the condenser is similar to that absorbed by water.

Figure 3.7 : Top view of mechanical heat pump R514

Figure 3.8 : Front view of mechanical heat pump R514

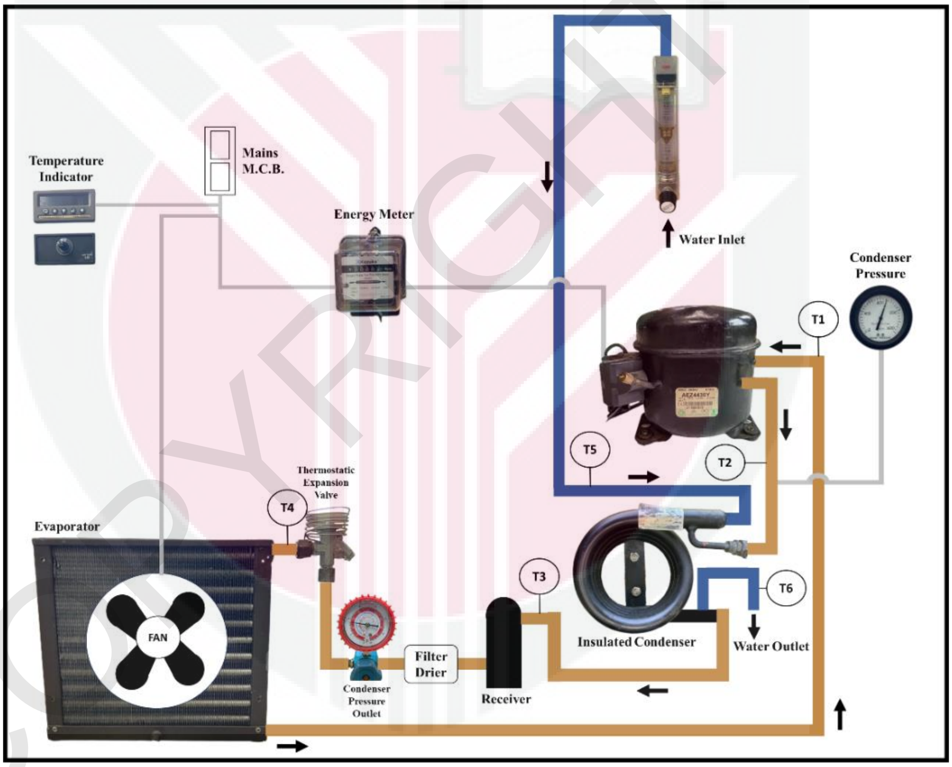

Figure 3.9 : Schematic mechanical heat pump R514 as the test rig

The detailed specifications parts of the system were:

1. Refrigerant: This system used R134a as a working fluid.
2. Compressor: It was a fully hermetic single cylinder-reciprocating type with a displacement value of 8.85 cm^3/rev.

Table 3.4 : Compressor descriptions

Type Compressor	AE4430Y (Tecumseh, L'UNIITE HERMETIQUE)
Rated Voltage (V)	220-240
Rated Frequency (Hz)	50
Refrigerant	R134a
Oil type	Polyol-ester (POE)
Oil Charge (cc)	400

3. Condenser: The water pipe was integrated into the condenser pipe; to minimise the wasted heat to the environment, the condenser pipe was insulated coiled concentric copper tube type.
4. Liquid receiver: Contained valves and the entire refrigerant charge if required.
5. Evaporator: Consists of a serpentine copper tube with aluminium fins and an integral fan.
6. Digital Thermometer: Resolution at 0.1 ^{o}C with a switch to select from six thermocouples.
7. Flow meter: It indicated the flow of the water in the condenser (range of 4 – 50 g/s).
8. Pressure Gauges (2): They indicated the high- pressure inlet and outlet of the condenser in kPa.
9. Energy Meter: It indicated the compressor works in kWh with a resolution of 0.1 kWh.

3.6 Temperature and Pressure Sensor system

There were six points for the placed temperature sensor and two points for the pressure sensor. Each point represented the temperature or the location of pressure.

- P_{cond_inlet} : High pressure of the system
- P_{cond_outlet} : High pressure of the system
- T_1 : Compressor suction temperature
- T_2 : Compressor delivery temperature
- T_3 : Condenser outlet temperature
- T_4 : Evaporator inlet temperature
- T_5 : Water inlet temperature
- T_6 : Water outlet temperature

Table 3.5 : Error tolerance for temperature sensor

Sensor	Error Tolerance (ºC)
T_1	0.047
T_2	0.042
T_3	0.042
T_4	0.038
T_5	0.035
T_6	0.047

3.7 Application of nano-lubricants in the test rig

The comparison discussed in the next chapter is related to enhancing the performance system using pure POE oil and three various concentrations of each used nanoparticle. Therefore, the first experiment was about the conventional mechanical heat pump for 2 hours. Afterwards, other solutions would be used alternately and run for the same time work. However, only two maximum experiments are conducted daily, and each nano-oil experiment must be repeated three times. Thereby, the production of nano-lubricant was carried out at least one day before the investigation starts to avoid sedimentation.

Prior to conducting the repetition of running the system with the same nano-lubricant, the first step that needs to be done was filling the refrigerant into the system and the nano-lubricant into the compressor.

First procedure (Filling the lubricant and refrigerant):

1. Removed the existing lubricant oil through the channels provided.
2. Filled 400 ml of pure POE oil or new concentration nano-lubricant into the compressor.
3. Vacuumed the heat pump machine to remove the existing refrigerant until the value - 30 psi.
4. Filled the refrigerant through the same channel slowly and turn on the engine so that the refrigerant flows evenly throughout the system.
5. Stopped filling the refrigerant until the pressure is stable at 25 psi-gauge.
6. Ran the system for 30 minutes to ensure stable pressure in the inlet compressor.
7. Turned off the machine and turn the pressure and temperature in the system back to normal.

Second procedure (Collecting data and repetition of running machine in the same nano-lubricant three times):

1. Checked the temperature of the compressor, condenser, expansion valve and evaporator until similar to the ambient temperature.
2. Set the water flow in the condenser to 4 g/s.
3. Turned on the system for 2 hours and collect the 10-minute data of each pressure and temperature sensor.

4. After 2 hours, turned off the machine and wait until the temperature of the engine becomes the same as in the environment.

Temperature and pressure were manually monitored and read every 10 minutes by switching the digital thermometer in the system for data collection. There were 13 data for each temperature and pressure. In addition, the same collection method was employed to obtain the required compressor work from the energy meter, the high and low-pressure system from the pressure gauge and the mass flow rate of refrigerant from the refrigerant flowmeter.

3.8 Equations used in the experimental

The raw data were obtained from the installed sensor in the machine using degree Celsius for temperature, kN/m2 for pressure and kWh for compressor work. Some of these units need to be converted to other units so that they can be analysed and used in the equation. As mentioned in Chapter 2, in Equation 2.11 and 2.12, both COP_{HP} and COP_{RE} require the data of compressor work as work input. Since $Q_{condenser}$ is the amount of heat absorbed by water from the condenser, while Q_{loss} is zero, it refers to Equation 2.5 and 2.6.

The temperature (T) and pressure (P) values of each point in the main components in the Vapour Compressor Refrigerant (VCR) system also require enthalpy (h) using the property table of saturation and superheated R134a. In Table 3.5, the correlation between the parameters is explained.

Table 3.6 : The main data of calculation in the refrigerant system

Enthalpy (kJ/kg)	Entropy (kJ/kg.K)	Temperature (Celcius)	Pressure (kPa)
h_1	s_1	T_1	P_1
h_2	s_2	T_2	P_2
h_3	s_3	T_3	P_3
h_4	s_4	T_4	P_{sat}

However, in the process of compression, which is from point 1 to point 2, the value was assumed to be the same as the reading data electricity meter. With this equation, the value of the refrigerant flow rate can be determined and assumed to be constant in each flow. In addition, the value of P1 is constant to maintain the pressure inlet, which is 25 psig or 273.69 kPa.

$$\dot{W}_{comp.EL} = \dot{W}_{comp} \quad (3.1)$$

$$\dot{m_{ref}} = \frac{\dot{W}_{comp}}{(h_2 - h_1)} \quad (3.2)$$

For the exergy part, the temperature and pressure in the dead state condition are T_0 = 25 °C and P_0 =101.325 kPa (Yıldız et al., 2022). The value of exergy can be found in the equation of exergy balance, and because of working in a continuous system, the exergy change is neglected (Ceylan, Yildiz, Gürel, Ergün, & Tosun, 2020). Equation 3.3 is the calculation for each point of system, while Equation 3.4 identifies the exergy destruction for each component of the system.

$$\dot{E}x = \dot{m}(h - h_0) - T_0(s - s_0) \quad (3.3)$$

$$\dot{E}x_{dest} = \sum E\,x_{in} - \sum E\,x_{out} \quad (3.4)$$

To examine the system performance, the equation of exergy destruction for each component can be calculated using the second law analysis (Gürel, Ağbulut, Ergün, & Yildiz, 2020).

$$\dot{E}x_{dest.condenser} = (\dot{E}x_2 - \dot{E}x_4) + (\dot{E}x_5 - \dot{E}x_6) \quad (3.5)$$

$$\dot{E}x_{dest.evaporator} = (\dot{E}x_4 - \dot{E}x_1) \quad (3.6)$$

$$\dot{E}x_{dest.compressor} = (\dot{E}x_1 - \dot{E}x_2) + \dot{W}_{comp.EL} \quad (3.7)$$

$$\dot{E}x_{dest.exp.valve} = (\dot{E}x_3 - \dot{E}x_4) \quad (3.8)$$

$$\dot{E}x_{dest.Total} = \dot{E}x_{dest.cond} + \dot{E}x_{dest.evap} + \dot{E}x_{dest.comp} + \dot{E}x_{dest.exp.val} \quad (3.9)$$

where:

$\dot{E}x_1$ = Exergy destruction inlet compressor (kJ/s)

$\dot{E}x_2$ = Exergy destruction outlet compressor (kJ/s)

$\dot{E}x_3$ = Exergy destruction outlet condenser (kJ/s)

$\dot{E}x_4$ = Exergy destruction outlet expansion valve (kJ/s)

$\dot{E}x_5$ = Exergy destruction inlet water (kJ/s)

$\dot{E}x_6$ = Exergy destruction outlet water (kJ/s)

3.9 Uncertainty Analysis

In scientific studies, there are no definite measurements; thus, uncertainty values can indicate doubt and lack of measurement. Uncertainty is the degree to which data values vary from one another and standard deviation is a method used to summarize the distance of each data to the average value or centre of the data (Siegel & Wagner, 2022). Equations 3.10 and 3.11 can be used for all parameters in the calculation system such as temperature, pressure, work input/output, COP, and exergy. This uncertainty analysis is necessary because the repetition of experiments was conducted for three times so that there is a possibility of differences in the data values obtained in each experiment.

$$\sigma = \sqrt{\frac{\text{Sum of squared deviations}}{\text{Number of population items}}} \tag{3.10}$$

$$\sigma = \sqrt{\frac{(X_1-\mu)^2+(X_2-\mu)^2+(X_3-\mu)^2}{N}} \tag{3.11}$$

where:

σ = standard deviation population

X_n = each data value (n = 1,2,3,…)

μ = the average of data

N = number of population items

In order to reduce experimental error, the experiments were repeated three times for each concentration of nano-lubricants. The first experiment was conducted using pure POE oil. Then, the lowest concentration in graphene nano-lubricants was replaced the pure POE oil. Before conducting experiments with other solutions, pure POE oil was put into the compressor first to reduce the possibility of reduction from the previous solution. If this was not done, it was likely that there would be residue from the previous nano-lubricant mixed with the new solution to be tested. After completing all graphene nano-lubricants, the experiment began again with the lowest concentration of MWCNT nano-lubricants. Furthermore, the temperature of the water entering the water pipe must be considered and kept somewhat constant throughout each experiment. The compressor's beginning temperature must also be the same as room temperature, therefore a break of around 2 to 3 hours is required between experiments.

3.10 Summary

In conclusion, all samples, including the full-size nano-lubricants, were prepared using the same method, which involved measurement, magnetic stirring, and sonication. The stability of the graphene and MWCNT nano-lubricants was evaluated through a stability of tests to identify the most stable concentrations. The stability tests were conducted in three stages: visual inspection, Ultraviolet-visible (UV-visible) spectrophotometry, and zeta potential. The results of these three tests indicated which concentration of each nano-lubricant exhibited the most stable characteristics. Subsequently, all selected samples were prepared in full size and replaced the pure compressor oil separately. The necessary basic parameters, such as temperature, pressure, and work input compressor during the system, were used to analyse the performance of the vapour compression refrigeration system.

CHAPTER 4

RESULTS AND DISCUSSIONS

4.1 Overview

In Chapter 4, all the raw data obtained from the experimental investigations are discussed to demonstrate the effectiveness of nano-lubricants in system performance. All equations used in the calculations have been mentioned in the previous chapter in more detail. However, to minimise the possibility of system blocking by using unstable nano-lubricants, the stability test results are displayed visually and numerically as consideration for further research. Comprehensive previous experiments related to this study also helped identify the results of this Vapour Compression Refrigeraation (VCR) system.

4.2 Stability Test of Nano-lubricant

After producing the different Graphene (Gr) and Multi-walled Carbon Nanotube (MWCNT) lubricant concentrations in sample size, each nano-lubricant's concentrations were immediately tested to minimise the potential of sediments.

4.2.1 Visual Inspection

It can be clearly seen in Fig 4.1 that deciding the concentrations of the most suitable nano-lubricant to replace pure Polyolester (POE) oil as compressor oil could be challenging. This is because the colour of each sample is very dark and concentrated, and no sediment can be seen at all in the bottom and top layers of the solution until three months of observation. Compared to the previous experiment, Choi et al. (2021) showed that by using 0.1 vol% MWCNT/POE oil, the visualisation was stable 72 hours after the preparation.

Besides, Salem (2020) observed the same nano-lubricant 0.5 wt% for 60 days and found no sedimentation in the solution.

It can be concluded that MWCNT is a nanoparticle that can be well dispersed in POE oil, thereby producing a solution that remains stable over a long period. Therefore, the following stability tests were used: Ultravoilet-vis sm and Zeta potential to obtain the three most optimal concentrations.

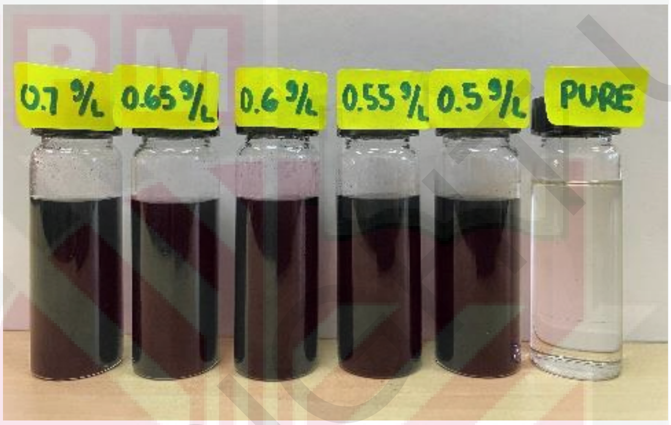

(i)

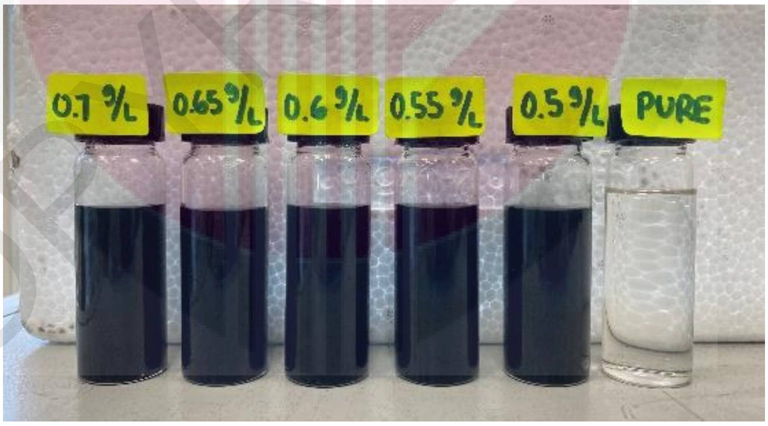

(ii)

Figure 4.1 : MWCNT nano-lubricant (i) After preparation, and (ii) After three months of preparation.

In contrast, the visual condition of some graphene samples can show the gap between nanoparticles and POE oil, as shown in Fig.4.2. The sedimentation on top of the bottles happened even after the preparation of samples. It can be seen clearly that the lowest concentration has the worst result for the first stability testing from the unbalanced mass of graphene and volume lubricant oil. Subsequently, the nanoparticles were dispersed in a large area but could not cover all surfaces. Besides, after 24 hours of observation samples, the 0.3 g/L (the highest concentration) experienced agglomeration and thick sedimentation on top of the surface nano-lubricant. The exact condition also happened for the next six days in 0.25 g/L nano-lubricant, but the solution was not as clear as the 0.3 g/L solution. In conclusion, the reliable concentration solutions for working in a refrigeration system are 0.2 g/L, 0.15 and 0.1 g/L.

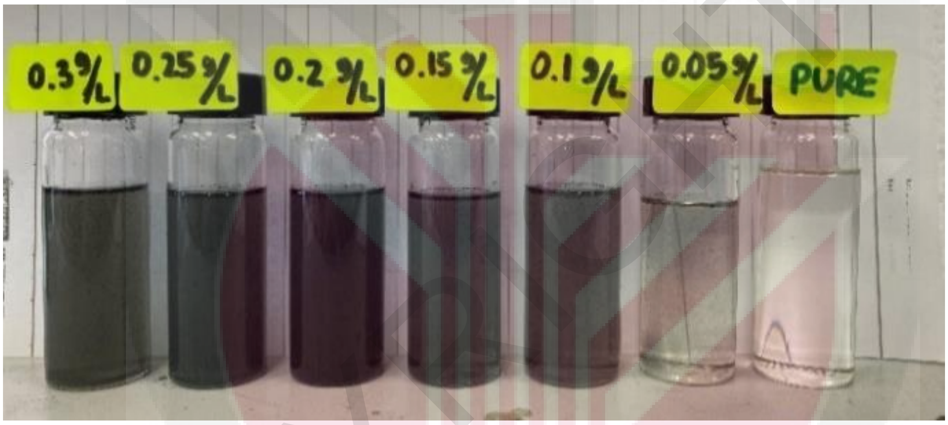

(i)

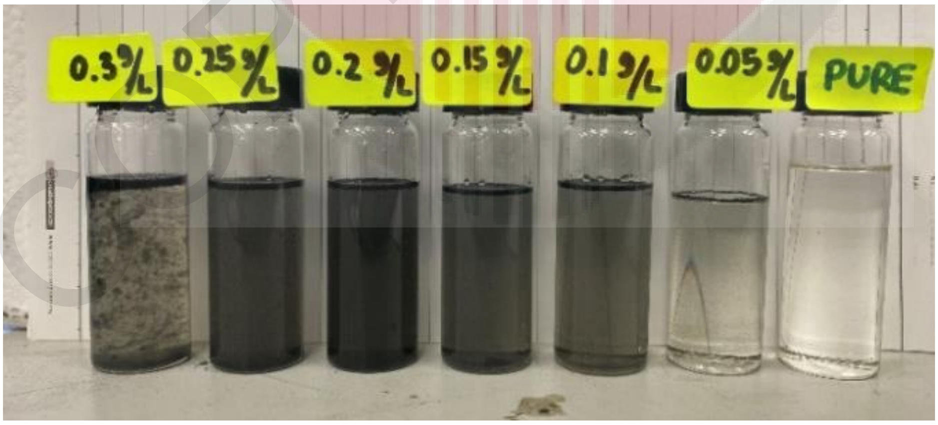

(ii)

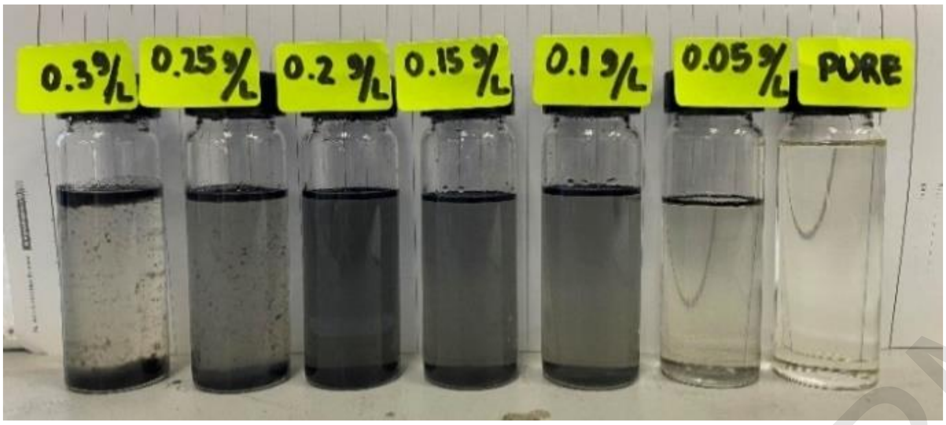

(iii)

Figure 4.2 : Graphene nano-lubricant (i) After preparation, (ii) After 24 hours of preparation, and (iii) After seven days of preparation.

4.2.2 Ultraviolet Visible Spectrophotometry

Another test should be conducted to select the three best MWCNT nano-lubricant concentrations: Ultraviolet Visible (UV-vis) spectrophotometry. At first, each sample was injected into the cuvette, as in Fig 4.3. It turned out that the darkest sample was next to pure oil, which was 0.5 g/L. Meanwhile, the other two samples were 0.55 g/L and 0.65 g/L, respectively. These results can also be proven on data using a UV-vis spectrophotometer in Table 4.1**.**

Figure 4.3 : The MWCNT samples on cuvette for UV-vis testing

Ahmad et al. (2020) suggested comparing the result of this testing by the outstanding peak absorption or the peak at the shortest wavelength. Based on Table 4.1, each concentration has its peak absorption at a different wavelength. After reaching its peak point, the absorbance value gradually decreased as the wavelength increased, as in previous research (Nugroho et al., 2021b). When 0.5 g/L was tested, its absorption value was the highest among other concentrations at a 200-700 nm wavelength range. However, the absorption at the single wavelength could be considered to compare each absorbance as the peak absorption has almost the same value. Therefore, 302 nm was chosen as the reference point for comparing the absorbance, with the prominent peak absorbance of 0.5, 0.55 and 0.65 g/L.

Table 4.1 : Result of UV-vis MWCNT nano-lubricants

Samples (g/L)	Peak Absorption (a.u.)	Wavelength (nm)
0.5	4.87	316
0.55	4.045	298
0.6	3.261	296
0.65	4.116	302
0.7	3.821	294

Table 4.2 : Result of UV-vis MWCNT nano-lubricant at 302 nm

Samples (g/L)	Absorption (a.u.)
0.5	4.197
0.55	3.383
0.6	2.861
0.65	4.116
0.7	2.908

Unlike MWCNT nano-lubricant, the previous stability test has confirmed the three best graphene nano-lubricant solutions. The result indicated that the peak absorbance wavelength for each concentration was 294 nm. The peak absorption value has confirmed the order of values from the visual inspection.

In another experiment with SiO_2/PAG, Sharif et al. (2017) proved that the UV-vis results on higher concentrations will have higher absorption by comparing 0.2, 0.7 and 1.5 vol%. However, the statement could be unsuitable for some concentrations or nano-lubricants since lower or higher concentrations still have a chance to agglomerate and sediment on the top or bottom layer of the nanofluid. Therefore, it is necessary to observe the nanofluid for a particular time to reduce the cost of testing and the potential to damage the work of the compressor after replacement.

Figure 4.4 : The Graphene samples on cuvette for UV-vis testing

Table 4.3 : Result of UV-vis Graphene nano-lubricants

Samples (g/L)	Peak Absorption (a.u.)	Wavelength (nm)
0.1	0.197	294
0.15	0.751	294
0.2	0.892	294

4.2.3 Zeta Potential Analysis

After selecting the three best MWCNT solutions, the value of zeta potential in the mV unit was tested to determine the stability of this nano-lubricant. The test was done twice for 0.5, 0.55 and 0.65 g/L to obtain a strong result.

As mentioned in the previous chapter, the value of zeta potential could be positive and negative. All MWCNT/POE oil samples were tested, and the results were more than ±60 mV, as in Table 4.4. Salem (2020) also checked the stability of MWCNT/POE 0.1 - 0.5 wt%; the result was between +30.34 and +31.5 mV. In addition, Al-Janabi et al. (2021) carried out another test with 0.1 v%; the zeta potential was -45.5 mV for MWCNT/POE without surfactant. Hence, these current MWCNT and POE oil mixture results showed more stability compared to the previous experiment and were ready to be prepared in large amounts to replace the compressor oil with a remarkable performance result.

Table 4.4 : The value of Zeta Potential for MWCNT nano-lubricant

Concentrations (g/L)	Testing 1	Testing 2
0.5	77.1	88.4
0.55	-75.7	-84.9
0.65	-51.7	-137

The contrast of each concentration's zeta potential value can be automatically detected from Table 4.5. The 0.1 and 0.15 g/L are classified as instability concentrations, although the solutions were better than 0.3, 0.25 and 0.05 g/L from visual inspection. The only graphene-lubricant concentration with more than ±30 mV that has good stability was 0.2 g/L. Consequently, this result could be considered before replacing pure compressor oil for long-term use in refrigerant systems, except for 0.2 g/L. This has been confirmed through experiments by various researchers if the 0.2 g/L application in different mass R600a had outstanding Coefficient of Performance (COP) compared to higher concentrations in domestic refrigeration systems (T. Babarinde et al., 2020; Madyira et al., 2022).

Table 4.5 : The value of Zeta Potential for Graphene nano-lubricants

Concentrations (g/L)	Testing 1	Testing 2
0.1	8.77	5.62
0.15	-9.41	15.3
0.2	-37.8	-37

4.3 Working in the refrigerant system

Seven types of lubricant oil were applied to the compressor to identify the system's performance. Each lubricant was run three times to obtain the average data. In the last related experiment, Yıldız et al. (2022) used 300 grams of R134a, thus making a variety of suction pressures in the compressor. However, in the current experiments, the initial pressure in part of the suction compressor was stated at 25 psi-gauge or 273.69 kPa constantly. This number was chosen based on the maximum pressure that can be set on this machine so that it is at least the closest to the pressure range in the previous experiment, namely 450-470 kPa absolute.

Besides the initial refrigerant pressure determined, the water flow rate is one of the essential parameters in this experiment. A higher water outlet temperature (T6) can be obtained using the lowest water flow rate, as seen in Table 4.6, to produce other benefits, including a water heater. It can be seen clearly that the highest difference in temperature by water was when the system applied a 4 g/s water-flow rate, around 25 °C. Referring to those data, in the present experiment, the water flow rate was set at 4 g/s to significantly improve the result in the water heater temperature.

Table 4.6 : The effect of application variety water flow rates

Nano-lubricants	Water Flow Rate (g/s)	T5 (°C)	T6 (°C)
POE OIL	4	27.3	52.3
	10		41.6
	20		36.5
	30		34.5
	40		33.5
	50		32.8

4.3.1 Graphene nano-lubricants in the system

After deciding the three suitable concentrations of graphene-lubricant oil, the pure oil in the compressor was replaced alternately from 0.2 g/L. The system first worked with 0.2 g/L to avoid clogged pipes due to the graphene nano-lubricant oil.

Even though the system was charged with the same pressure as the refrigerant, the compressor worked differently, as can be observed and analysed from the data in Table 4.7. While working with pure oil, the system needed more work in the compressor part, which was more than 35% compared to graphene-oil results. However, high pressure was obtained in the discharge of the compressor part, thus creating a high temperature in the condenser. This result dramatically impacted the heat transferred from the condenser to the water, which is the reason why the temperature of the water inlet and outlet was higher than that using the graphene-lubricant oil.

Conversely, decreasing the system's high pressure will undoubtedly decrease the pressure and temperature in the evaporator section. This is what caused the temperature of the evaporator to get lower and even below 0 °C. Compared to the pure oil and all graphene concentrations, the 0.2 g/L of graphene oil has a remarkable result in terms of the evaporator temperature at -1.41 °C and the reduction of compressor work input at 30%.

Table 4.7 : Graphene nano-lubricant results in VCR system

Lubricant oil (g/L)	Pressure (kPa)				Temperature (°C)						Work Input (kJ/s)
	1	2	3	4	1	2	3	4	5	6	
PURE	273.69	1457	1454.3	309.27	26.67	86.68	52.73	1.50	27.33	53.38	0.500
Gr 0.1	273.69	1309.2	1308.9	279.60	24.67	83.88	48.86	-1.29	27.26	48.38	0.365
Gr 0.15	273.69	1315.2	1313.1	279.93	24.05	83.77	49.18	-1.26	27.33	48.82	0.373
Gr 0.2	273.69	1306.2	1304	278.33	24.75	83.66	48.85	-1.41	27.33	48.66	0.350

The highlight in comparison results between pure POE oil and graphene nano-lubricant was the drastically dropping energy required by the compressor. Having a certain amount of graphene in compressor oil made the system require less energy to work more optimally. Even though the heat transfer in the condenser part also decreased using nanoparticles in compressor oil, all graphene nano-lubricant performance results showed that the system worked effectively, as can be seen clearly from the increment of Coefficient of Performance in heat pump (COP_{HP}) value in Table 4.8.

In the cooling process, the value of heat of evaporation (Q_{evap}) and Coefficient of Performance in refrigerant effect (COP_{RE}) are the main parameters to identify the system's performance. Based on the COP_{RE} the system performed with no significant differences with all types of lubricant oil. Therefore, the role of nanoparticles, which are graphene in this process, seemed to not have a prominent contribution by increasing the cooling performance. In contrast, in refrigerant flow rate parameters, the value decreased by increasing the concentration of graphene nano-lubricant and decreasing the compressor work in the system. It means that there is a strong relation between the rate of work input and the refrigerant flow.

Table 4.8 : Comparison results of graphene and POE oil of working system

Lubricant oil (g/L)	W_{comp} (kJ/s)	Q_{evap} (kJ/s)	Q_{cond} (kJ/s)	COP_{HP}	COP_{RE}	Refrigerant flow rate (kg/s)
PURE	0.500	1.821	0.438	0.875	3.641	0.01240
Gr 0.1	0.365	1.338	0.355	0.972	3.666	0.00886
Gr 0.15	0.373	1.349	0.361	0.967	3.613	0.00899
Gr 0.2	0.350	1.293	0.358	1.024	3.695	0.00855

4.3.2 MWCNT nano-lubricants in the system

The same method with graphene nano-lubricant was used to obtain the result of MWCNT nano-lubricants. In MWCNT nano-lubricants, the concentrations were higher than graphene's, which were at 0.5, 0.55 and 0.65 g/L.

The advantages of using the nanoparticles in the POE oil have been shown in the MWCNT experiment results. The trend of decrement pressure in the compressor discharge, heat transferred by the condenser and outlet water temperature were the same in the graphene experiments. These results highlighted a drastic reduction in the compressor work with 0.65 g/L, which was roughly 40% less than the pure POE lubricant result in Table 4.9. Compared to other concentrations in MWCNT nano-lubricants, the required work input for

0.55 g/L was higher than 0.65 g/L, which was around 15%. However, at point 4, the temperature reached -2.44 °C, which was the lowest temperature. Hence, between 0.5 and 0.55 g/L with the same amount of compressor work, using 0.55 g/L in the VCR system is more optimal owing to the lowest temperature inlet evaporator.

Table 4.9 : MWCNT nano-lubricant results in VCR system

Lubricant oil (g/L)	Pressure (kPa)				Temperature (°C)						Work Input (kJ/s)
	1	2	3	4	1	2	3	4	5	6	
PURE	273.69	1456.99	1454.32	309.27	26.67	86.68	52.73	1.50	27.33	53.38	0.50
MWCNT 0.5	273.69	1290.66	1284.99	274.63	22.86	82.67	48.12	-1.78	27.33	48.72	0.353
MWCNT 0.55	273.69	1331.49	1325.52	268.03	22.12	81.81	47.98	-2.44	27.30	48.55	0.350
MWCNT 0.65	273.69	1394.66	1391.23	279.67	25.37	85.34	51.13	-1.28	27.33	51.08	0.303

By working with 0.65 g/L, the value of COP_{HP} increased by 50%, where the least amount of work compressor and highest heat transferred in the condenser were around 0.303 kJ/s and 0.399 kJ/s, respectively, as in Table 4.10. At the same time, the refrigerant flow rate was 0.00742 kg/s, which is the lowest rate among other subjects.

The same improvement with graphene results occurred to the MWCNT nano-lubricant in the cooling process, where there were no significant increments in COP_{RE}. The only condition that demonstrated the impact of using MWCNT in Q_{evap} was by using 0.55 g/L, as the COP_{RE} was 0.97% higher than using the blank POE oil in the VCR system. This condition also happened in 0.5 g/L and 0.55 g/L in terms of all parameters, such as Q_{cond}, W_{comp}, Q_{evap}, and COP_{HP}. This could happen because the difference in the value of the concentration tested is so small that it will be challenging to detect the differences in the system's performance

Table 4.10 : Comparison results of MWCNT and POE oil of working system

Lubricant oil (g/L)	W_{comp} (kJ/s)	Q_{evap} (kJ/s)	Q_{cond} (kJ/s)	COP_{HP}	COP_{RE}	Refrigerant flow rate (kg/s)
PURE	0.500	1.821	0.438	0.875	3.641	0.01240
MWCNT 0.5	0.353	1.27	0.359	1.017	3.608	0.00847
MWCNT 0.55	0.350	1.2870	0.357	1.020	3.676	0.00853
MWCNT 0.65	0.303	1.099	0.399	1.315	3.622	0.00742

4.3.3 P-h Diagram Analysis

As mentioned previously, all the presented data in the p-h diagram were based on the pressure and temperature in the experiment. However, on point 4, the enthalpy was assumed to be the same as on point 3. It means there was no outside heat supplied/absorbed or adiabatic expansion. Furthermore, at point 4, there was no installed pressure gauge, so the value was assumed to be the same as the saturation pressure at the existing temperature at this point (T4).

One of the reasons the refrigerant system's process was indicated in the P-h diagram is to identify the quality of each phase process, which could be compared to the ideal process. At points 2 and 4, the system can be categorised as working ideally. This is because on point 2, the quality of refrigerant was in superheated (x = 1), and on point 4, it was in saturated liquid (x = 0). Besides, the high pressure in the system slightly decreased from the inlet to the outlet condenser, suggesting the absence of pressure drop. Apart from points 2 and 3, the quality of refrigerant at point 4 was a mix of liquid and vapour, which were also in an ideal state. On the other hand, the low pressure in the evaporation was different before and after the process. The pressure sensor should be installed to ensure the pressure value enters the evaporator to make the data more accurate. Although the difference was quite significant, the refrigerant temperature after the evaporation process was in superheated condition at the initial pressure-charged of the system. This point is crucial since the refrigerant must be at least in saturation vapour (ideal cycle) before entering the compressor to ensure the refrigerant has already been wholly vapourised.

Basically, the P-h diagram to pure oil-, graphene and MWCNT nano-lubricant experiments have the same quality of each point as in Fig. 4.5, 4.6 and 4.7. In details:

1. Point 1: Superheated (Ideal: Saturated vapor)
2. Point 2: Superheated
3. Point 3: Saturated liquid
4. Point 4: Mix (no throttling losses assumed)

After substituting the pure POE oil with the graphene and MWCNT nano-lubricant, the refrigerant temperature was seen to lower, affecting the reading of pressure at this point. If the temperature at point 4 is lower, the process of absorbing heat from the environment will be more straightforward and frequent. This fact has been proven with the data enthalpy between point 1 and point 4, even in graphene and MWCNT experiments. By using the pressure saturation at T4, there was more dropped pressure at this point, making the pressure in evaporation more stable and temperature (T4) close to temperature saturation at P1.

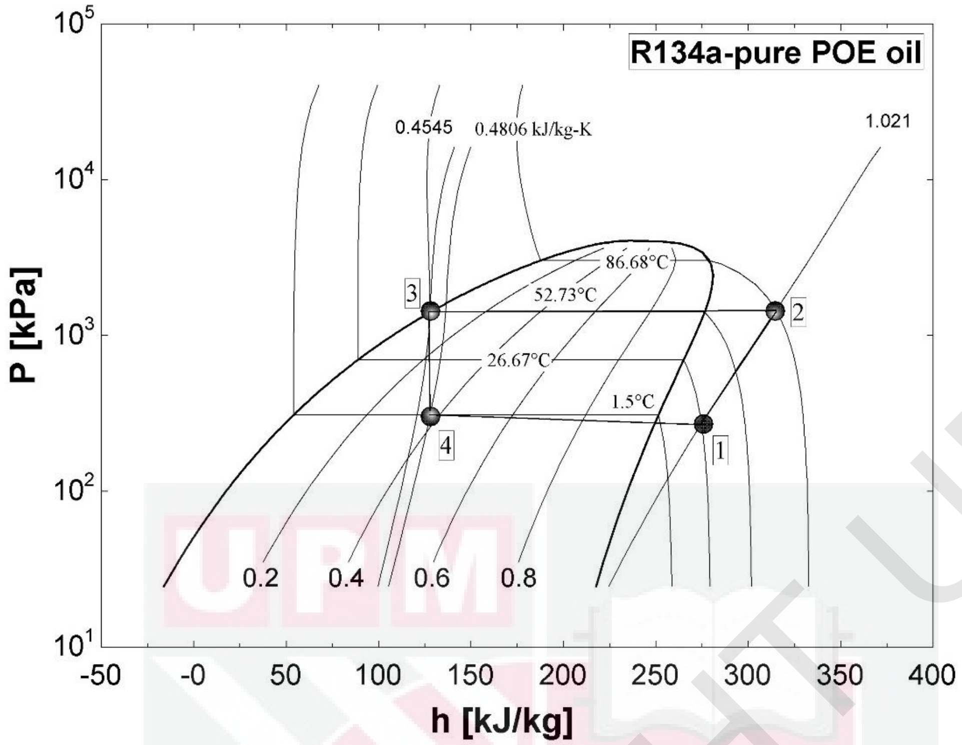

Figure 4.5 : P-h Diagram pure POE oil in refrigerant system

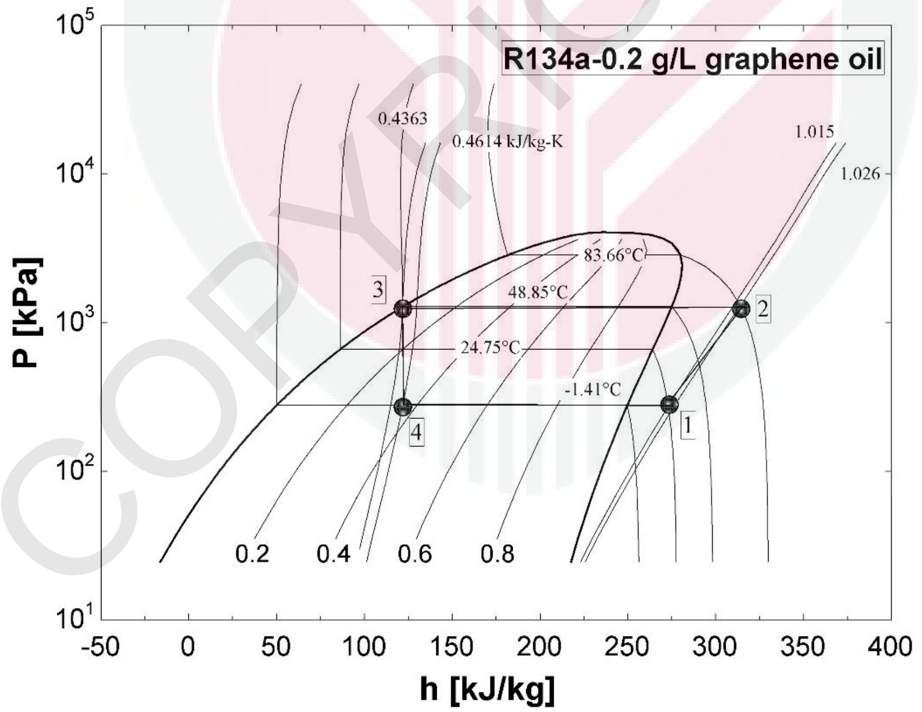

Figure 4.6 : P-h Diagram Graphene nano-lubricant 0.2 g/L in refrigerant system

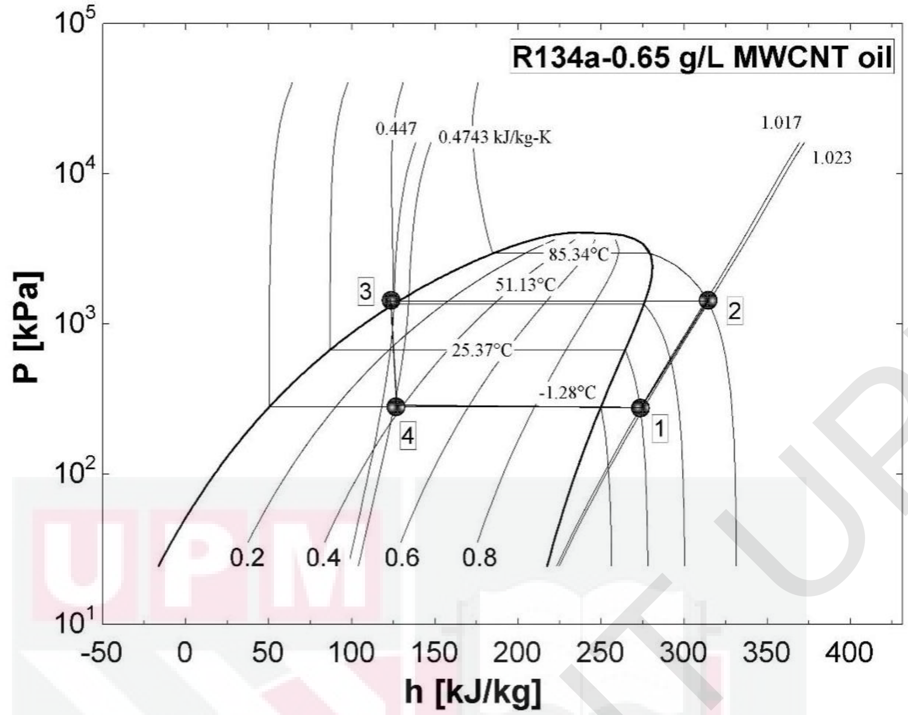

Figure 4.7 : P-h Diagram MWCNT nano-lubricant 0.2 g/L in refrigerant system

4.4 Performance analysis of nano-lubricants

Some parameters can be used to indicate the system's performance, such as heat transfer, COP and exergy analysis. In using the various nanoparticles and the concentrations of the nano-lubricants, the outcome of the performance system must be different in terms of temperature, pressure and heat transfer. In general, system performance was determined by calculating the flow rate of heat transfer in the evaporation and condensation process. Moreover, the compressor work is one of the essential parameters due to the high electricity consumption.

4.4.1 Heat Transfer and Coefficient of Performance (COP) system

In experimental studies, the compressor work value was assumed to be similar to the installed energy meter value. It can be clearly seen in Figure 4.8 that the highest electricity consumption in the test rig system was when using pure POE oil. Compared with conventional oil, the most optimal concentration of graphene lubricant was 0.2 g/L due to a 30% reduction in compressor work. In MWCNT experimental working, the same result was shown using 0.5 and 0.55 g/L, around 0.350 kJ/s. It was noticeable that the system required the lowest energy when working with 0.65 g/L, which was about 0.303 kJ/s. This value suggests that the reduction was almost 40% lower than pure POE oil. In previous research, T. O. Babarinde et al. (2020) investigated 0.6 g/L MWCNT/Mineral Oil/R600a, and the maximum reduction of compressor work was around 22% from the pure result. Another result shown in the D. K. Singh et al. (2021) experiments demonstrated that the compressor work was reduced by 31% using 0.5 wt% in the mineral oil-R134a system. It was then concluded that the mixture of MWCNT and POE oil has a great impact on the R134a system, and 0.6 g/L is the most optimal concentration for MWCNT-lubricant to gain low energy consumption in the vapour compression refrigeration system.

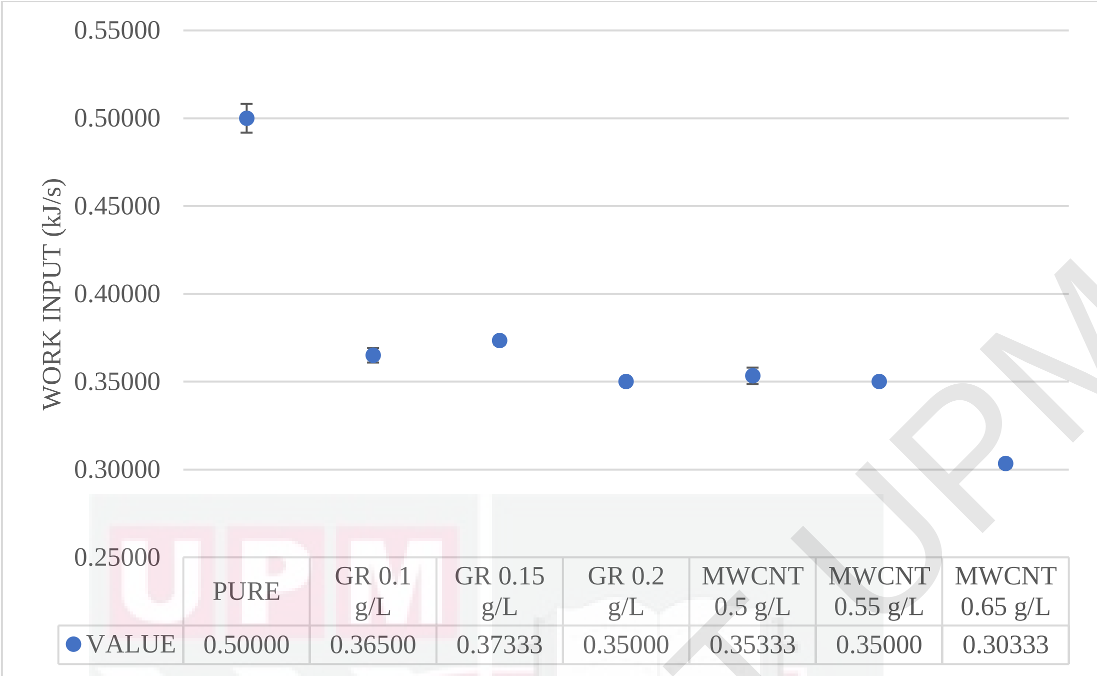

Figure 4.8 : The comparison of the compressor work in the experimental study

All the heat absorbed by the water through the pipe was assumed to be the same as the heat transferred by the condenser. Figure 4.9 shows that when using pure POE oil in the system, the heat transferred to the water was higher than in other results. However, this value is related to the compressor work, which was also high using pure POE oil simultaneously.

Working with the graphene nano-lubricant in different concentrations, the heat transferred was almost the same, in the range of 0.350-0.362 kJ/s. This also happened with 0.5 and 0.55 g/L MWCNT nano-lubricants. Nevertheless, the effect of using nanoparticles in lubricant oil can be easily noticed using 0.65 g/L MWCNT nano-lubricant as the heat absorbed was relatively high, which was around 0.3999 kJ/s, 14% greater than other nano-lubricants. This happened because by using a 0.65 g/L solution, the compressor worked less which made the refrigerant flow rate also low. By having a low refrigerant flow rate, one of the values that has a big influence is the outlet water temperature (T_6) which is the higher the value. As mentioned earlier, the $Q_{condenser}$ value is obtained from Q_{water}, so the T_6 value greatly influences the absorbed heat in the condenser section of the system. This also happened in the Yıldız et al., (2022) experiment, which showed that variations in the refrigerant flow rate value affected the exit temperature of the water integrated with the condenser, which was the same as the experimental equipment carried out in the current experiment.

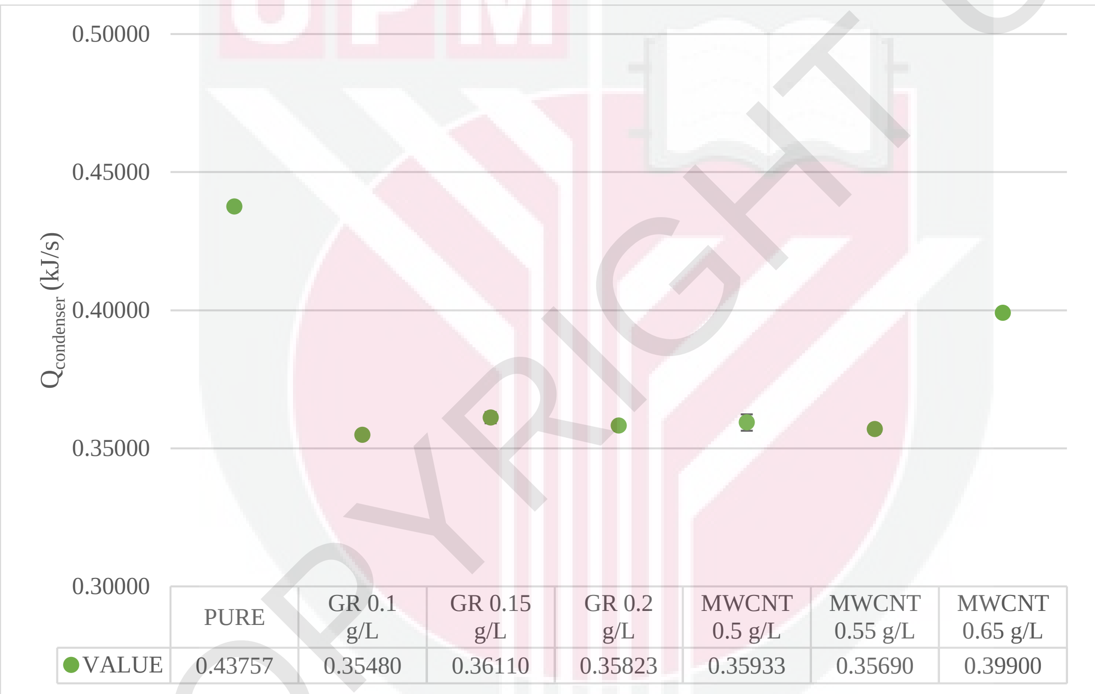

Figure 4.9 : The comparison of $Q_{condenser}$ in the experimental study

The ratio between the heat transferred by the condenser to the environment and the work input to the system is represented as the COP_{HP} value of the system. The system can be categorised as performing poorly if the COP value is lower than 1. It is caused by the outcome of the system being lower than the input energy. After three repetitions of experimental working for each nano-lubricant, the system's performance using pure POE oil, 0.1 and 0.15 g/L graphene-lubricant resulted in low performance. Even though the POE system worked optimally by transferring the heat to another medium, the electricity consumption was simultaneously high and unequal to the least expected outcome.

By replacing POE oil with 0.2 g/L in the VCR system, the performance value tended to be more stable from the minimum error among the repetitions. Moreover, the COP value of 0.2 g/L was around 17% higher than that of the system without nanoparticle lubricants. On the other hand, while working with MWCNT nano-lubricants, the overall system's performance was more than 1, which indicates good performance. From Figure 4.10, particularly for the MWCNT nano-lubricant part, the COP value increased by adding more concentration in the VCR system, showing the role of nanoparticles in lubricant oil to help reduce the compressor workload and increase the heat transferred to the environment. Additionally, the significant improvement was with 0.65 g/L, which was approximately 51% compared to the COP's pure-POE system.

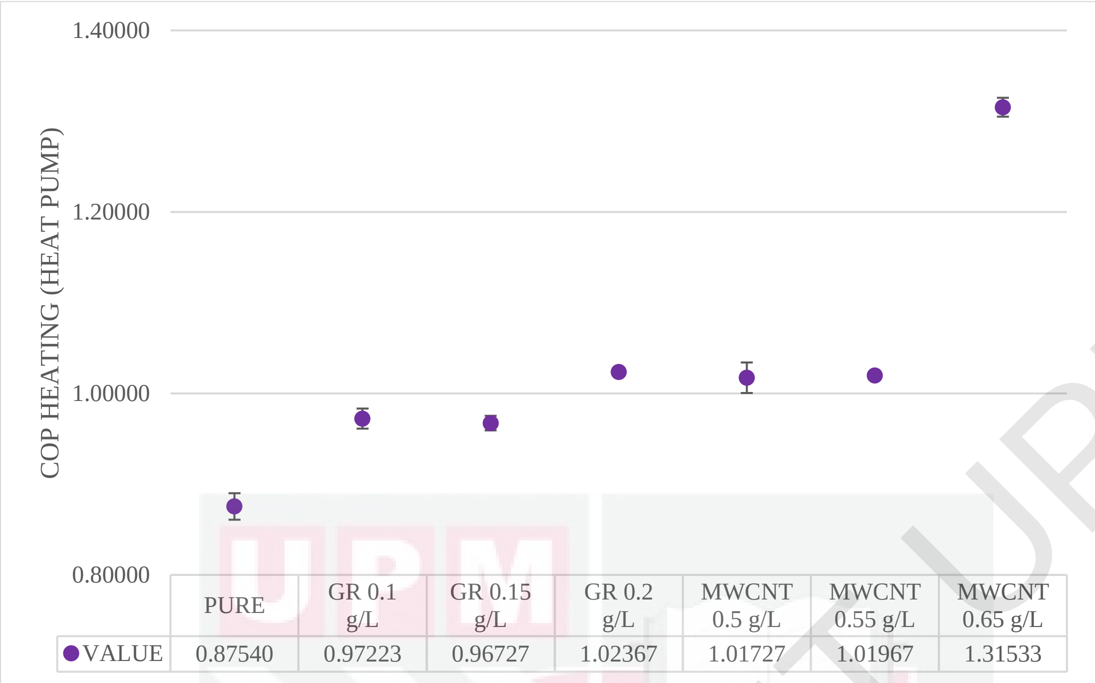

Figure 4.10 : The comparison of COP_{HP} in the experimental study

In the test rig system, the load absorbed by the evaporator was from the environment. The value of heat absorbed by the evaporator was also three times more than the heat transferred by the condenser. Overall, the result indicated that the POE oil, graphene, and MWCNT nano-lubricant performed well in the R134a system for the cooling part. The most optimal absorption of the load was with pure POE lubricant oil, which was 1.821 kJ/s. Figure 4.11 shows that using nanoparticles in the R134a system made the rate of heat absorption low.

The highest heat transfer rate among graphene nano-lubricants was 1.338 kJ/s, with 0.1 g/L. It also happened in the experimental study with the second lowest concentrations of MWCNT nano-lubricants, with the result of 1.287 kJ/s. This result is even lower than that obtained using graphene nano-lubricants. The effect of having more concentrated graphene and MWCNT in the refrigerant system created a low rate of heat absorption in the evaporation process.

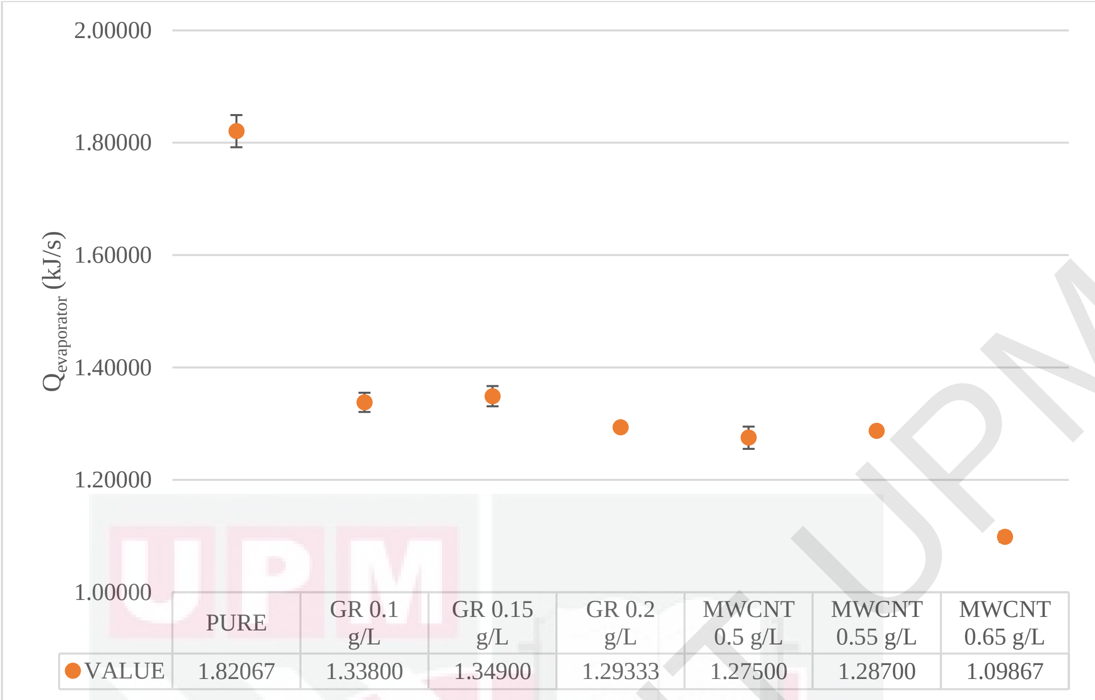

Figure 4.11 : The comparison of $Q_{evaporator}$ in the experimental study

From Figure 4.12, the graph shows a COP value of more than 3 in all experimental studies using blank, graphene and MWCNT nano-lubricants, meaning the absorption of the load by the evaporator was higher than the work input by the compressor. However, the resulting system performance in the cooling process was quite close, making the effect of using nanoparticles in this study appear insignificant. The most prominent result was shown by 0.2 g/L graphene nano-lubricant, which was 1.5% higher than pure POE oil in the system. This result remained stable in the experimental study by having the most negligible error data repetition. The second option to perform well is applying the 0.1 g/L graphene nano-lubricant, as the COP value was almost the same as 0.2 g/L.

In MWCNT nano-lubricant research, the highest possibility of replacing the pure POE oil with the optimal performance was working with 0.55 g/L. This is because the result was higher than pure POE oil, MWCNT and graphene concentrations, except for 0.2 g/L graphene lubricant. Therefore, to obtain the better performance of the POE/R134 system, the most optimal nano-lubricants and their concentrations to be considered are 0.2 g/L graphene nano-lubricant and 0.55 g/L nano-lubricant.

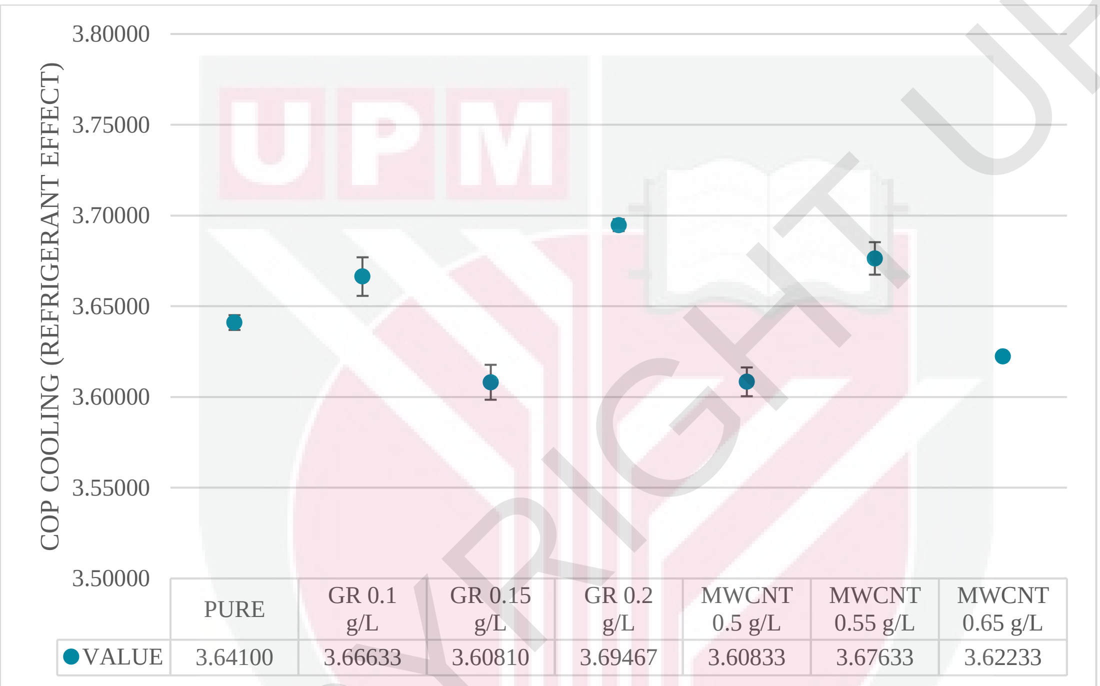

Figure 4.12 : The comparison of COP_{RE} in the experimental study

In addition to the heat transfer rate and system COP, the refrigerant flow rate dramatically influences nano-lubricant use. The significance of dropping refrigerant flow rate can be seen clearly in Figure 4.13, which is approximately 30% in all nano-lubricants, except 0.65 g/L MWCNT nano-lubricant. Working with the highest concentration of MWCNT nano-lubricant in this study slowed the refrigerant flow in the system. The flow rate decreased by nearly 40% using 0.65 g/L MWCNT nano-lubricant compared to the pure POE oil.

In more detail, the trend of the effect of nano-lubricant in the VCR in the required energy in the compressor graph is the same as the refrigerant flow rate trend. Therefore, the impact of applying nanoparticles in compressor oil can be shown from the result of the amount of work input and the rate of refrigerant flowing in the working system. This statement has been approved by (Yıldız et al., 2022) in their experimental research. By adding nanoparticles in lubricant oil such as Al_2O_3, TiO_2, and CuO in POE oil, the refrigerant flow rate dropped by nearly 11% compared to the pure POE oil.

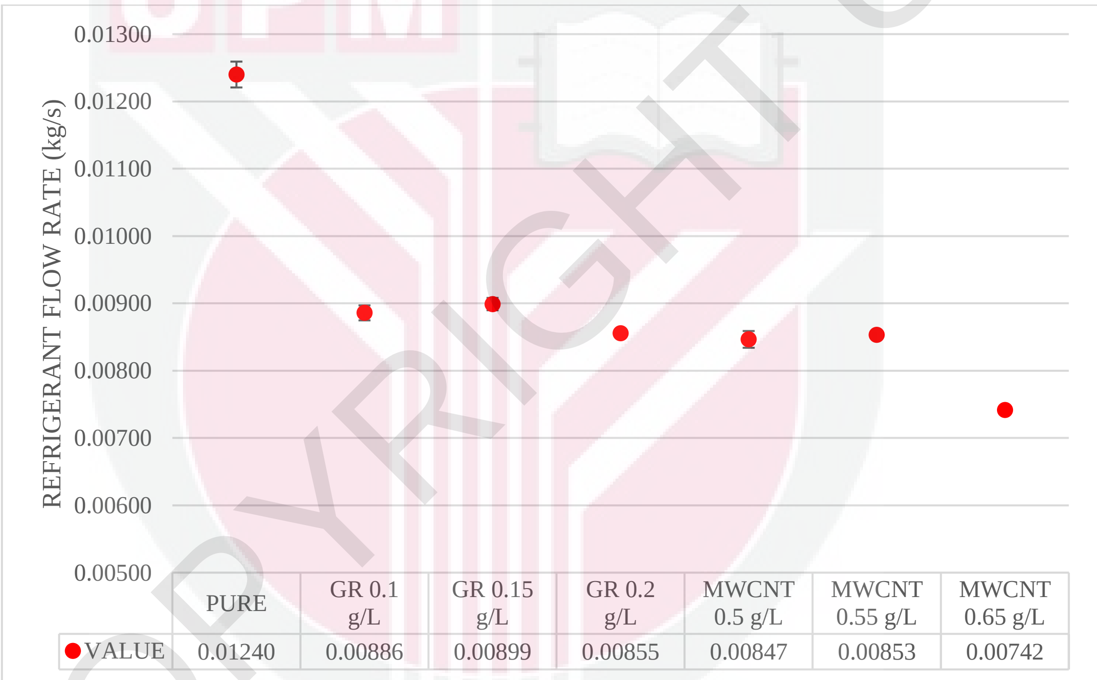

Figure 4.13 : The comparison of refrigerant flow rate in the experimental study

4.4.2 Exergy destruction analysis

Exergy analysis can assist in designing, optimising and assessing such systems by identifying the sources of exergy destruction and emphasising potential areas for improvement (Dincer & Rosen, 2021; Wan et al., 2023). Furthermore, the analysis can help establish the least amount of work required to obtain the desired result in work-consuming operations (Dincer & Rosen, 2021). Exergy destruction in components may not be induced by flaws or decreased by self-optimisation, like refrigerant, which has a substantial role in the VCR system (Cui, Wang, Wei, & Shi, 2022). However, in this experimental study, the exergy destructions of each component were analysed as the parameter of the optimisation mechanical heat pump system as in Table 4.11.

Table 4.11 : Exergy destruction for all components system

Lubricant oil (g/L)	Exergy Destruction (kJ/s)				
	Compressor	Evaporator	Condenser	Exp.valve	TOTAL
PURE	0.00172	0.17540	0.20543	0.09617	0.47873
Gr 0.1	0.02976	0.12280	0.13190	0.06596	0.35043
Gr 0.15	0.03247	0.12427	0.13383	0.06762	0.35819
Gr 0.2	0.02687	0.11827	0.12603	0.06393	0.33509
MWCNT 0.5	0.03686	0.11697	0.12203	0.06244	0.33830
MWCNT 0.55	0.02643	0.11687	0.12707	0.06481	0.33517
MWCNT 0.65	0.01259	0.10026	0.11213	0.06024	0.28523

For the compressor part, the minimum exergy destruction was with pure POE oil. Adding nanoparticles would make more destructive exergies. In the MWCNT result, the value decreased when more concentrations of nanoparticles were added. However, the results were not lower than those using pure POE oil. In graphene analysis, the results were higher than pure POE oil and all concentrations in MWCNT, which were more than 0.02687 kJ/s. In contrast, in the other components, the evaporator, condenser and expansion valve, the impact of using nanoparticles in the lubricant oil can be easily detected due to the most drastically reduced exergy destruction. It is also recognisable that having more concentrated nanoparticles in the POE lubricant oil makes the system the least exergy-destructive value.

Based on all result data in Table 4.11, the evaporator and condenser are the most considered components that should be identified due to the high value of exergy destructions. Even after including nanoparticles in the lubricating oil, both parts' values remained higher than the exergy destructions of the compressor and expansion valve. Therefore, the system's performance can be improved significantly by reducing the exergy destruction in the condenser and evaporator parts, which means improving the work of both parts.

Aside from detecting the exergy destructions of each component, the overall exergy destructions can be used to detect the decrease in exergy destruction value after utilising nanoparticles in lubricating oil. The highest value came from using pure POE oil as compressor oil in the VCR system, which was around 0.479 kJ/s. Figure 4.14 depicts the notable drop caused by adding a modest amount of graphene to the lubricating fluid. The most minimal exergy destruction occurred at 0.2 g/L (0.335 kJ/s). The figure also shows the value of exergy destruction for each component, which was the lowest among the graphene nano-lubricant concentrations. Compared to the MWCNT nano-lubricant results, 0.65 g/L in the VCR system resulted in the fewest destructions, with a lowering value of around 40% from the POE oil result. Meanwhile, other concentrations in the same lubricant oil were nearly identical, namely 0.2 g/L graphene nano-lubricant oil.

Figure 4.14 : The comparison of Total Exergy Destruction in the experimental study

4.5 Uncertainty analysis

In the raw data obtained while the system was run for 2 hours with three times repetition, there was an error reading of each sensor temperature, pressure inlet condenser, pressure outlet condenser and energy meter. The values were ±0.025°C, 0.4714 kPa, 0.4623 kPa, 0.0024 kJ/s respectively. Other than that, the error for all important parameters is determined and shown in Table 4.12.

Table 4.12 : Error for the data calculation in percentage

W_{comp}	Q_{evap}	Q_{cond}	COP_{HP}	COP_{RE}	m_{refg}	Exergy Destructions				
						Comp	Evap	Cond	Exp. valve	TOTAL
0.78	0.98	0.39	0.99	0.26	0.92	0.89	1.04	1.02	0.90	0.83

By obtaining the smaller error value, the closer the value obtained from each experiment carried out. It can be seen from Table 4.12, the error values obtained are almost all below 1% of the average data value for each parameter, only two parameters are above that value, namely exergy destruction of evaporator and exergy destruction of condenser. However, these values only range from 1.04% and 1.02% respectively. This error value also serves to determine the range of values that can be obtained when the experiment is carried out.

4.6 Summary

Compared to prior studies, the usage of graphene 0.2 g/L and MWCNT 0.65 g/L, which are the most optimal concentrations among the samples, is appropriate for reducing compressor work. The resulting decrease in value ranges between 30% and 39.34%. In the previous study, the highest ideal concentration for graphene, 0.2 g/L, was only about 19% when compared to pure R600a compressor oil (Madyira et al., 2022). The same effect happened in the MWCNT 0.6 g/L solution, which resulted in the highest reduction among the samples. However, the value is only about 20% of pure R600a (Babarinde et al., 2021b). As a result, employing R134a in the VCR system can help reduce compressor work, which is significantly lower than that of other refrigerants. Using R134a as a refrigerant in the VCR system dramatically increases the effectiveness of the graphene and MWCNT application. More details, the massive drop in input work will certainly affect the condensation and evaporation processes. The COP_{RE} value in the two prior investigations was only 2.9 for graphene 0.2 g/L and MWCNT 0.6 g/L, however the value in this work, which did not use extra nanoparticles, is greater than 3.6. That is, in terms of COP_{RE} value, the current study is significantly more efficient than earlier investigations.

CHAPTER 5

CONCLUSIONS AND RECOMMENDATIONS

5.1 Conclusions

All experiments that have been done yielded remarkable results that can be used for further research and new ideas for the application of nanoparticles in pure lubricant oil. Based on the general objective, the Vapour Compression Refrigeration (VCR) system had the great improvement by using the graphene and Multi-Walled Carbon Nanotubes (MWCNT) nano-lubricants.

More details, the result of stability testing of graphene and MWCNT were the initial specific objective that must be achieved before replace the pure compressor oil in the VCR system. Among other concentrations, in graphene nano-lubricant there were three most stable concentrations, which were 0.1, 0.15, and 0.2 g/L. While for MWCNT nano-lubricants, they were 0.5, 0.55 and 0.65 g/L. Therefore, only these six concentrations and pure Polyolester (POE) oil applied in the VCR system to prevent damage to the flow of refrigerant in the system.

In addition, based on the performance system after replacing the pure POE oil, it was found the remarkable result by the improvement parameters. The highlight result of using the graphene nano-lubricant was working with 0.2 g/L. The result showed that the reduction of work compressor and total exergy destruction, improvement of COP_{HP}, as well as COP_{HP} which were 30%, 30%, 16.94% and 1.04% respectively. This result also happened while system working with 0.65 g/L MWCNT nano-lubricant. This concentration made the compressor worked more effortless, which around 39.33% of reduction work. Other than that, the COP_{HP} value increased by 50.26% and the total exergy destruction decreased by 40.4% compared to the result's pure POE oil.

5.2 Recommendations

For future experiments, some recommendations could be considered in the process of selecting the nanoparticles, preparing nano-lubricants and running the system.

1. Using Graphene/CTAB/POE oil and MWCNT/POE oil in R134a system with the different variety of concentrations
2. Changing the water flow rate, it can be lower or higher than 4 g/s. because it can help to have the higher performance of condenser instead of using the basic Vapour Compression Refrigeration (VCR) system
3. Comparing other types of nanoparticles to obtain different performance results.
4. Using a variety of pure oil, such as Polyalkylene Glycol (PAG) oil, Mineral Oil (MO) and Alkyl Benzene (AKB) oil depending on the required compressor.
5. Substituting Refrigerant-134a to the other refrigerants, those with a lower environmental impact for long-term application.
6. Setting a higher water flow rate helps to identify the better performance of the system.
7. Installing the reading meter for refrigerant flow rate and pressure in the evaporator to have more accurate data in actual work

REFERENCES

Ahmad, A., Amir, M., Alshadidi, A. A., Hussain, M. D., Haq, A., & Kazi, M. (2020). Central composite design expert-supported development and validation of HPTLC method: Relevance in quantitative evaluation of protopine in Fumaria indica. *Saudi Pharmaceutical Journal*, *28*, 487–494.

Ahmadi, M. H., Alhuyi Nazari, M., Ghasempour, R., Madah, H., Shafii, M. B., & Ahmadi, M. A. (2018). Thermal conductivity ratio prediction of Al2O3/water nanofluid by applying connectionist methods. *Colloids and Surfaces A: Physicochemical and Engineering Aspects*, *541*, 154–164.

Akhtar, M. J., & Rajput, S. P. S. (2023). Performance analysis of ice plant using R134a/POE blended with MWCNTs nano-refrigerant–An experimental approach. *International Journal of Refrigeration*, *155*, 333–347.

Akhtar, M. J., & Rajput, S. p. s. (2024). Energy and exergy analysis of vapour compre ssion test rig using R134a blended with GN- MWCNT/POE hybrid nano-lubricants. *Energy Sources, Part A: Recovery, Utilization, and Environmental Effects*, *46*, 188–208.

Akkaya, M., Sarilmaz, A., Balci, S., & Ozel, F. (2023). Numerical and experimental analysis of refrigerating performance for hybrid nanolubricants with sepiolite additives. *Thermal Science and Engineering Progress*, *37*, 101576.

Al-Janabi, A. S., & Hussin, M. (2020). Stability and thermal conductivity of graphene in polyester nanolubricant. *AIP Conference Proceedings*, *2267*, 020066.

Al-Janabi, A. S., Hussin, M., & Abdullah, M. Z. (2021). Stability, thermal conductivity and rheological properties of graphene and MWCNT in nanolubricant using additive surfactants. *Case Studies in Thermal Engineering*, *28*, 101607.

Al-Janabi, A. S., Hussin, M., Abdullah, M. Z., & Ismail, M. A. (2022). Effect of CTAB surfactant on the stability and thermal conductivity of mono and hybrid systems of graphene and FMWCNT nanolubricant. *Colloids and Surfaces A: Physicochemical and Engineering Aspects*, *648*, 129275.

Aljuwayhel, N. F., Ali, N., Ebrahim, S. A., & Bahman, A. M. (2023). Experimental investigation of thermophysical properties, tribological properties and dispersion stability of nanodiamond-based nanolubricant for air conditioning systems. *International Journal of Refrigeration*, *145*, 325–337.

Alrwashdeh, S. S., & Ammari, H. (2019). Life cycle cost analysis of two different refrigeration systems powered by solar energy. *Case Studies in Thermal Engineering*, *16*, 100559.

Anwar, T., & Randa, D. R. (2020). *Experimental Study of Vapour Compression Refrigeration System by Using Aluminium Oxide Nanoparticles as Lubricant Additive*. *6*, 6.

Awang, N. W., Ramasamy, D., Kadirgama, K., Samykano, M., Najafi, G., & Sidik, N. A.
C. (2019). An experimental study on characterization and properties of nano lubricant containing Cellulose Nanocrystal (CNC). *International Journal of Heat and Mass Transfer*, *130*, 1163–1169.

Azman, N. F., & Samion, S. (2019). Dispersion Stability and Lubrication Mechanism of
Nanolubricants: A Review. *International Journal of Precision Engineering and Manufacturing-Green Technology*, *6*, 393–414.

Azmi, W. H., Ismail, M. F., Zawawi, N. N. M., Mamat, R., & Safril, S. (2024). Tribological
and residential air conditioning performance using SiO2-TiO2/PVE nanolubricant. *International Journal of Refrigeration*. https://doi.org/10.1016/j.ijrefrig.2024.01.002

Babarinde, T., Akinlabi, S., Madyira, D., Adedeji, P., & Ekundayo, F. (2021). Improving
the performance of LPG with graphene-nanolubricant in a domestic refrigerator: An artificial intelligence approach. *International Journal of Ambient Energy*, 1–29.

Babarinde, T., Akinlabi, S., Madyira, D., & Ekundayo, F. (2020). Enhancing the energy
efficiency of vapour compression refrigerator system using R600a with graphene nanolubricant. *Energy Reports*, *6*, 1–10.

Babarinde, T. O., Akinlabi, S. A., & Madyira, D. M. (2020). Energy performance evaluation of R600a/MWCNT-nanolubricant as a drop-in replacement for R134a in household refrigerator system. *Energy Reports*, *6*, 639–647.

Babarinde, T. O., & Madyira, D. M. (2023). Assessment of TiO2, Al2O3, and SiO2
nanolubricant with eco-friendly refrigerant as substitute for R134a in a vapour compression system: An experimental approach. *Energy Reports*, *9*, 326–331.

Babarinde, T. O., Madyira, D. M., Mashinini, P. M., & Marangwanda, G. T. (2021a).
Performance of multi-walled CNTs suspended with hydrocarbon refrigerant (R600a) and lubricating oil in vapour compression refrigeration system. *Fuel Communications*, 100036.

Babarinde, T. O., Madyira, D. M., Mashinini, P. M., & Marangwanda, G. T. (2021b).
Performance of multi-walled CNTs suspended with hydrocarbon refrigerant (R600a) and lubricating oil in vapour compression refrigeration system. *Fuel Communications*, 100036.

Bahman, A. M., & Saleh, D. (2024). Parametric analysis for nanolubricant in vapor
compression refrigeration cycle. *Journal of Engineering Research*.

Bian, Q. (2020). Waste heat: The dominating root cause of current global warming.
Environmental Systems Research, *9*, 8.

Bibi Cassim, S., Aziz Hairuddin, A., & Vira, C. (2024). The effects of Multiwalled Carbon
Nanotube to the performance of a refrigeration system. Retrieved August 25, 2024.

Ceylan, İ., Yildiz, G., Gürel, A. E., Ergün, A., & Tosun, A. (2020). The effect of malfunctions in air handling units on energy and exergy efficiency. *Heat Transfer Research*, *51*.

Chavhan, S., Choudhary, S. K., & Maheshwary, P. (2023). Performance analysis of
vapor compression refrigeration system using varying concentrations of copper oxide (CuO)/mineral oil (MO) based nanosuspension. *Materials Today: Proceedings*.

Che Abdullah, C. A., & Albert, E. L. (2019). Chapter 6—Carbon Nanotubes as Biological Transporters and Tissue-Engineering Scaffolds. In S. A. Rashid, R. N. I. Raja Othman, & M. Z. Hussein (Eds.), *Synthesis, Technology and Applications of Carbon Nanomaterials* (pp. 135–156). Elsevier.

Choi, T. J., Kim, D. J., Jang, S. P., Park, S., & Ko, S. (2021). Effect of polyolester oil-based multiwalled carbon-nanotube nanolubricant on the coefficient of performance of refrigeration systems. *Applied Thermal Engineering*, *192*, 116941.

Colbourne, D., Suen, K. O., Li, T.-X., Vince, I., & Vonsild, A. (2020). General framework for revising class A3 refrigerant charge limits – a discussion. *International Journal of Refrigeration*, *117*, 209–217.

Cui, M., Wang, B., Wei, F., & Shi, W. (2022). A modified exergy analysis method for vapor compression systems: Splitting refrigerant exergy destruction. *Applied Thermal Engineering*, *201*, 117728.

Dağıdır, K., & Bilen, K. (2023). Experimental investigation of usage of POE lubricants with Al2O3, graphene or CNT nanoparticles in a refrigeration compressor. *Beilstein Journal of Nanotechnology*, *14*, 1041–1058.

Dai, N., & Li, S. (2018). Simulation and performance analysis on condenser coil in household heat pump water heater. *Sustainable Cities and Society*, *36*, 176–184.

de Paula, C. H., Duarte, W. M., Rocha, T. T. M., de Oliveira, R. N., & Maia, A. A. T. (2020). Optimal design and environmental, energy and exergy analysis of a vapor compression refrigeration system using R290, R1234yf, and R744 as alternatives to replace R134a. *International Journal of Refrigeration*, *113*, 10–20.

Devecioğlu, A. G., & Oruç, V. (2018). Improvement on the energy performance of a refrigeration system adapting a plate-type heat exchanger and low-GWP refrigerants as alternatives to R134a. *Energy*, *155*, 105–116.

Deymi-Dashtebayaz, M., Baranov, I. V., Nikitin, A., Davoodi, V., Sulin, A., Norani, M., & Nikitina, V. (2022). An investigation of a hybrid wind-solar integrated energy system with heat and power energy storage system in a near-zero energy building-A dynamic study. *Energy Conversion and Management*, *269*, 116085.

Dincer, I., & Rosen, M. A. (2021). Chapter 14—Exergy analyses of cryogenic and liquefaction systems. In I. Dincer & M. A. Rosen (Eds.), *Exergy (Third Edition)* (pp. 383–410). Elsevier.

Duarte, M., Pires, L., Silva, P., & Gaspar, P. (2017). Experimental comparison between R409A and R437A performance in a heat pump unit. *Open Engineering*, *7*.

Ekundayo, F., & Babarinde, T. (2019). *Performance Investigation Of Tio 2 Nano Fluid Based Lubricant On Exergy Of VCRS Working With A Mixture Of R290/R600*.

Fukuchi, Y., Yoshitake, K., & Yokota, K. (2019). *Development of simplified condenser model considering the effect of phase change*.

Gürel, A. E., Ağbulut, Ü., Ergün, A., & Yildiz, G. (2020). ENERGY, EXERGY, AND ENVIRONMENTAL (3E) ASSESSMENTS OF VARIOUS REFRIGERANTS IN THE REFRIGERATION SYSTEMS WITH INTERNAL HEAT EXCHANGER. *Heat Transfer Research*, *51*. https://doi.org/10.1615/HeatTransRes.2020033716

Hansen, J. E., Sato, M., Simons, L., Nazarenko, L. S., Sangha, I., Kharecha, P., … Li, J. (2023). Global warming in the pipeline. *Oxford Open Climate Change*, *3*, kgad008.

Hansen, J., Sato, M., & Ruedy, R. (2022). Global temperature in 2021. *Diponível Em Http://Www. Columbia. Edu/~ Jeh1/Mailings/2022/Temperature2021. 13January2022. Pdf. Acesso Em*, *1*.

Hiralal, K. A., & Ali, M. (2024). Performance Evaluation Using Graphene Oxide Nanomaterial as a Nano-Lubricant for R600a Refrigeration Systems. *Nanotechnology Perceptions*, 1133–1142.

Husainy, A. S., Gurav, A. R., Pawar, A. N., Kate, S. S., Daphale, D. D., & Kirtane, A. A. (2018). *Preparation, Properties, Stability and Applications of Different Nanofluids: A Review*. 9.

Ismail, M. F., Azmi, W. H., Mamat, R., Sharma, K. V., & Zawawi, N. N. M. (2023). Stability Assessment of Polyvinyl-Ether-Based TiO2, SiO2, and Their Hybrid Nanolubricants. *Lubricants*, *11*, 23.

Jacobson, M. Z., Krauland, A.-K. von, Coughlin, S. J., Dukas, E., Nelson, A. J. H., Palmer, F. C., & Rasmussen, K. R. (2022). Low-cost solutions to global warming, air pollution, and energy insecurity for 145 countries. *Energy & Environmental Science*, *15*, 3343–3359.

Jagadeesan, A. K., Thangavelu, K., & Dhananjeyan, V. (2020). Carbon Nanotubes: Synthesis, Properties and Applications. In *21st Century Surface Science—A Handbook*. IntechOpen.

Jatinder, G., Ohunakin, O. S., Adelekan, D. S., Atiba, O. E., Daniel, A. B., Singh, J., & Atayero, A. A. (2019). Performance of a domestic refrigerator using selected hydrocarbon working fluids and TiO2–MO nanolubricant. *Applied Thermal Engineering*, *160*, 114004.

Jing, S., Chen, Q., Zhou, Y., & Yu, J. (2023). Thermodynamic analysis of a modified booster-assisted ejector heat pump cycle with dual condensers. *Applied Thermal Engineering*, *235*, 121351.

Joshi, Y. G., Zanwar, D., Gupta, V., Dhandale, P. N., Patil, A., & Kudawale, A. (2023). Synthesis and performance investigation of novel graphene nanoplatelets-based nanosuspension in PAG and MO refrigeration lubricants. *Materials Today: Proceedings*.

Joshi, Y. G., Zanwar, D. R., Kinkar, T., Dongre, V., & Barai, V. (2022). Experimental investigation for thermophysical properties of reduced Graphene-Based nanosuspension for refrigeration lubricant. *Materials Today: Proceedings*, *62*, 3651–3657.

Kaggwa, A., & Carson, J. K. (2019). Developments and future insights of using nanofluids for heat transfer enhancements in thermal systems: A review of recent literature. *International Nano Letters*, *9*, 277–288.

Kandhaswamy, K., Periasamy, S., Mayilsamy, S., & Thangavel, S. (2017). Experimental investigations on automobile air conditioners working with R134a and R290/R600a as an alternative. *Thermal Science*, *21*, 515–522.

Kasaeian, A., Hosseini, S. M., Sheikhpour, M., Mahian, O., Yan, W.-M., & Wongwises, S. (2018). Applications of eco-friendly refrigerants and nanorefrigerants: A review. *Renewable and Sustainable Energy Reviews*, *96*, 91–99.

Kasi, P., & Cheralathan, M. (2023). Performance analysis of cascade refrigeration system with alternative refrigerants to reduce carbon emission. *Journal of Thermal Analysis and Calorimetry*, *148*, 4389–4399.

Kaygusuz, K. (2017). Second law of thermodynamics and heat pumps for domestic heating. *Journal of Engineering Research and Applied Science*, *6*, 668–679.

Kim, D. K., & Sunderland, P. B. (2021). Viability of Various Sources to Ignite A2L Refrigerants. *Energies*, *14*, 121.

Kinloch, I. A., Suhr, J., Lou, J., Young, R. J., & Ajayan, P. M. (2018). Composites with carbon nanotubes and graphene: An outlook. *Science*, *362*, 547–553.

Kong, L., Sun, J., & Bao, Y. (2017). Preparation, characterization and tribological mechanism of nanofluids. *RSC Advances*, *7*, 12599–12609.

Kulkarni, S., Chavali, S., & Dikshit, S. (2023). A review on analysis of Vapour Compression Refrigeration System (VCRS) for its performance using different ecofriendly refrigerants and nanofluids. *Materials Today: Proceedings*, *72*, 878–883.

Kumar, V., Karimi, M. N., & Kamboj, S. K. (2020). Mathematical Simulation of Fourth Generation Refrigerant R1243zf in Single Stage and Double Stage Vapour Compression Refrigeration System. *International Journal of Innovative Technology and Exploring Engineering*, *1*, 100.

Kutlu, C., Erdinc, M. T., Li, J., Wang, Y., & Su, Y. (2019). A study on heat storage sizing and flow control for a domestic scale solar-powered organic Rankine cycle-vapour compression refrigeration system. *Renewable Energy*, *143*, 301–312.

Le Ba, T., Mahian, O., Wongwises, S., & Szilágyi, I. M. (2020). Review on the recent progress in the preparation and stability of graphene-based nanofluids. *Journal of Thermal Analysis and Calorimetry*, *142*, 1145–1172.

Li, Z., Jiang, H., Chen, X., & Liang, K. (2019). Comparative study on energy efficiency of low GWP refrigerants in domestic refrigerators with capacity modulation. *Energy and Buildings*, *192*, 93–100.

Liang, K., Li, Z., Chen, M., & Jiang, H. (2019). Comparisons between heat pipe, thermoelectric system, and vapour compression refrigeration system for electronics cooling. *Applied Thermal Engineering*, *146*, 260–267.

Liu, D., Yuan, L., Chun, L., Gong, G., Fang, X., Wang, H., … Peng, P. (2023). Thermodynamic performance analysis of a novel air conditioning system integrating solar absorption compression refrigeration and vacuum membrane-based dehumidification (SACV). *Energy and Buildings*, *288*, 113021.

Liu, Z., Tian, Q., Guo, X., Huang, Y., & Xu, Z. (2023). Pulse cyclone electrowinning of gallium recovery for higher current efficiency and lower energy consumption. *Separation and Purification Technology*, *326*, 124801.

Madyira, D. M., & Babarinde, T. O. (2024). TiO2, CNTs, and SiO2 nanolubricant: An approach to improving the efficiency of a domestic refrigerator. *Journal of Physics: Conference Series*, *2748*, 012003.

Madyira, D. M., Babarinde, T. O., & Mashinini, P. M. (2022). Performance improvement of R600a with graphene nanolubricant in a domestic refrigerator as a potential substitute for R134a. *Fuel Communications*, *10*, 100034.

Malwe, P. D., Shaikh, J., Gawali, B. S., Panchal, H., Dalkilic, A. S., Rahman, S., & Alrubaie, A. J. (2022). Dynamic simulation and exergy analysis of an Organic Rankine Cycle integrated with vapor compression refrigeration system. *Sustainable Energy Technologies and Assessments*, *53*, 102684.

Manoj Kumar, P., Mukesh, G., Naresh, S., Mohana Nitthilan, D., & Kishore Kumar, R. (2021). Study on Performance Enhancement of SPV Panel Incorporating a Nanocomposite PCM as Thermal Regulator. In S. Mohan, S. Shankar, & G. Rajeshkumar (Eds.), *Materials, Design, and Manufacturing for Sustainable Environment* (pp. 587–597). Singapore: Springer.

Megdouli, K., Tashtoush, B. M., Ezzaalouni, Y., Nahdi, E., Mhimid, A., & Kairouani, L. (2017). Performance analysis of a new ejector expansion refrigeration cycle (NEERC) for power and cold: Exergy and energy points of view. *Applied Thermal Engineering*, *122*, 39–48.

Mohd Zaki, S., Azmi, W., Redhwan, A. A. M., Zawawi, N. N. M., & Mamat, R. (2017). Improvement of nanofluid stability using 4-step UV-vis spectral absorbency analysis. *Journal of Mechanical Engineering*, 233–247.

Nair, V., Parekh, A. D., & Tailor, P. R. (2020). Experimental investigation of a vapour compression refrigeration system using R134a/Nano-oil mixture. *International Journal of Refrigeration*, *112*, 21–36.

Nandanwar, Y. N., Walke, P. V., Kalbande, V. P., & Mohan, M. (2023). Performance improvement of vapour compression refrigeration system using phase change material and thermoelectric generator. *International Journal of Thermofluids*, *18*, 100352.

Narayanasarma, S., & Kuzhiveli, B. T. (2019). Evaluation of the properties of POE/SiO2 nanolubricant for an energy-efficient refrigeration system – An experimental assessment. *Powder Technology*, *356*, 1029–1044.

Nikhil Babu, P., Mohankumar, D., Manoj Kumar, P., Makeshkumar, M., Gokulnath, M., Gurubalaji, K., … Ashok, M. (2021). Energy efficient refrigeration system with simultaneous heating and cooling. *Materials Today: Proceedings*, *45*, 8188–8194.

Nugroho, A., Bo, Z., Mamat, R., Azmi, W. H., Najafi, G., & Khoirunnisa, F. (2021a). Extensive examination of sonication duration impact on stability of Al2O3-Polyol ester nanolubricant. *International Communications in Heat and Mass Transfer*, *126*, 105418.

Nugroho, A., Bo, Z., Mamat, R., Azmi, W. H., Najafi, G., & Khoirunnisa, F. (2021b). Extensive examination of sonication duration impact on stability of Al2O3-Polyol ester nanolubricant. *International Communications in Heat and Mass Transfer*, *126*, 105418.

Obodo, R. M., Ahmad, I., & Ezema, F. I. (2019). Introductory Chapter: Graphene and Its Applications. In *Graphene and Its Derivatives—Synthesis and Applications*. IntechOpen.

Ogbonnaya, M., Ajayi, O. O., & Waheed, M. A. (2023). Influence of Refrigerant Type, Nanoparticle’s Concentration and Size on the Performance and Exergy Efficiency of the Vapour Compression Refrigeration System Using Al2O3 Based Nanolubricant. *Journal of Nanofluids*, *12*, 712–722.

Ohunakin, O. S., Adelekan, D. S., Gill, J., Atayero, A. A., Atiba, O. E., Okokpujie, I. P., & Abam, F. I. (2018). Performance of a hydrocarbon driven domestic refrigerator based on varying concentration of SiO2 nano-lubricant. *International Journal of Refrigeration*, *94*, 59–70.

Otsuka, A. (2023). Industrial electricity consumption efficiency and energy policy in Japan. *Utilities Policy*, *81*, 101519.

Ozair Arshad, M., Azam, Q., Twaha Irfan Ahmad, S., Khan, F., & Atif Wahid, M. (2021). Analysis of vapour compression refrigeration system with R-12, R-134a and R-22: An exergy approach. *Materials Today: Proceedings*, *46*, 6748–6752.

Ozsipahi, M., Kose, H. A., Kerpicci, H., & Gunes, H. (2022). Experimental study of R290/R600a mixtures in vapor compression refrigeration system. *International Journal of Refrigeration*, *133*, 247–258.

Patel, H., Kumar Singh, D., & Prakash Verma, O. (2024). An examination of the vapour compression refrigeration system performance utilizing several environmentally friendly refrigerants and the effect of nanoparticles- a review. *Materials Today: Proceedings*.

Pavía, M., Alajami, K., Estellé, P., Desforges, A., & Vigolo, B. (2021). A critical review on thermal conductivity enhancement of graphene-based nanofluids. *Advances in Colloid and Interface Science*, *294*, 102452.

Phiri, J., Gane, P., & Maloney, T. C. (2017). General overview of graphene: Production, properties and application in polymer composites. *Materials Science and Engineering: B*, *215*, 9–28.

Pinamonti, M., & Baggio, P. (2020). Energy and economic optimization of solar assisted heat pump systems with storage technologies for heating and cooling in residential buildings. *Renewable Energy*, *157*, 90–99.

Poachaiyapoom, A., Leardkun, R., Mounkong, J., & Wongwises, S. (2019). Miniature vapor compression refrigeration system for electronics cooling. *Case Studies in Thermal Engineering*, *13*, 100365.

Raviram, R. P. D., Vijayaganapathy, D., & Dhinakaran, V. (2020). Performance Consideration and Result Analysis Using Various Alternative Refrigerants in a Vapour-Compression Refrigeration System. *IOP Conference Series: Materials Science and Engineering*, *988*, 012126.

Rudrapati, R. (2020). Graphene: Fabrication Methods, Properties, and Applications in Modern Industries. In *Graphene Production and Application*. IntechOpen.

Said, Z., Rahman, S. M. A., Sohail, M. A., & B s, B. (2023). Analysis of thermophysical properties and performance of nanorefrigerants and nanolubricant-refrigerant mixtures in refrigeration systems. *Case Studies in Thermal Engineering*, *49*, 103274.

Sakhir, A. A., & Qaid, D. S. (2023). Experimental investigation for the effect of using CuO/PAG nano-lubricant on the coefficient of performance in a VCR system. *AIP Conference Proceedings*, *2787*, 030027.

Salem, M. R. (2020a). Performance enhancement of a vapor compression refrigeration system using R134a/MWCNT-oil mixture and liquid-suction heat exchanger equipped with twisted tape turbulator. *International Journal of Refrigeration*, *120*, 357–369.

Salem, M. R. (2020b). Performance enhancement of a vapor compression refrigeration system using R134a/MWCNT-oil mixture and liquid-suction heat exchanger equipped with twisted tape turbulator. *International Journal of Refrigeration*, *120*, 357–369.

Sánchez, D., Cabello, R., Llopis, R., Arauzo, I., Catalán-Gil, J., & Torrella, E. (2017). Energy performance evaluation of R1234yf, R1234ze(E), R600a, R290 and R152a as low-GWP R134a alternatives. *International Journal of Refrigeration*, *74*, 269–282.

Sanjeevi, B., & Loganathan, K. (2020). Synthesis of multi wall carbon nanotubes nanofluid by using two step method. *Thermal Science*, *24*, 519–524.

Sánta, R. (2022). Investigations of the performance of a heat pump with internal heat exchanger. *Journal of Thermal Analysis and Calorimetry*, *147*, 8499–8508.

Santhana Krishnan, R., Arulprakasajothi, M., Logesh, K., Dilip Raja, N., & Rajendra, M. (2018). Analysis and Feasibilty of Nano-Lubricant in Vapour Compression Refrigeration System. *Materials Today: Proceedings*, *5*, 20580–20587.

Sanukrishna, S. S., Raju, A. V., Krishnan, A., Harikrishnan, G. H., Amal, A., Kumar, T. S. K., & Prakash, M. J. (2019). Enhancing the thermophysical properties of PAG lubricant using graphene nano-sheets. *Journal of Physics: Conference Series*, *1355*, 012041.

Sarsam, W. S. (2024). Assessment of using different ozone-friendly R22 alternative refrigerants in residential air conditioners in a high-ambient temperature country. *Journal of Engineering and Applied Science*, *71*, 114.

Saufi, M. A., & Mamat, H. (2022). Comparison of dispersion techniques of graphene nanoparticles in polyester oil. *Materials Today: Proceedings*, *66*, 2747–2751.

Saxena, A., & Tangellapalli, S. (2022). Performance analysis of solar-powered integrated desalination and air conditioning system. *Energy Sources, Part A: Recovery, Utilization, and Environmental Effects*, *44*, 6281–6302.

Senthilkumar, A., Abhishek, P. V., Adithyan, M., & Arjun, A. (2021). Experimental investigation of CuO/Sio2 hybrid nano-lubricant in R600a vapour compression refrigeration system. *Materials Today: Proceedings*, *45*, 6083–6086.

Senthilkumar, A., & Anderson, A. (2021). Experimental investigation of Sio2 nanolubricants for R410A vapour compression refrigeration system. *Materials Today: Proceedings*, *44*, 3613–3617.

Senthilkumar, A., Mohammed Sahaluddeen, P. A., Nufais Noushad, M., & Mohammed Musthafa, E. K. (2021). Experimental investigation of ZnO / Sio2 hybrid nano-lubricant in R600a vapour compression refrigeration system. *Materials Today: Proceedings*, *45*, 6087–6093.

Senthilkumar, A., Prabhu, L., Sathish, T., Saravanan, R., Casmir Jeyaseelan, G. A., Ağbulut, Ü., … Ahamed Saleel, C. (2023). Enhancement of R600a vapour compression refrigeration system with MWCNT/TiO2 hybrid nano lubricants for net zero emissions building. *Sustainable Energy Technologies and Assessments*, *56*, 103055.

Sezer, N., Atieh, M. A., & Koç, M. (2019). A comprehensive review on synthesis, stability, thermophysical properties, and characterization of nanofluids. *Powder Technology*, *344*, 404–431.

Shakya, A., Faisal, N., & Chauhan, T. (2019). Performance Analysis of Vapour Compression Cascade Refrigeration Using Refrigerants R404A And R134a. *Int. J. Sci. Dev. Res*, *4*, 319–325.

Sharif, M. Z., Azmi, W. H., Redhwan, A. A. M., & Zawawi, N. M. M. (2017). Preparation and stability of silicone dioxide dispersed in polyalkylene glycol based nanolubricants. *MATEC Web of Conferences*, *90*, 01049.

Sharif, M. Z., Azmi, W. H., Zawawi, N. N. M., & Ghazali, M. F. (2022a). Comparative air conditioning performance using SiO2 and Al2O3 nanolubricants operating with Hydrofluoroolefin-1234yf refrigerant. *Applied Thermal Engineering*, *205*, 118053.

Sharif, M. Z., Azmi, W. H., Zawawi, N. N. M., & Ghazali, M. F. (2022b). Comparative air conditioning performance using SiO2 and Al2O3 nanolubricants operating with Hydrofluoroolefin-1234yf refrigerant. *Applied Thermal Engineering*, *205*, 118053.

She, X., Cong, L., Nie, B., Leng, G., Peng, H., Chen, Y., … Luo, Y. (2018). Energy-efficient and -economic technologies for air conditioning with vapor compression refrigeration: A comprehensive review. *Applied Energy*, *232*, 157–186.

Siegel, A. F., & Wagner, M. R. (2022). Chapter 5 - Variability: Dealing with Diversity. In A. F. Siegel & M. R. Wagner (Eds.), *Practical Business Statistics (Eighth Edition)* (pp. 105–134). Academic Press.

Silva, L. I., Mirabella, D. A., Pablo Tomba, J., & Riccardi, C. C. (2020). Optimizing graphene production in ultrasonic devices. *Ultrasonics*, *100*, 105989.

Singh, D. K., Kumar, S., Kumar, S., & Kumar, R. (2021). Potential of MWCNT/R134a nanorefrigerant on performance and energy consumption of vapor compression cycle: A domestic application. *Journal of the Brazilian Society of Mechanical Sciences and Engineering*, *43*, 540.

Sonawan, H., Saputro, P., & Kurniawan, I. M. (2018). Utilization of air conditioner condenser as water heater in an effort to energy conservation. *Renewable Energy and Environmental Sustainability*, *3*, 1.

Srithar, K., Rajaseenivasan, T., Arulmani, M., Gnanavel, R., Vivar, M., & Fuentes, M. (2018). Energy recovery from a vapour compression refrigeration system using humidification dehumidification desalination. *Desalination*, *439*, 155–161.

Subhedar, D. G., Patel, J. Z., & Ramani, B. M. (2022). Experimental studies on vapour compression refrigeration system using Al2O3/mineral oil nano-lubricant. *Australian Journal of Mechanical Engineering*, *20*, 1136–1141.

Thachnatharen, N., Khalid, M., Arulraj, A., & Sridewi, N. (2021). Tribological performance of hexagonal boron nitride (hBN) as nano-additives in military grade diesel engine oil. *Materials Today: Proceedings*.

Vaghela, J. K. (2017). Comparative Evaluation of an Automobile Air Conditioning System Using R134a and Its Alternative Refrigerants. *Energy Procedia*, *109*, 153–160.

Vashisht, S., & Rakshit, D. (2021). Recent advances and sustainable solutions in automobile air conditioning systems. *Journal of Cleaner Production*, *329*, 129754.

Venkataraman, A., Amadi, E. V., Chen, Y., & Papadopoulos, C. (2019). Carbon Nanotube Assembly and Integration for Applications. *Nanoscale Research Letters*, *14*, 220.

Wan, T., Bai, B., & Zhou, W. (2023). Exergy destruction analysis of a power generation system utilizing the cold energy of LNG. *Heliyon*, *9*, e19393.

Wu, H., Ge, Y., Chen, L., & Feng, H. (2021). Power, efficiency, ecological function and ecological coefficient of performance optimizations of irreversible Diesel cycle based on finite piston speed. *Energy*, *216*, 119235.

Xia, X., Liu, Z., Wang, Z., Sun, T., & Zhang, H. (2023). Multi-layer performance optimization based on operation parameter-working fluid-heat source for the ORC-VCR system. *Energy*, *272*, 127103.

Xu, J., Luo, E., & Hochgreb, S. (2021). A thermoacoustic combined cooling, heating, and power (CCHP) system for waste heat and LNG cold energy recovery. *Energy*, *227*, 120341.

Yaakop, S. N., Fauadi, M. M., & Damanhuri, A. M. (2023). Experimental Study on Heat Recovery of Air Dryer from Waste Heat Energy of Condensing Unit from VCRS Air Conditioner. *Nature Environment and Pollution Technology*, *22*, 149–157.

Yan, G., Liu, Y., Qian, S., & Yu, J. (2019). Theoretical study on a vapor compression refrigeration system with cold storage for freezer applications. *Applied Thermal Engineering*, *160*, 114091.

Yang, L., Jiang, W., Ji, W., Mahian, O., Bazri, S., Sadri, R., … Wongwises, S. (2020). A review of heating/cooling processes using nanomaterials suspended in refrigerants and lubricants. *International Journal of Heat and Mass Transfer*, *153*, 119611.

Yang, S., Cui, X., Zhou, Y., & Chen, C. (2020). Study on the effect of graphene nanosheets refrigerant oil on domestic refrigerator performance. *International Journal of Refrigeration*, *110*, 187–195.

Yarmand, H., Gharehkhani, S., Shirazi, S. F. S., Goodarzi, M., Amiri, A., Sarsam, W. S., … Kazi, S. N. (2016). Study of synthesis, stability and thermo-physical properties of graphene nanoplatelet/platinum hybrid nanofluid. *International Communications in Heat and Mass Transfer*, *77*, 15–21.

Yıldırım, R., Gungor, A., Akyüz, A., & Tuncer, A. D. (2023). A new approach for environmental analysis of vapor compression refrigeration systems: Environmental impact index. *Thermal Science and Engineering Progress*, *42*, 101871.

Yıldız, G., Ağbulut, Ü., Gürel, A. E., Ergün, A., Afzal, A., & Saleel, C. A. (2022). Energetic, exergetic, and thermoeconomic analyses of different nanoparticles-added lubricants in a heat pump water heater. *Case Studies in Thermal Engineering*, *33*, 101975.

Yu, X., Cheng, H., Zhang, M., Zhao, Y., Qu, L., & Shi, G. (2017). Graphene based smart materials. *Nature Reviews Materials*, *2*, 17046.

Zawawi, N. N. M., Azmi, W. H., Hamisa, A. H., Hendrawati, T. Y., & Aminullah, A. R. M. (2024). Experimental investigation of air-conditioning electrical compressor using binary TiO2–SiO2 polyol-ester nanolubricants. *Case Studies in Thermal Engineering*, *54*, 104045.

Zawawi, N. N. M., Hamisa, A. H., Azmi, W. H., Hendrawati, T. Y., & Safril, S. (2023). Performance of hybrid electric vehicle air-conditioning using SiO2/POE nanolubricant. *Case Studies in Thermal Engineering*, *52*, 103717.

APPENDICES

Appendix A.1: Average raw data for POE oil experiment.

Time (mins)	T5 (°C)	T6 (°C)	T1 (°C)	T2 (°C)	T3 (°C)	T4 (°C)	P2 (kPa)	P3 (kPa)	P1 (kPa)
0	27.33	27.33	27.33	27.33	27.33	27.33	663.33	653.78	273.694
10	27.33	51.1	26.83	74.4	50.53	0.5	1281.67	1278.14	273.694
20	27.3	51.8	26.53	81.27	51.23	1.3	1303.33	1297.75	273.694
30	27.33	53.33	26.53	86.3	51.9	1.47	1333.33	1333.71	273.694
40	27.33	53.37	26.59	86.6	52.1	1.47	1338.33	1336.98	273.694
50	27.33	53.33	26.8	86.6	52.63	1.5	1346.67	1343.51	273.694
60	27.33	53.23	26.87	86.8	52.47	1.47	1351.67	1346.78	273.694
70	27.33	53.43	26.93	86.8	52.7	1.57	1356.67	1353.32	273.694
80	27.3	53.43	26.6	86.73	52.6	1.4	1358.33	1353.32	273.694
90	27.27	53.5	26.67	86.7	52.87	1.6	1360	1359.86	273.694
100	27.37	53.3	26.47	86.73	53.4	1.5	1366.67	1363.13	273.694
110	27.3	53.4	26.63	86.83	53.3	1.57	1375	1369.66	273.694
120	27.4	53.43	26.57	86.7	53.3	1.47	1370	1369.66	273.694

Appendix A.2: Average raw data for 0.1 g/L Graphene/POE experiment.

Time (mins)	T5 (°C)	T6 (°C)	T1 (°C)	T2 (°C)	T3 (°C)	T4 (°C)	P2 (kPa)	P3 (kPa)	P1 (kPa)
0	27.3	27.3	27.3	27.3	27.3	27.3	636.67	640.7	273.694
10	27.27	47.85	24.95	77.85	48	-1.85	1160	1160.46	273.694
20	27.3	48.1	24.8	81.35	48.45	-1.48	1195	1193.14	273.694
30	27.33	48.4	24.65	82.8	48.8	-1.3	1203.33	1202.95	273.694
40	27.27	48.45	24.5	83.55	48.85	-1.3	1210	1212.76	273.694
50	27.2	48.4	24.63	83.8	48.95	-1.3	1207.67	1206.22	273.694
60	27.23	48.41	24.73	83.8	48.93	-1.3	1207.67	1212.76	273.694
70	27.3	48.47	24.87	84.25	48.9	-1.3	1215	1216.03	273.694
80	27.37	48.33	24.77	84.25	48.9	-1.27	1212.67	1212.76	273.694
90	27.3	48.3	24.55	84.25	49	-1.27	1205	1206.22	273.694
100	27.2	48.33	24.75	84.15	48.75	-1.27	1205	1196.41	273.694
110	27.17	48.4	24.6	84.1	48.65	-1.3	1205	1212.76	273.694
120	27.27	48.35	24.6	83.85	48.9	-1.3	1207	1196.41	273.694

Appendix A.3: Average raw data for 0.15 g/L Graphene/POE experiment.

Time (mins)	T5 (°C)	T6 (°C)	T1 (°C)	T2 (°C)	T3 (°C)	T4 (°C)	P2 (kPa)	P3 (kPa)	P1 (kPa)
0	27.33	27.33	27.33	27.33	27.33	27.33	617.5	622.72	273.694
10	27.37	48.48	23.83	78.28	48.65	-1.6	1191.67	1193.14	273.694
20	27.33	49.98	23.67	82	50.25	-1.2	1249.17	1243.81	273.694
30	27.33	48.9	24.05	83.37	49.2	-1.23	1231.67	1230.74	273.694
40	27.27	48.73	23.78	83.53	49.17	-1.3	1209.17	1212.76	273.694
50	27.33	48.67	23.87	83.53	49.1	-1.27	1209.17	1207.85	273.694
60	27.33	48.8	23.97	83.58	49	-1.23	1209.17	1207.85	273.694
70	27.3	48.88	23.97	83.7	49.15	-1.23	1209.17	1207.85	273.694
80	27.37	48.87	24.1	84	49.23	-1.27	1211.67	1207.85	273.694
90	27.27	48.67	24.27	83.82	49.2	-1.27	1215	1209.49	273.694
100	27.37	48.87	24.17	84.13	49.3	-1.27	1213.33	1211.12	273.694
110	27.37	48.9	24.13	84.07	49.23	-1.23	1215	1209.49	273.694
120	27.37	48.93	24.23	84	49.18	-1.27	1215.83	1212.76	273.694

Appendix A.4: Average raw data for 0.2 g/L Graphene/POE experiment.

Time (mins)	T5 (°C)	T6 (°C)	T1 (°C)	T2 (°C)	T3 (°C)	T4 (°C)	P2 (kPa)	P3 (kPa)	P1 (kPa)
0	27.33	27.33	27.33	27.33	27.33	27.33	630	627.63	273.694
10	27.23	46.87	24.9	77.47	47.4	-1.8	1150	1147.38	273.694
20	27.33	48.27	24.77	82.07	48.57	-1.5	1186.67	1186.61	273.694
30	27.3	48.6	24.7	83.5	48.67	-1.4	1201.67	1199.68	273.694
40	27.3	48.8	24.7	83.53	49.2	-1.4	1216.67	1216.03	273.694
50	27.4	48.7	24.8	83.7	48.97	-1.43	1216.67	1216.03	273.694
60	27.4	48.67	24.7	83.67	48.73	-1.43	1200	1194.78	273.694
70	27.3	48.53	24.77	83.57	48.83	-1.4	1200	1194.78	273.694
80	27.3	48.63	24.6	83.77	48.97	-1.4	1200	1199.68	273.694
90	27.27	48.63	24.73	83.7	48.7	-1.4	1201.67	1202.95	273.694
100	27.33	48.63	24.9	83.73	48.77	-1.37	1205	1202.95	273.694
110	27.43	48.7	24.67	83.8	48.8	-1.4	1201.67	1199.68	273.694
120	27.3	48.67	24.97	83.63	48.87	-1.43	1205	1199.68	273.694

Appendix A.5: Average raw data for 0.5 g/L MWCNT/POE experiment.

Time (mins)	T5 (°C)	T6 (°C)	T1 (°C)	T2 (°C)	T3 (°C)	T4 (°C)	P2 (kPa)	P3 (kPa)	P1 (kPa)
0	27.33	27.33	26.37	26.37	26.37	26.37	630	617.82	273.694
10	27.4	47.3	23.03	76.37	47.23	-2.4	1145	1134.3	273.694
20	27.37	48.4	22.93	80.13	48.13	-1.8	1171.67	1170.26	273.694
30	27.27	48.6	22.93	81.83	48.13	-1.73	1186.67	1180.07	273.694
40	27.3	48.77	22.9	82.67	48.07	-1.8	1186.67	1183.34	273.694
50	27.37	48.87	23	82.5	48.07	-1.77	1191.67	1186.61	273.694
60	27.33	48.77	22.67	82.87	48.2	-1.77	1191.67	1183.34	273.694
70	27.33	48.8	22.67	82.8	48.1	-1.77	1191.67	1186.61	273.694
80	27.37	48.73	22.8	82.73	48.2	-1.8	1186.67	1180.07	273.694
90	27.4	48.7	22.83	82.77	47.9	-1.77	1188.33	1183.34	273.694
100	27.23	48.63	22.93	82.8	47.87	-1.8	1186.67	1180.07	273.694
110	27.33	48.57	22.97	82.9	48.4	-1.8	1193.33	1189.88	273.694
120	27.33	48.73	22.93	82.8	48.3	-1.77	1190	1183.34	273.694

Appendix A.6: Average raw data for 0.55 g/L MWCNT/POE experiment.

Time (mins)	T5 (°C)	T6 (°C)	T1 (°C)	T2 (°C)	T3 (°C)	T4 (°C)	P2 (kPa)	P3 (kPa)	P1 (kPa)
0	27.3	27.3	26.17	26.17	26.17	26.17	646.67	634.16	273.694
10	27.3	47.5	22.43	74.5	47	-2.8	1183.33	1180.07	273.694
20	27.3	48.17	22.2	79.3	47.6	-2.63	1205	1199.68	273.694
30	27.27	48.43	22.23	80.27	47.97	-2.4	1211.67	1206.22	273.694
40	27.23	48.5	22.03	80.63	47.63	-2.43	1215	1209.49	273.694
50	27.3	48.43	22.07	81.23	47.77	-2.5	1216.67	1212.76	273.694
60	27.3	48.47	22.07	81.93	47.93	-2.43	1228.33	1225.83	273.694
70	27.33	48.53	22.13	82.53	48.1	-2.43	1236.67	1229.1	273.694
80	27.3	48.77	22.07	82	48.13	-2.43	1238.33	1232.37	273.694
90	27.33	48.47	22.17	82.27	48.13	-2.43	1233.33	1232.37	273.694
100	27.27	48.7	22.03	82.4	48	-2.43	1240	1232.37	273.694
110	27.33	48.53	22.27	82.43	48	-2.43	1238.33	1229.1	273.694
120	27.37	48.63	22.17	82.4	48.1	-2.43	1243.33	1232.37	273.694

Appendix A.7: Average raw data for 0.65 g/L MWCNT/POE experiment.

Time (mins)	T5 (°C)	T6 (°C)	T1 (°C)	T2 (°C)	T3 (°C)	T4 (°C)	P2 (kPa)	P3 (kPa)	P1 (kPa)
0	27.33	27.33	26.07	26.07	26.07	26.07	643.33	637.43	273.694
10	27.33	50.77	24.9	80.3	50.4	-1.7	1281.67	1274.87	273.694
20	27.37	51.47	25	83.77	51.3	-1.4	1295	1287.94	273.694
30	27.3	51.7	25.3	84.7	51.67	-1.27	1303.33	1301.02	273.694
40	27.3	51.77	25.47	85.1	51.57	-1.3	1310	1307.56	273.694
50	27.33	51	25.6	85.07	50.9	-1.27	1293.33	1291.21	273.694
60	27.37	51.3	25.6	85.4	50.6	-1.3	1288.33	1284.67	273.694
70	27.37	50.7	25.3	85.2	51.3	-1.27	1291.67	1287.94	273.694
80	27.37	51.07	25.3	85.5	51.27	-1.3	1290	1284.67	273.694
90	27.3	50.9	25.27	85.8	51.27	-1.3	1288.33	1284.67	273.694
100	27.33	50.8	25.4	85.4	50.9	-1.3	1288.33	1284.67	273.694
110	27.3	50.7	25.27	85.7	50.97	-1.27	1288.33	1284.67	273.694
120	27.33	50.87	25.23	85.5	50.9	-1.27	1291.67	1287.94	273.694

Appendix B.1: Sample calculation using EES program (Pure Data)

```
T[4] = 1.50 [C]
P[4] = P_SAT(R134a,T=T[4])
h[4] = h[3]
s[4] = ENTROPY(R134a,T=T[4],h=h[4])

T[3] = 52.73 [C]
P[3] = 1454.3 [kPa]
h[3] = ENTHALPY(R134a,T=T[3],P=P[3])
s[3] = ENTROPY(R134a,T=T[3],P=P[3])

T[2] = 86.68 [C]
P[2] = 1457 [kPa]
h[2] = ENTHALPY(R134a,T=T[2],P=P[2])
s[2] = ENTROPY(R134a,T=T[2],P=P[2])

T[1] = 26.67 [C]
P[1] = 273.69 [kPa]
h[1] = ENTHALPY(R134a,T=T[1],P=P[1])
s[1] = ENTROPY(R134a,T=T[1],P=P[1])

m_dot_water = 0.004 [kg/s]
c_water = 4.2 [kJ/kg.C]
Delta_Twater = T[6]-T[5]
Q_water = m_dot_water*c_water*Delta_Twater
Q_cond = Q_water

W_compEL = 0.500 [kJ/s]
W_comp = W_compEL
m_dot_refrigerant = W_comp/ (h[2]-h[1])

Q_evap = m_dot_refrigerant*(h[1] -h[4])

COP_heating = Q_cond/W_compEL
COP_cooling = Q_evap /W_compEL

{EXERGI PART }
T[0] = 25 [C]
P[0] = 101.325 [kPa]
h[0] = ENTHALPY(Air,T=T[0])
s[0] = ENTROPY(Air,T=T[0],P=P[0])

T[00]= 298 [K]
m_dot_refrigerant_exergy = m_dot_refrigerant
i[4] = m_dot_refrigerant_exergy*((h[4]-h[0])-T[00]*(s[4]-s[0]))
i[3] = m_dot_refrigerant_exergy*((h[3]-h[0])-T[00]*(s[3]-s[0]))
i[2] = m_dot_refrigerant_exergy*((h[2]-h[0])-T[00]*(s[2]-s[0]))
i[1] = m_dot_refrigerant_exergy*((h[1]-h[0])-T[00]*(s[1]-s[0]))
```

T[5] = 27.33 [C]
P[5] = P[0]
h[5] = ENTHALPY(Water,T=T[5],P=P[5])
s[5] = ENTROPY(Water,T=T[5],P=P[5])

T[6] = 53.38 [C]
P[6] = P[0]
h[6] = ENTHALPY(Water,T=T[6],P=P[6])
s[6] = ENTROPY(Water,T=T[6],P=P[6])

m_dot_water_exergy = m_dot_water
i[5] = m_dot_water_exergy *((h[5]-h[0])-T[00]*(s[5]-s[0]))
i[6] = m_dot_water_exergy *((h[6]-h[0])-T[00]*(s[6]-s[0]))

i_comp = m_dot_refrigerant_exergy*T[00]*(s[2]-s[1])
i_cond = (i[2]-i[3])+(i[5]-i[6])
i_expval = i[3]-i[4]
i_evap = i[4]-i[1]

The result from this program:

1. Enthalpy per point
2. Entropy per point
3. Q_water = Heat transfer in water
4. Q_cond = Heat transfer in condenser part
5. Q_evap = Heat transfer in evaporator part
6. m_dot_refrigerant = Refrigerant flow rate
7. i_comp = Exergy destruction compressor
8. i_cond = Exergy destruction condenser
9. i_expval = Exergy destruction expansion valve
10. i_evap = Exergy destruction evaporator
11. i[5] = Exergy destruction inlet water
12. i[6] = Exergy destruction outlet water

Appendix B.2: Data Enthalpy and Entropy Pure POE Oil and Graphene nano-lubricants

Lubricants Oil	Enthalpy (kJ/kg)				Entropy (kJ/Kg-K)			
	1	2	3	4	1	2	3	4
PURE	274.6	314.9	127.6	128	1.02	1.02	0.4541	0.4801
GR 0.1 g/L	272.8	314	121.7	122	1.02	1.03	0.4364	0.4614
GR 0.15 g/L	272.2	313.8	122.2	122	1.01	1.03	0.4379	0.4631
GR 0.2 g/L	272.9	313.8	121.7	122	1.02	1.03	0.4363	0.4614

Appendix B.3: Data Enthalpy and Entropy Pure POE Oil and MWCNT nano-lubricants

Lubricants Oil	Enthalphy (kJ/kg)				Entrophy (kJ/Kg-K)			
	1	2	3	4	1	2	3	4
PURE	274.6	314.9	127.6	128	1.02	1.02	0.4541	0.4801
MWCNT 0.5 g/L	271.2	312.9	120.6	121	1.01	1.02	0.4329	0.4576
MWCNT 0.55 g/L	270.5	311.4	120.3	120	1.01	1.02	0.432	0.4574
MWCNT 0.65 g/L	273.4	314.3	125.2	125	1.02	1.02	0.4471	0.4743

Appendix C1. Sampel calculation for uncertainty

Nano-lubricants	Trial 1	Trial 2	Trial 3	Average	Standart Deviation	Error (%)
Pure	0.490	0.510	0.500	0.500	0.0082	1.63
Graphene 0.1 g/L	0.367	0.364	0.363	0.365	0.0017	0.47
Graphene 0.15 g/L	0.368	0.375	0.375	0.373	0.0033	0.89
Graphene 0.2 g/L	0.350	0.350	0.350	0.350	0.0000	0.00
MWCNT 0.5 g/L	0.350	0.350	0.360	0.353	0.0047	1.33
MWCNT 0.55 g/L	0.352	0.350	0.349	0.350	0.0012	0.36
MWCNT 0.65 g/L	0.305	0.305	0.300	0.303	0.0024	0.78
AVERAGE ERROR FOR WORK COMPRESSOR (%)						0.78

Average = (data Trial 1 + Trial 2 + Trial 3)/ Jumlah Trial (3)

Standart Deviation = STDEV.P(Trial 1: Trial 3)

Error = Standart Deviation/ Average

Average error for work compressor = AVERAGE(Pure : MWCNT 0.65 g/L)

LIST OF PUBLICATIONS

Cassim, S. B., Hairuddin, A. A., & Cut, V. (2024). The effects of Multiwalled Carbon Nanotube to the performance of a refrigeration system. Proceedings of the Institution of Mechanical Engineers, Part C: Journal of Mechanical Engineering Science, 09544062231224955.

Vira, C., Aziz Hairuddin, A., & Mazlan, N. (2022). Promising use nanoparticles in the base fluid of a system (preparation, stability test and critical analysis): A review. Materials Today: Proceedings, 66, 3135–3139.

Vira, C., Aziz Hairuddin, A., & Mazlan, N. (2024). Dispersion and Stability Behaviour of Graphene and MWCNT Based Nano-Lubricant for Vapour Compression Refrigeration (VCR) System. Communications on Applied Nonlinear Analysis, 32(1s), 314-323. 10.52783/cana.v32.2173